Energy and Structural Performance of Thermoactive Piles in Cold Regions

By

Maryam Saaly

A Thesis submitted to the Faculty of Graduate Studies of

The University of Manitoba

in partial fulfillment of the requirements of the degree of

MASTER OF SCIENCE

Department of Civil engineering

University of Manitoba

Winnipeg

Abstract

The objective of this thesis was to develop and apply thermal and thermo-mechanical analyses to evaluate the structural and energy efficiency of a Geothermal Energy Pile Foundation System in cold regions. Such systems were used to re-harvest the buildings energy loss through their below-grade enclosures for providing heating and cooling energy demand.

To investigate the energy performance of the below-grade envelope of a building in cold regions, a thermal analysis was carried out for an institutional building, the Stanley-Pauley Engineering Building (SPEB) located in the campus of the University of Manitoba. Knowing the amount of the annual heat dissipation from the sub-grade enclosure of the building to the ground, soil temperature increase was calculated. To efficiently harness the leaked heat from the basement, a geothermal energy system was proposed to be integrated to the foundation of the SPEB and the energy efficiency of such a system was assessed. In addition to the energy efficiency of the proposed system, the thermo-mechanical response of the proposed thermo-active foundation to the applied thermal and mechanical loads was also evaluated.

Results showed that 8% of the annual energy consumption of the SPEB in terms of space heating was leaked into the ground. This energy loss increased the temperature of the soil underneath the building. Using the geothermal energy foundation system, the lost energy was aimed to

be re-harvested. Results showed that the thermoactive foundation system could supply 4-15% of the building heating demand during Nov–Apr and 7–41% of the building cooling demand during May-Oct. It should be noted that application of such foundation system necessitated larger factor of safety effective on the allowable load.

Acknowledgement

I would like to express my sincere gratitude to my academic advisor, Dr. Pooneh Maghoul, for her excellent guidance and supports through my research. I was so blessed to work under her supervision during the past two years. Her perfect leadership, strong academic background and her great attitude encouraged me to put more effort on my work.

I am so glad to be surrounded with great friends to help me through my master's program. I would like to thank Mr. Hongwei Liu for his advice and patience and my best friend Mr. Nozhan Bayat for his infinite support and kindness during this program.

Last but not least, I would like to thank my parents, my brothers and my sister who were always by my side and encouraged me through this way. There is no word to express my gratitude to their support and love.

Maryam Saaly

Contents

List of Figures

List of Tables

1 Introduction and Overview

> *The way to get started is to quit talking and begin doing.*
>
> **— Walt Disney**

In Northern countries due to the cold climate and long winters, the energy demand allocated to space heating is high in buildings. In addition, due to the high thermal gradient between the building's indoor air temperature and outdoor air temperature in cold regions, the energy loss through the building envelopes is high compared to buildings that are located in regions with a moderate climate. The estimation of such energy dissipation through the building enclosures in direct contact with the ground (i.e., below-grade envelope) can be challenging. The reason is that in cold regions, freezing and thawing cycles may occur in the pore water of the soil especially near the ground surface which is more influenced by seasonal air temperature variations compared to deeper levels of ground. This phenomenon impacts the thermal properties of the soil, which have important consequences on predicting the energy efficiency of the sub-grade enclosure of buildings.

Nowadays, numerical modeling provides civil engineers with a tool to design and monitor the performance of new infrastructure in different conditions. For instance, using numerical models, the challenges associated with freeze/thaw cycles in the ground in cold regions can be addressed appropriately.

The objective of this thesis was to propose a hypothetical geothermal pile system to re-inject the energy loss through the below-grade envelope of an institutional building. The proposed thermoactive pile system was aimed at supplying the building's heating and cooling demand. The performance of the energy foundation system was assessed using a thermal analysis as well as thermo-mechanical modeling.

1.1 Problem Statement

1.1.1 Energy Loss through Below-Grade Enclosure

A significant component of the global energy consumption is allocated to space heating and cooling of buildings. For example, in Canada in 2009, 49% and 63% of all energy consumption in residential and institutional buildings, respectively, were allocated to space heating [48]. A significant portion of costs related to keeping indoor thermal conditions of buildings within acceptable limits is wasted through energy leakage from the structural envelopes.

Evaluating the annual heat loss through the building's below-grade enclosure, which is in direct contact with the ground, and assessing the efficiency of the mitigation approaches are challenging due to seasonal freeze and thaw cycles in foundation soils. In fact, the thermo-physical properties of soils are temperature- and moisture-dependent. When the soil temperature drops below the freezing point, pore water starts freezing. As freezing occurs in the soil, thermo-physical properties of soil changes compared to the non-freezing state because thermo-physical properties of ice is different from thermo-physical properties of water. Using an appropriate thermal modeling, such variations in soil thermo-physical properties can be included in studying the building's below-grade energy performance.

In this thesis, the energy loss from the basement of an institutional building in cold regions is addressed using 2D and 3D analyses. The institutional building that is the Stanley Pauley Engineering Building (SPEB) that is located at the campus of the University of Manitoba, Winnipeg where is a city with an annual cold climate. Knowing the annual energy loss through the below-grade enclosure of the building, the potential energy efficient strategies can be implemented to decrease the amount of energy loss and the corresponding budget waste in the building. In spite of application of energy efficiency improvement techniques, thermal profile of the ground is affected by the energy loss through the SPEB's below-grade envelope. Therefore, the objective of this work is to re-harvest the energy loss through basement via proposing a geothermal energy pile system.

1.1.2 Design and Performance Analysis of Geothermal Energy Pile Foundations

A practical way to re-harvest the dissipated heat from the sub-grade structures is the application of the geothermal energy technology for space heating and cooling. One of the promising technologies in this regard is the Ground Source Heat Pump system (GSHP). This system has three main constituents (i) heat pump, (ii) ground heat exchanger (GHE), and (iii) a heat distribution system [116]. Traditionally, a Ground Heat Exchanger (GHE) consists of one or more loops of absorber pipe in different shapes (i.e., U-shaped, W-shaped, and spiral). The heat carrier pipes are inserted into boreholes by which heat is extracted and rejected from/into the ground. These boreholes are traditionally independent of the building's foundation system. To decrease the costs of drilling boreholes for the purpose of using the energy stored in the ground, the pile foundation which is designed to support the structural load of the building can also be

used as a ground heat exchanger. Such bi-functional foundations are called thermoactive piles or geothermal energy piles [4].

In regions with long and cold winters, the annual energy demand of residential buildings that is allocated for space heating purposes is higher than the cooling demand. Therefore, the application of geothermal energy piles in cold regions may contribute to an excessive heat extraction from the ground which leads to a gradual decrease in the ground temperature after few years of operation of the system [159]. This phenomenon is called underground thermal imbalance which can cause the malfunction of the GSHP system. Therefore, the appropriate design of thermo-active foundations necessitates the consideration of such factors.

As mentioned earlier, building's heat loss through their basement enclosure leads to an increase in the ground temperature which can be re-harnessed by using thermo-active piles. Reviewing the literature, there is a lack of knowledge regarding the application of geothermal energy foundations while considering the building's heat leakage through their basement. The outcomes of this thesis can give a better insight into the energy and structural performance of the geothermal energy piles which are intended for extracting the stored heat in the ground as well as re-harvesting the leaked heat through the buildings below-grade enclosure.

1.2 Hypotheses and Objectives

In this section, the objectives and scopes of each part of this study are presented.

1.2.1 Energy Loss through the Below-Grade Structures

Hypothesis:

The thermal performance of the below-grade envelope of the SPEB is analyzed using a thermal modeling. The important assumptions made in the numerical model are as follows: i) the soil underneath and surrounding the building is fully-saturated although the granular backfill material that is used around the basement walls is assumed to be dry due to its high permeability and drainage feature; ii) thermal properties of the soil is assumed to be isotropic; iii) transient heat transfer in the soil occurs only through conduction; iv) volume change of water due to freezing of the soil pore water is ignored.

Since soil temperature especially near the ground surface is a function of the seasonal air variations, hourly air temperature data, provided by ASHRAE Weather Data Viewer Version 5.0, are assigned to the model as one of the inputs. Given this, the impacts of seasonal outdoor air temperature on the energy performance of the building's below-grade enclosure are investigated.

Objectives of Research:

The objective of this part is to assess the amount of energy loss through the below-grade envelope of SPEB and to determine the ground thermal profile beneath the SPEB considering the energy loss from the SPEB's surrounding buildings. In addition, to alleviate the energy loss through the basement of the building, some potential strategies will be proposed and a comparative cost analysis between the various mitigation methods will be carried out.

1.2.2 Design and Performance Analysis of Geothermal Energy Pile Foundations

This part of the thesis is targeted by performing two interrelated studies: i) energy performance of a hypothetical geothermal energy pile foundation system for the SPEB (Study I) and ii)

thermo-mechanical modeling of the energy piles to assess their mechanical response to the applied thermal loading (Study II).

Hypothesis:

The ground temperature especially at shallower depths varies with seasonal air variations. The input data regarding the hourly air temperature provided by ASHRAE Weather Data Viewer Version 5.0 is assigned to the numerical model to determine the ground temperature.

In the Study I (i.e., energy performance analysis), the following assumptions are considered in the energy modeling: a) the physical and thermal properties of the concrete used in geothermal piles are constant; b) properties of the soil depends on temperature, latent heat of fusion, and the fraction of water and ice in the pores; c) the modeled soil surrounding the SPEB assumed to be fully-saturated.

Study II (i.e, structural analysis) includes a thermo-mechanical model to assess the structural performance of the proposed geothermal energy pile foundation subjected to both structural and thermal loadings. It should be noted that the operation of the thermo-active pile is suggested in a way to avoid the occurrence of an underground thermal imbalance as well as freezing at the pile-soil interface. The following assumptions have been made: a) the materials used in piles are assumed to be solid, isotropic, and linear elastic; b) a perfect contact is assumed at the interface between the pile and soil; c) the soil is modeled as an isotropic, and elastoplastic material. The size of the yield surface is defined by using the Mohr-Coulomb criterion.

Objectives of Research:

A hypothetical geothermal energy pile foundation system is proposed and the thermal response of the ground as well as a potential underground thermal imbalance due to the operation of the

system will be studied. To improve the efficiency of the system, different approaches will be proposed and their impacts on the efficiency of the system will be investigated.

Furthermore, to assess the application of such foundation systems from a structural point of view, the structural behavior of the pile associated with both thermal and mechanical loadings will be analyzed. In addition to the thermal loading applied to the piles, the impacts of the dissipated heat through the below-grade enclosure of the building on the behavior of the thermo-active foundation system will be studied as well. The outcomes of this research will pave the way for further expansion of the application of thermoactive foundations in cold regions.

1.3 Thesis Structure

Chapter 1

Chapter 1 provides the problem statement which will be addressed in this thesis as well as objectives and scopes of different chapters. In addition, the outline of this thesis is provided in this chapter.

Chapter 2

In Chapter 2, the impact of freeze and thaw cycles in foundation soils on the annual energy loss through the below-grade envelope of an institutional building, the Stanley Pauley Engineering Building, in Winnipeg, Canada is investigated. Moreover, a parametric study is conducted to asses the effects of various factors such as insulation thickness, backfill material and additional insulation layer, on the energy efficiency of the sub-grade enclosure of the building. Finally, an overall cost analysis is carried out to evaluate the annual budget loss upon the energy loss through the basement enclosure.

Chapter 3

Chapter 3 presents a comprehensive review of the ground source heat pump (GSHP) application. In addition, one of the most common impediments for broad application of geothermal energy in cold regions, the underground thermal imbalance, is studied and potential solutions for this problem provided in the literature are presented. The solutions, which are intended to be reviewed, include the application of the auxiliary units and hybrid systems such as solar-assisted heat pump system, GSHP integrated with air-source units, waste water units or fossil fuels. In addition to the auxiliary heat and cold units, some of the solutions deal with the changes in the configuration and properties of the borehole heat exchangers.

Chapter 4

In Chapter 4, a hypothetical energy pile foundation system is proposed to re-harvest the building's heat dissipation through its below-grade enclosure. The thermal performance of such an energy pile system is then studied using thermal modeling. Moreover, the soil response to heat extraction and rejection is investigated. Finally, solutions for potential occurrence of the thermal imbalance in the ground are assessed and the performance of the system due to implementation of such solutions is evaluated.

Chapter 5

In Chapter 5, the thermo-mechanical response of a single pile of the geothermal energy foundation system of the SPEB due to the applied thermal and mechanical loadings is studied. The reason is that the application of the proposed thermo-active foundation system is feasible only if the pile displacements as well as the maximum compressive stress induced by thermal and mechanical loads are within the admissible limit. Such criteria are assessed in this chapter.

Chapter 6

Chapter 6 provides some conclusions of the works that are carried out in this thesis and indicates the limitations and future works.

1.4 Dissemination and Authorship Contribution

The outcomes of this thesis have been disseminated as follows:

Journal Papers:

1. Saaly M., Maghoul P., Kavgic M., Polyzois D., 2019. Performance Analysis of a Proposed Geothermal Pile System for Heating and Cooling Energy Demand for a Building in Cold Regions, *Sustainable Cities and Societies (Elsevier)*, 45, pp: 669–682.

    - Saaly M.: Prepared the manuscript, conducted the simulations in COMSOL Multiphysics, processed and interpreted the data.
    - Maghoul P.: Suggested and supervised this research and assisted with editing of the manuscript.
    - Kavgic M.: Conducted the building energy modeling.
    - Polyzois D.: Supervised this research.

2. Saaly M., Maghoul P., 2019. Thermal Imbalance Due to Application of Geothermal Energy Piles and Mitigation Strategies for Sustainable Development in Cold Regions: A Review, *Innovative Infrastructure Solutions (Springer)*, 4: 39. DOI: 10.1007/s41062-019-0224-1.

    - Saaly M.: Prepared the manuscript.

- Maghoul P.: Suggested and supervised this research and assisted with editing of the manuscript.

3. Saaly M., Bobko K., Maghoul P., Kavgic M., 2019. Energy Performance of Below-Grade Envelope of an Institutional Building in Cold Regions, *Journal of Building Engineering (Elsevier)*, Under Review.

    - Saaly M.: Prepared the manuscript, conducted the simulation in COMSOL Multiphysics, processed and interpreted the data.
    - Bobko K.: Conducted the simulation in COMSOL Multiphysics, processed and interpreted the data.
    - Maghoul P.: Suggested and supervised this research and assisted with editing of the manuscript.
    - Kavgic M.: Conducted the building energy modeling.

4. Saaly M., Maghoul P., Holläder H., 2019. Thermo-mechanical performance of a proposed geothermal energy pile system , *Acta Geotechnica (Elsevier)*, Under Review.

    - Saaly M.: Prepared the manuscript, conducted the simulation in COMSOL Multiphysics, processed and interpreted the data.
    - Maghoul P.: Suggested and supervised this research and assisted with editing of the manuscript.
    - Holläder H.: Supervised this research and assisted with editing of the manuscript.

Conference Papers:

1. Saaly M., Maghoul P., Holländer H., 2019. Thermo-mechanical performance of a geothermal energy pile system for re-harvesting the energy loss through the basement of a building in cold regions, 72th Canadian Geotechnical Conference (Geo St John's 2019), St.John's, Canada.

    - Saaly M.: Prepared the manuscript, conducted the simulation in COMSOL Multiphysics, processed and interpreted the data.
    - Maghoul P.: Suggested and supervised this research and assisted with editing of the manuscript.
    - Holläder H.: Supervised this research and assisted with editing of the manuscript.

2. Saaly M., Maghoul P., 2019. Thermal Performance of a Proposed Geothermal Piles System for Re-harvesting Heat Loss through the Building Below-Grade Enclosure in Cold Regions, 18th International Conference on Cold Regions Engineering and the 8th Canadian Permafrost Conference, Quebec City, Canada.

    - Saaly M.: Prepared the manuscript, conducted the simulation in COMSOL Multiphysics, processed and interpreted the data.
    - Maghoul P.: Suggested and supervised this research and assisted with editing of the manuscript.

3. Bobko K., Maghoul P., Kavgic M., Saaly M., 2018. Energy Performance of Below-Grade Envelope of Stanley-Pauley Building in Winnipeg, 71st Canadian Geotechnical Conference (GeoEdmonton 2018), Edmonton, Canada.

- Bobko K.: Prepared the manuscript, conducted the simulation in COMSOL Multiphysics, processed and interpreted the data.
- Maghoul P.: Suggested and supervised this research and assisted with editing of the manuscript.
- Kavgic M.: Conducted the building energy modeling.
- Saaly M.: Assisted with editing of the manuscript.

2

Energy Loss through the Below-Grade Envelope of an Institutional Building in Cold Regions [1]

Abstract

The effects of freeze-thaw cycles on the thermal properties of foundation soils is often ignored in many building energy simulation programs. Consequently, the energy dissipation through the below-grade enclosure of buildings in cold regions, where freeze-thaw occurs in soils, has been lagged behind. In this chapter, the energy performance of the below-grade envelope of the Stanley Pauley engineering building (SPEB) located in the Fort-Garry campus of the University of Manitoba, Winnipeg, Canada has been numerically investigated using 3-D and 2-D analyses. For this purpose, the energy loss through the below-grade structure of the building has been estimated using two scenarios. Each scenario was assessed considering two different approaches. In the first scenario, no insulation was considered for the basement walls and floor while the second scenario simulated the basement structure having the actual insulation layers of the SPEB (i.e., a 230 mm thick insulation layer underneath the floor slab and a 125 mm thick insulation layer surrounding the basement walls). The approaches by which the

[1] **Saaly M.,** Bobko K., Maghoul P., Kavgic M., 2019. Energy Performance of Below-Grade Envelope of an Institutional Building in Cold Regions, *Journal of Building Engineering*, Under Review.

thermal analysis have been done include: (i) constant soil thermal properties (Approach 1), and (ii) temperature-dependent soil thermal properties by which phase change of pore water in freezing soil is considered (Approach 2). Results showed that the energy loss through the below-grade building fabric decreased by 61% if the insulation layers, as suggested in the structural plans, cover the basement walls and floor slab. In addition, it was observed that the simulations within Approach 1 underestimated the energy loss through the basement envelope of the building by 25% and 8% compared to Approach 2 and within Scenario 1 and Scenario 2, respectively. Although decreased yet considerable energy was leaked through the basement of the building in comparison to the energy loss of the building's above-grade enclosure. As such, mitigation approaches were proposed that could decrease the annual energy loss through the basement enclosure especially basement walls. Such mitigation methods include using an additional horizontal insulation layer, and increasing the thermal resistance of the basement walls. Finally, the results of the 3-D analysis were compared to an equivalent 2-D analysis of the energy performance of the SPEB which showed up to 22% overestimation in the 2-D analysis's results.

2.1 Introduction

The global consumption of fossil fuels is increasing year by year due to high energy demand all over the world. As a result, emission of greenhouse gases and their following impacts on environment such as climate change have recently promoted the mitigation strategies to reduce the energy loss in buildings. A significant component of the total global energy consumption relates to the energy used to heat and cool buildings [134, 35]. For instance in Canada in 2009, 49% and 63% of all energy use in residential and institutional buildings, respectively were allocated to space heating [48]. Although gains in efficiency produced a 24% decrease in energy

needed for space heating of a single family dwelling between 1990 and 2009, a 36% increase in the number of households in Canada resulted in a 12% net increase in required total for heating [48].

The accumulated heat in the building can be dissipated in different ways, one of which is natural ventilation heat loss. Such process happens due to non-complete air tightness of buildings which causes the heated air to ex-filtrate through gaps and be replaced by cold air [45]. Another mechanism of heat loss is through the building enclosure's material such as glass and concrete using conduction, and radiation. Energy performance of the above-grade elements of buildings, such as walls, windows and ceiling's built-up has been well studied in the literature [134, 132, 137, 80, 61] since they initially posed the most substantial potential of heat loss. However, significant heat losses may still occur due to the flow of heat from inside a building through ground-floor slabs into soil [38, 19, 83, 30, 29, 125, 122, 2]. The basement enclosure of a building is in the direct contact with the foundation soil. The thermal gradient between the foundation soil and building's indoor air leads to the heat dissipation via the thermal conduction through the basement enclosure. It can pose a significant impact on the building's energy efficiency, especially during the cold seasons of the year.

Rantala and Leivo [122] showed that depending on the material properties of a floor slab, up to 19% of the total heat loss can occur through the basement floor. Also, Rees et al. [124] assessed the influence of the soil's moisture content on the heat leakage from the basement floor. It was observed that a higher soil moisture content increases the heat flux through the basement floor up to 20% and 40% in two-dimensional and three-dimensional thermal analyses, respectively.

Aside from the thermal properties of the materials used in a building's below-grade enclosure, the thermal properties of the foundation soil which are affected by the soil's moisture content,

can affect the building's energy loss. Also, the configuration of the insulation layer covering the basement walls and floor slabs is another important factor in the intensity of the building's heat leakage through the below-grade envelope [13]. Hagentoft [64] showed that the heat leakage through the basement can contribute to 30% of a building's total energy loss if a low quality insulation is applied. Therefore, the investigation into a more efficient insulation, which meets the required thermal properties, for the below-grade envelope of buildings is critical.

Through the analytical studies, Karti et al. [72] estimated the heat loss through a slab-on-grade floor using a three-dimensional model that can estimate the energy loss more accurately compared to an one-dimensional study. It was shown that the energy loss through the floor slab calculated by a three-dimensional analysis is more accurate comparing to a two-dimensional model. The reason is modeling of the building's basement corners where most of the heat loss through slab occurs due to the thermal bridge [72, 73, 71]. It is worth mentioning that Lachenbruch [79] and Delsante et al. [43] have developed a three-dimensional model for the heat exchange between the slab and ground prior to Karti et al.[72]. However, neither of the latter methods considered the slab-on-grade to be insulated.

Aside from the above-mentioned analytical studies, few researchers investigated the performance of the below-grade envelope of buildings through empirical studies [108, 109, 133]. It should be noted that in the aforementioned studies, the main emphasis has been placed on the basement floor slab as the main source of below-grade heat loss of residential buildings.

In another work, Adjali et al. [1] conducted a set of in-situ measurements in order to monitor the thermal behavior of a slab-on-ground floor. Results were compared with a standard conductive numerical model which was added to the general building energy simulation program APACHE aimed at simulating the earth-contact heat flow. The temperature at different depths of the soil

in contact with the building floor slab estimated by the numerical analysis adapted well with the measured data. However, some discrepancies were noticed in leaked energy from the floor slab. Adjali et al. [1] speculated that such discrepancies stemmed from the inevitable reduction of the large 3-D domain due to an excessive number of nodes that resulted in prohibitive run-time.

One of the important parameters that affects the thermal properties of soils is the moisture content. The reasons are higher heat capacity and thermal conductivity of water than grain particles. Therefore, the effective thermal conductivity of soil increases when voids are filled with water [45]. Temperature changes generated in surrounding soils by heat losses from the foundation to the ground may contribute to a strongly-coupled, nonlinear moisture and energy flow (heat and mass transfer). Cold climates may cause freezing of pore water at shallower levels of the ground. Freezing involves temperature gradients and moisture migration due to cryo-suction. This phenomenon, with or without frost heave, has significant consequences in foundation engineering in areas where both seasonal frost and permafrost exist. The thermal conductivity of soils in frozen and unfrozen states have been studied by Johansen [70], Farouki [55] and Andersland and Ladanyi [8] who attempted to formulate the thermal conductivity of soils as a combination of the thermal conductivities of all components (soil particles, water, air, and ice). In spite of the attempts in estimating the thermal properties of soils coupled with their ice and water content, in building energy simulation programs such as EnergyPlus and TRNSYS it is often assumed that the thermal properties of soils are constant which means that they do not depend on such factors as seasonal freeze-thaw cycles and variations in moisture content. However, it was shown in the literature [1, 45, 44] that by ignoring the presence of pore water in soils, the energy loss through the floor slab cannot be determined appropriately.

This chapter aims to investigate the energy efficiency of the newly constructed SPEB at the Fort-Garry campus of the University of Manitoba in Winnipeg, Canada. Since Winnipeg experiences extreme cold weather and low temperatures during winter, freezing occurs in the ground, as deep as 2.5 m below the ground surface, which affects soil's thermal properties.

2.2 Overview of the SPEB

The SPEB is a new addition to the Engineering and Information Technology Complex of the University of Manitoba in Winnipeg, Canada. The building is composed of three floors above grade with an overall footprint of 862.5 m^2 and a basement at 4.250 m below grade that spreads over 287.5 m^2. Fig.2.1 demonstrates the basement plan of the SPEB. According to this plan, the structural load of the building is transferred into a group of piles underneath a 230 mm thick insulation layer underlying the concrete slab of the basement. The properties of the insulation (i.e. extruded polystyrene) and concrete are presented in Section 2.3.6.

2.2.1 Site Investigation and Soil Stratigraphy

Winnipeg soil consists of the Precambrian basement of bedrock underneath the fine-grained deposits of glaciolacustrine clays and tills of Lake Agassiz. Since frost penetration reaches ~2.5 m in Winnipeg area, the top glaciolacustrine clays and tills would be mostly affected by this seasonal changes [56].

Based on the geotechnical reports, construction site has topsoil cover and asphalt followed by gravel pack of approximately 250 mm. Clays are encountered until the depth of 16.7 m which are classified as very soft to very stiff in consistency. The first two meters of the soil consists

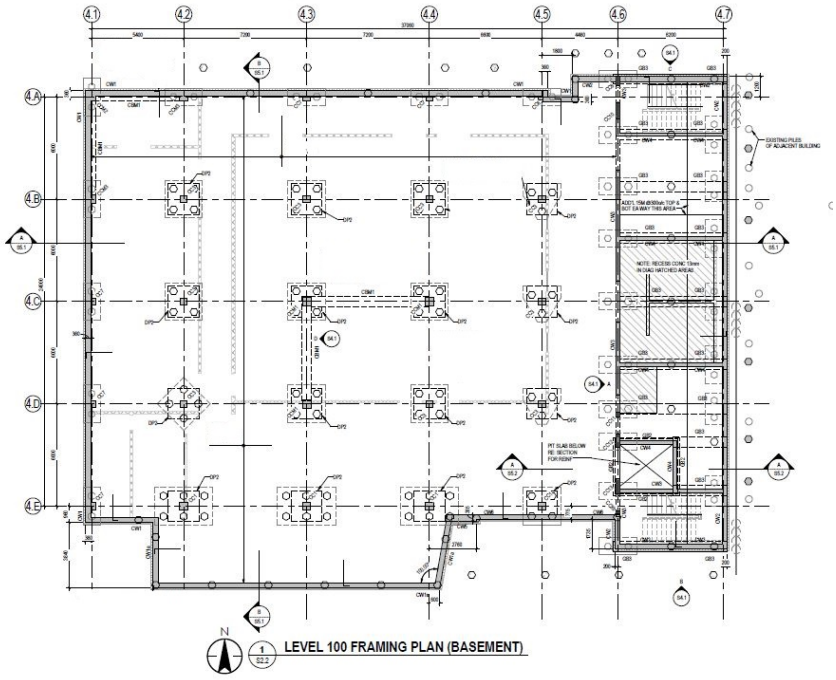

Fig. 2.1: Basement plan view at elevation -4.250 m (courtesy of Stantec and the University of Manitoba).

of dark grey clay containing organic compounds overlaying a stiffer layer of brown clay. The moisture content of the soil increases with depth and varies within a range of 27% to 61% [52].

Fig. 2.2: Locations in the site from where soil samples were retrieved [16].

The stratigraphy of the site consists of three layers with thicknesses of 1.5 m, 2.95 m and 10.55 m. To determine the variability of soil thermal properties at different depths, 18 different samples were obtained from elevations of 1-1.5 m, 2 m and 4.5 m below ground. As shown in Fig. 2.2, samples were retrieved from three different locations in the site.

Disturbed soil sampling in layers one and two were conducted using three trenches with the depths of 1-1.5m and 2m that were dug at the locations shown in Fig. 2.2. The obtained disturbed samples consist of twelve 20 × 20 cm cohesive cubical specimens. It should be noted that the collected samples were preserved and sealed before tests to avoid moisture loss as this noticeably affects the estimated thermal conductivity and heat capacity of samples. Also, another six undisturbed samples were taken from the depth of -4.5 m using Shelby tubes according to ASTM D1587-15 standard (Fig. 2.3b). The retrieved tubes were preserved and stored in a refrigerator before accomplishing the required tests.

(a) (b)

Fig. 2.3: Preparation of (a) disturbed sample (b) undisturbed samples for the tests [16].

Measurements for determination of thermal properties of the samples were taken using KD2-Pro that was manufactured by Decagon Devices, Inc (Fig. 2.4). This device was previously calibrated in the laboratory according to manufacturing instructions [40]. This system is attached to two sensors known as TR-1 and SH-1 which consist of needles that contain a heater and temperature sensor for estimating the thermal conductivity of the soil. Both sensors used the transient line heat source technique. In addition to thermal conductivity, the dual-needle SH-1 sensor yields the information on diffusivity and volumetric heat capacity. Using SH-1, volumetric heat capacity is measured through the heat impulse induced by needle 1 and captured by needle 2 located in a distance of 6 mm.

Both TR-1 and SH-1 sensors work within low and high-power modes. The low power mode facilitates the sensor to generate temperature impulse of very small fractions of °C. This makes the sensor capable of being used for measurements in temperature- sensitive substances such as liquids or frozen samples where forced convection may affect the results of measurements. In contrast, high power mode makes stronger temperature increments, more than 10°C, which is used in less temperature-sensitive materials such as rocks and clays. Both power modes were used to measure the thermal properties of frozen samples.

Overall, laboratory tests were aimed to determine the basic thermal properties of different layers of the soil. Each thermal measurement was instantly accompanied with tests of physical properties such as density and water content. Table 2.1 and Table 2.2 provide the properties of the soil samples in unfrozen and frozen states, respectively that are measured in the laboratory. The frozen soil samples in comparison with unfrozen ones have lower specific heat capacity while density of the soils was less sensitive to variation of frozen pore water content. It should

Fig. 2.4: Disturbed sample during thermal conductivity measurement test [16].

be noted that initially, the unfrozen properties of the soil of the construction site have been used in the numerical model.

Layer's Thickness (m)	Thermal Conductivity (W/m°C)	Heat Capacity (J/kg°C)	Density (kg/m^3)	Porosity [-]
0.0 -1.5 m	1.10	1564	1802	0.32
1.5 - 4.5 m	1.12	1513	1862	0.31
4.5 -16.7 m	1.06	2205	1744	0.34

Tab. 2.1: Summary of the soil properties of the construction site - unfrozen state.

Layer's Thickness (m)	Thermal Conductivity (W/m°C)	Heat Capacity (J/kg°C)	Density (kg/m^3)	Porosity [-]
0.0 -1.5 m	1.55	1533	1820	0.31
1.5 - 4.5 m	1.41	1310	1830	0.31
4.5 -16.7 m	1.69	1411	1720	0.38

Tab. 2.2: Summary of the soil properties of the construction site - frozen state.

2.2.2 Energy Consumption of the SPEB

To better realize the scale of the SPEB's energy loss through its below grade envelope, information regarding the annual energy use of the SPEB have been provided in this section. Such information has been presented in a study conducted by Al-Janabi et al. [68]. Energy consumption has been determined using a multi-zone model according to the as-built drawings of the SPEB which has been developed in EnergyPlus using SketchUp Make/ Euclid 0.9.3 [49]. To estimate the building's energy consumption, solar heat gains and performance of the systems need to be modeled accurately. As such, 98 thermal zones have been assigned to the model based on load and scheduling characteristics, type of HVAC system and orientation.

The enclosure of the building is an assembly of several layers each of which represents a specific type of material. Physical and thermal properties of the material specified for each layer have been assigned according to Manitoba Energy Code for Buildings (MECB) [101]. Also, thickness of each layer is equal to the values reported at the final construction drawings of the building.

In addition to the specifications noted above, Al-Janabi et al. [68] considered the internal loads which have a significant impact on SPEB energy consumption that is estimated using the EnergyPlus model. To this end, equipment, internal lights and plug-loads have been taken into account as the sources of internal gain.

Fig. 2.5 provides the obtained results regarding the total annual heating and cooling consumption of the SPEB as well as heating load of the building's basement using EnergyPlus model. In addition, detailed monthly heating and cooling load of the building is also provided in Fig. 2.6.

Results signify that heating and cooling consumption loads exist all over a year. This is due to the reason that SPEB accommodates various space types including graduate study spaces,

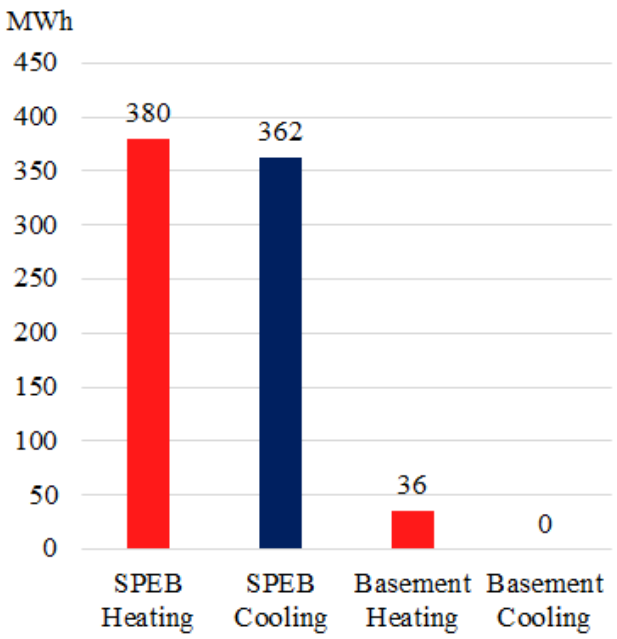

Fig. 2.5: The annual heating and cooling energy consumption of the SPEB; data from Al-Janabi et al. [68].

laboratories, fabrication spaces and data centers which cause high internal gains from the equipment and occupants. Consequently, there is a need for cooling the core zones, lab spaces and data centers even during the winter months. Moreover, the building's window to wall ratio is almost equal to 60%. This contributes to an increase in heating and cooling loads of the perimeter zones throughout a year.

2.3 Thermal Modeling of the Below-Grade Envelope of the Building

This section is intended to investigate the annual energy loss through the below-grade enclosure of the SPEB using COMSOL Multiphysics. In the current research, the below-grade envelope of the building is investigated using a 3-D analysis. Furthermore, to highlight the consequences

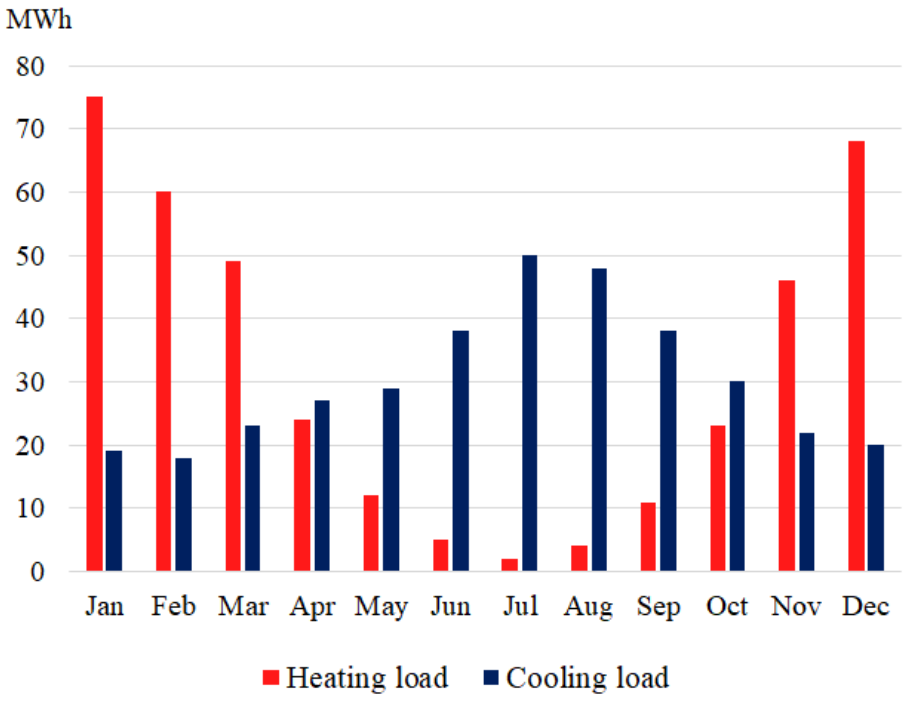

Fig. 2.6: Monthly heating and cooling energy consumption of the SPEB; data from Al-Janabi et al. [68].

of the thermal bridge through the corners of the basement structure, the results of the 3-D simulation is compared with 2-D numerical analyses and further suggestions are provided.

2.3.1 Modeling Methodology

Scenario 1: In the new construction practices not only the insulation is included in the design of a building envelope but also the emphasis is put on minimizing the amount of the energy loss by optimizing the properties, dimensions and installation practices of insulation layers. However, in some of the institutional and commercial buildings, the insulation performance degrades over the life-time of the building to the point that the building's envelop performs as low energy efficient as a non-insulated enclosure which necessitates implementing further thermal performance improvement techniques [127]. Therefore, to quantitatively demonstrate

the importance of promising performance of the basement enclosure's insulation over the life-span of the building, in Scenario 1 it has been assumed that the basement concrete walls and floor slab are not insulated. This Scenario is considered as the base case.

Scenario 2: Within Scenario 2, the below-grade enclosure of the SPEB is insulated according to the structural drawings by using two 230 mm and 125 mm thick layers of extruded polyester underneath the floor slab and surrounding the walls, respectively. The energy loss of the building was further estimated by measuring the heat transferred from the building's basement to the ground using COMSOL Multiphysics.

Scenario 3: The energy performance of the below-grade enclosure especially basement walls is reliant on seasonal temperature variations. To alleviate the effects of the ambient air temperature variation on heat exchange between the ground and the basement walls, Scenario 3 is proposed in which an additional horizontal insulation layer is applied. The aforementioned insulation layer which is 100 mm thick and 1.2 m wide, is located at 0.5 m below the ground level.

Such horizontal insulation layer which is intended for decreasing the ground temperature variation due to seasonal climate changes, make an stop to propagation of the freezing front. Therefore, temperature of the ground around the perimeter of the basement will not decrease significantly during winter months. Consequently, due to lower thermal gradient between the ground and temperature of the walls, less heat will be dissipated to the ground from the basement walls.

2.3.2 Governing Equations

First Approach: Constant Thermal Properties

Based on the first approach, which is a simplified method, the thermal and physical properties of the soil (i.e., thermal conductivity, specific heat capacity and density) are constant and equal to the average values reported in Table 2.1. Therefore, the heat transfer in the model is governed by the following equation:

$$\rho C_p \frac{\partial T}{\partial t} + \nabla . q_c = Q \tag{2.1}$$

where, ρ [kg/m^3] is the density of material (i.e., concrete and insulation), C_p [J/kg·K] is the specific heat capacity, T [°C] is the temperature, t [s] denotes time, $\nabla\cdot$ is the divergence operator ($\nabla\cdot \mathbf{F} = \frac{\partial \mathbf{F}_x}{\partial x} + \frac{\partial \mathbf{F}_y}{\partial y} + \frac{\partial \mathbf{F}_z}{\partial z}$) and Q[W/m^3] is the heat source. q_c is also the heat flux which is defined by Fourier's law as follows:

$$q_c = -k\nabla T \tag{2.2}$$

where, k is the thermal conductivity of the material and ∇ denotes the gradient operator ($\nabla = \frac{\partial}{\partial x}, \frac{\partial}{\partial y}, \frac{\partial}{\partial z}$).

Second Approach: Variable Thermal Properties

In approach 2, the concrete and insulation are modeled as solid domains with constant thermal and physical properties. The heat transfer occurs through such materials only by conduction as

shown in Equation 4.1. However, for estimating the heat transfer in the soils surrounding the below-grade envelope using approach 2, the following assumptions have been made:

- Soil is homogeneous, isotropic and incompressible.
- The initial temperatures of the soil, concrete, and insulation layer are uniform.
- The thermal properties of the concrete and insulation are considered constant.
- The thermal properties of the soil are temperature-dependent and vary as the temperatures drops down below the freezing temperature (T_0). In other words, the thermal properties of the soil depend on latent heat of fusion and the fraction of water and ice in the soil pores.

The governing equations for transient heat conduction in freezing soils considering the latent heat released during the phase change of pore water can be defined according to Zhu and Michalowski [164]. To derive the partial differential equations for heat transfer in freezing soils, following assumptions need to be made: 1) it is assumed that the soil is fully-saturated, 2) frost heave due to volume change of pore water as a result of freezing assumed to be negligible, 3) heat is transferred into the soil only through the heat conduction mechanism. Based on the mentioned assumptions, the governing equation for transient heat transfer in the soil can be described as below:

$$\left(\rho C_p - L_f \rho_i \frac{\partial \theta_i}{\partial T}\right) \frac{\partial T}{\partial t} + \nabla . q_c = Q \tag{2.3}$$

where ($\rho C_p - L_f \rho_i \frac{\partial \theta_i}{\partial T}$) is the apparent volumetric heat capacity, L_f denotes the latent heat of fusion per unit mass of water (approximately 3.33×10^5 J / kg), ρ_i is the density of ice and θ_i is the volumetric fraction of ice in pores, ρC_p is the volumetric heat capacity of the soil which

can be estimated by the sum of the volumetric heat capacity of each constituent of a saturated freezing soil (solid skeleton, water, and ice) multiplied by its volumetric fraction as described below:

$$\rho C_p = \rho_w C_w \theta_w + \rho_i C_i \theta_i + \rho_s C_s \theta_s \tag{2.4}$$

It should be mentioned that w, i, s subscripts denote water, ice and soil skeleton, respectively. Also, the effective thermal conductivity of a saturated soil sample having ice and water components can be described as below:

$$k = k_w \theta_w + k_i \theta_i + k_s \theta_s \tag{2.5}$$

According to Michalowski [105], as temperature of the soil drops below the freezing temperature (T_0), some fraction of water in the pores freezes. In order to determine the unfrozen water content of the soil, the following equation has been proposed:

$$\theta_w = \theta_{wr} + (\theta_{w0} - \theta_{wr})\, e^{a(T - T_0)} \tag{2.6}$$

In the above equation, θ_{wr} represents the residual unfrozen water content which is assumed to be 0.05 in this study [164], θ_{w0} denotes the initial unfrozen water content which is equal to the porosity of the soil, a $[1/^\circ C]$ is a parameter that controls the curvature, taken here 0.16 [164]. Also, the volumetric fraction of ice can be determined using the following equation:

$$\theta_i = \theta_{w0} - \theta_w \tag{2.7}$$

2.3.3 2D Model Description

The 2D model has been set up in the axisymmetric space dimension of COMSOL Multiphysics. Soil domain extends at a depth of 11 m below the building's foundation and reaches to the elevation of -15 m. The axisymmetric condition has been assigned to the left boundary of the soil domain. The total length of the model spreads for 17 m which is almost half of the total length of the SPEB that is reported in construction plans.

In Fig. 2.7 a general view of the geometry of the 2D model has been shown for the case which contains no insulation. In addition, Fig. 2.8 provides the geometry of the 2D model including the insulation that has been applied in the design of the SPEB below-grade envelope. The mesh of the models has been built using the physic-controlled sequence type with fine mesh refinement near the basement structure, as shown in Fig. 2.7 and Fig.2.8.

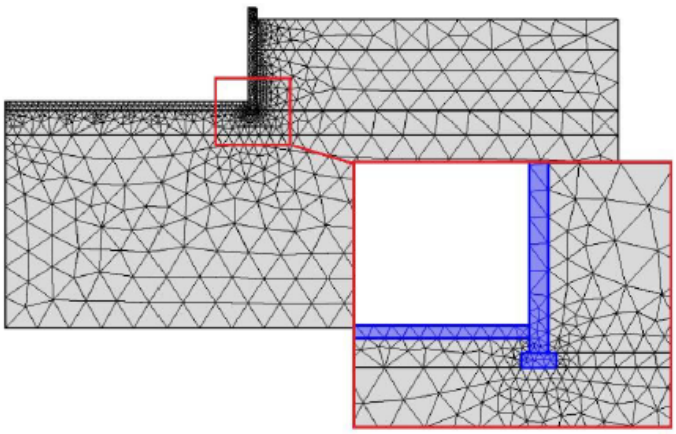

Fig. 2.7: General view of the 2-D model developed in COMSOL Multiphysics for the basement envelope of the SPEB for the case that no insulation is applied to the walls and floors [16].

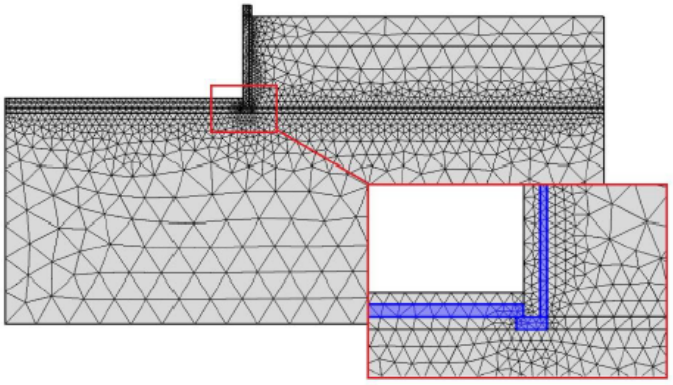

Fig. 2.8: General view of the 2-D model developed in COMSOL Multiphysics for the basement envelope of the SPEB including basement walls and floor insulation layers [16].

2.3.4 3D Model Description

Fig.2.9 provides the 3D model geometry of the SPEB's below grade envelope developed in COMSOL Multiphysics. The dimensions of the domain are considered to be 70 m × 65 m × 15 m. In other words, the bottom of the domain is located at the elevation of -15m. It should be noted that dimensions of the model have been selected in a way that boundaries have the least effects on the results.

Automatic physics-controlled sequence type with fine mesh has been applied to the model as presented in Fig.2.9. As can be observed, denser and smaller mesh has been set up to the corner point to increase the accuracy of outputs. It should be noted that mesh refinement using "finer" automatic physic-controlled sequence has also been applied to the model that showed negligible effect on the results.

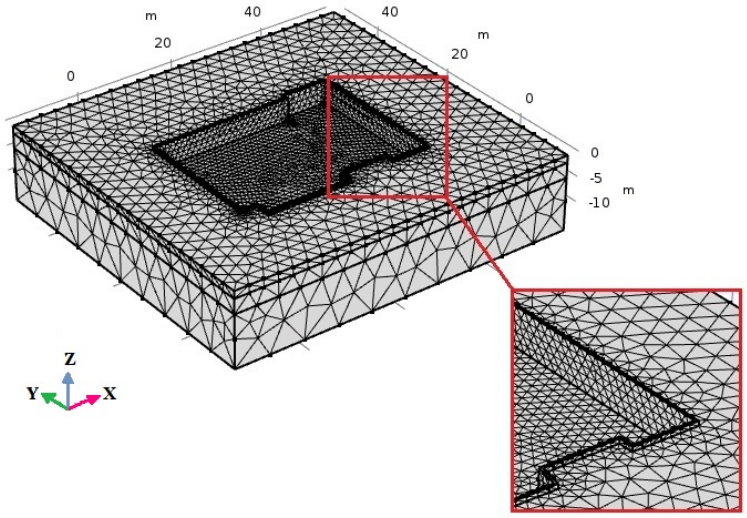

Fig. 2.9: General view of the 3-D model of the SPEB below-grade envelope in COMSOL Multiphysics.

2.3.5 Boundary and Initial Conditions of the 2D and 3D Models

Temperature of the soil especially near the ground surface is dependent on seasonal changes To consider the impacts of seasonal temperature variation on the ground temperature, the following convective heat flux $q_{conv}[W/m^2]$ has been assigned to the top boundary of the soil domain (i.e. ground surface) which is in direct contact with the ambient air:

$$q_{conv}(t) = h(T_{air}(t) - T_s(t)) \tag{2.8}$$

where, h $[W/m^{2\circ}C]$ is the convective heat flux coefficient whose value is dependent on the wind speed and temperature condition of each specific boundary [67]. T_{air} $[^\circ C]$ is the hourly average ambient air temperature which is provided by ASHRAE Weather Data Viewer version

5.0. T_s [$^\circ C$] is the temperature at the ground surface which is calculated for each time step by the software.

The boundary conditions at the interface between the basement structure (wall and floor slab) and the soil is also defined by a convective heat flux q_{indoor} [W/m^2] which can be determined as follows:

$$q_{indoor} = h\left(T_{indoor} - T_g\right) \tag{2.9}$$

According to the literature [44, 94], h can be considered to be 8 and 6 [$W/m^{2\circ}C$] for the heat transfer through the walls and floor of the basement, respectively. T_{indoor} is the basement's indoor air temperature, which is assumed equal to 20°C over a year due to the operation of the heating, ventilation and air conditioning (HVAC) system. T_g is the temperature of the soil surrounding the below-grade envelope of the building.

In the 2D model, an adiabatic condition was assigned to the left and right boundaries of the model where no heat flow was assumed. The surrounding boundaries of 3D model are also considered as adiabatic surfaces where no heat flow occurs. In addition, a constant temperature of 6°C has been assigned to the bottom boundary of both 2D and 3D models.

The initial temperature of the soil domain in both 2D and 3D models is assumed to be equal to 6°C [56]. Also, the concrete slab and insulation layer are assumed to have the initial temperature of 15°C.

2.3.6 Material Properties

The governing equations according to section 2.3.2 have been used to estimate the heat loss through the below-grade envelope of the building over 8760 h (i.e., one year). This model

simulates the building's surrounding soil, a 200 mm concrete slab, a 230 mm thick insulation layer underneath the slab and a 125 mm thick insulation layer surrounding the basement walls. According to Eqs. 2.3-2.7, to determine the thermal properties of the soil, the thermal properties of each of its constituents are required. Based on the results obtained from laboratory experiments (Table 2.1), the properties of soil constituents that are used in the simulation were obtained (Table 2.3). The thermal properties of concrete and insulating material are also required to conduct the thermal analysis of the model. As mentioned before, the thermal properties of concrete and insulation layers assumed to be constant and equal to the values shown in Table.2.3.

Constituent	Thermal conductivity [W/m°C]	Heat Capacity [J/kg°C]	Density [kg/m^3]
Soil Skeleton	1.58	942	2560
Water	0.56	4188	1000
Ice	2.2	2117	950
Concrete	1.8	880	2300
Insulation	0.041	1450	34

Tab. 2.3: Thermal properties of the model materials.

2.4 Results and Discussion

2.4.1 Energy Loss Through the Below-Grade Enclosure under Different Scenarios

Table 2.4 shows the results of the thermal analysis for the base case (i.e., Scenario 1) by using approaches 1 and 2. It can be seen that analyzing the model within approach 2, 34% more energy loss has been resulted compared to the model that was analyzed within approach 1. The reason is the fact that occurrence of phase change in the soil's pore water significantly

affects the energy loss through the basement structure. In other words, as the pore water starts freezing, the thermal conductivity of the ground increases. Consequently, a larger magnitude of heat will be transferred into the ground through the basement wall and floor slab.

According to the results for the second approach, the energy loss through the basement floor and walls, respectively, consist of almost 35% and 65% of the total annual energy loss through the below-grade envelope of the SPEB. This emphasizes the importance of a promising insulation for the walls.

Results of the first Scenario (base case) is compared with Scenario 2 in which heat loss of the insulated basement enclosure of the SPEB is studied. According to Table 2.4, the energy loss of the insulated basement of SPEB consist of almost 43% and 57% of the total annual energy loss through the floor and the walls, respectively. Comparing the results of the Scenario 1 and 2 that are obtained from analyzing the model within approach 1, insulation of the below-grade envelope of the building caused 51% increase in the overall energy efficiency of the basement. Such energy efficiency enhancement increases to 60% once phase change occurs in the soil domain of the model (approach 2).

Energy loss	Approach 1	Approach 2
Walls (Scenario 1) [MWh]	48.229	51.167
Floor (Scenario 1) [MWh]	19.861	26.687
Total (Scenario 1) [MWh]	57.990	77.854
Walls (Scenario 2) [MWh]	17.628	18.448
Floor (Scenario 2) [MWh]	10.429	12.065
Total (Scenario 2) [MWh]	28.057	30.514

Tab. 2.4: Annual energy loss through the below-grade enclosure of SPEB - Scenario 1 and Scenario 2.

As mentioned earlier, Winnipeg experiences cold and long winters which significantly affects the thermal profile of the ground especially at shallower depths. The temperature of the soil

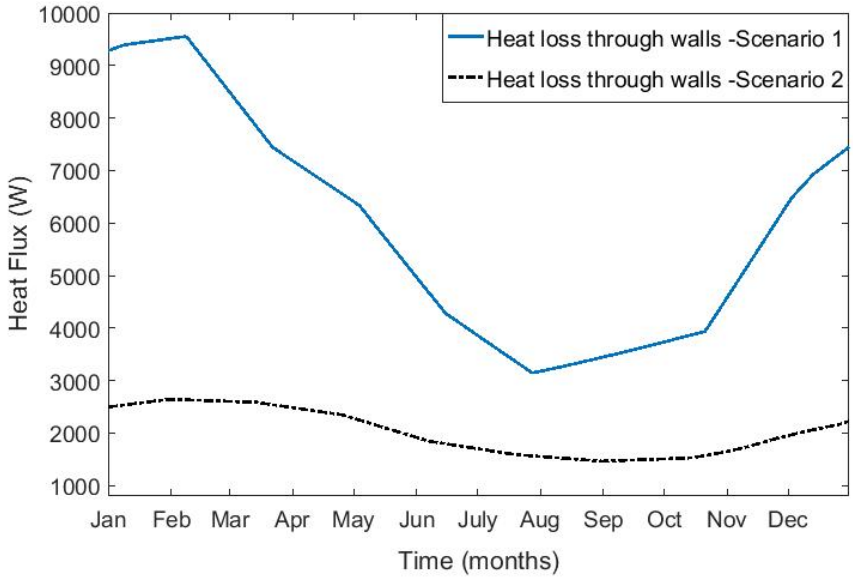

Fig. 2.10: Heat flux through the basement walls of the SPEB simulated within Scenario 1 and Scenario 2 using approach 1.

surrounding the basement wall is a function of the outdoor air temperature that drops below 0°C during the cold seasons. This causes a higher temperature gradient between the indoor air of the basement and the soil surrounding the basement walls. As such, it can be observed in Fig. 2.10 that the heat flux through the walls is higher during the cold months (January–April) compared to the warmer months (May–Dec). However, as the ambient air temperature increases during summer, the soil temperature increases as well (Fig. 2.11) which contributes to lower temperature gradient with the indoor air temperature of the building. Therefore, it can be seen that during the second half of the year, the heat flux through the walls decreased noticeably.

Fig. 2.12 shows that the seasonal temperature variations of the soil are less sensitive to the ambient air temperature at deeper depths in comparison to shallower levels. Therefore, it can be expected that the heat flux through the basement floor, which is located at 4.2 m below the

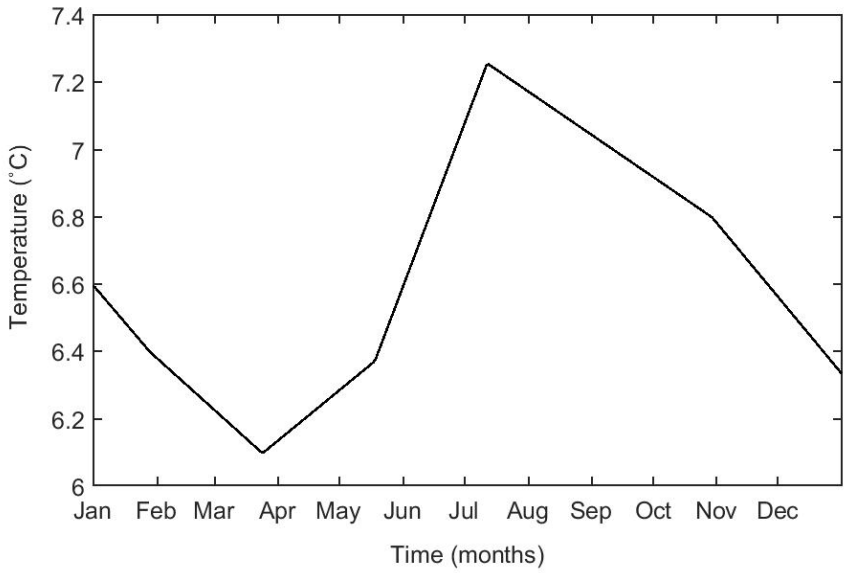

Fig. 2.11: Average temperature variation of the soil surrounding the SPEB over a year.

Case study	Energy loss through the walls [MWh]		Energy loss through the floor [MWh]	
	Approach 1	Approach 2	Approach 1	Approach 2
Scenario 1	48.229	51.167	19.861	26.687
Scenario 2	17.628	18.448	10.429	12.065

Tab. 2.5: Summary of the energy loss obtained using different approaches and scenarios.

ground surface, follows a steadier trend than heat flux through the walls over a year. In this regard, Fig. 2.13 illustrates the heat loss through the floor slab for two different scenarios. In the first case, the concrete slab is in direct contact with the soil (i.e., Scenario 1) and in the second case, the concrete slab overlays a 230 mm insulation layer (i.e., Scenario 2).

Comparing the results obtained from Scenario 1 and Scenario 2 within approach 2 (Table 2.5), a 125 mm thick layer of insulation surrounding the basement walls decreased the annual building energy loss through the walls by 64%. The buildings heat loss through the basement floor slab also declined by 55% using a 230 mm thick layer of extruded polyester underneath the concrete

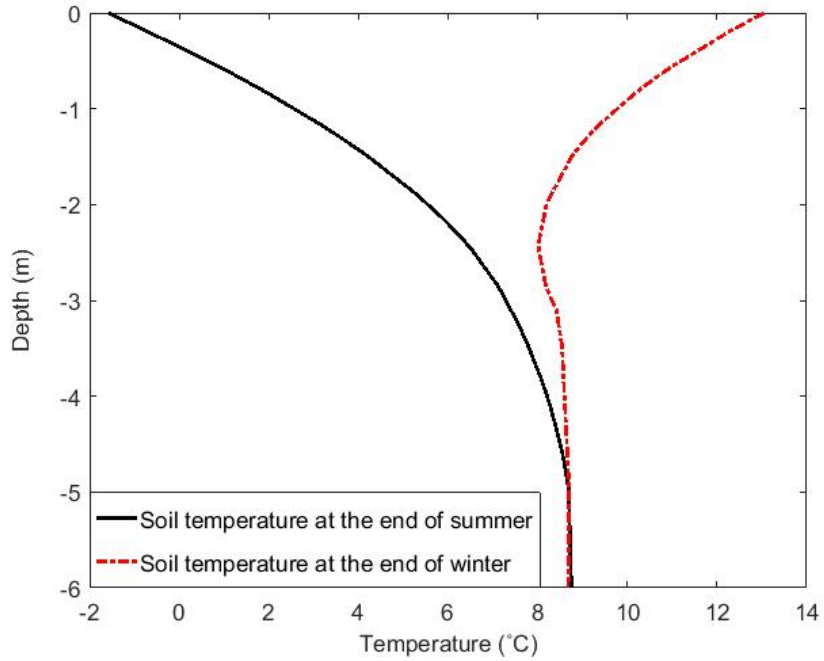

Fig. 2.12: Temperature variation of the soil surrounding the SPEB with depth.

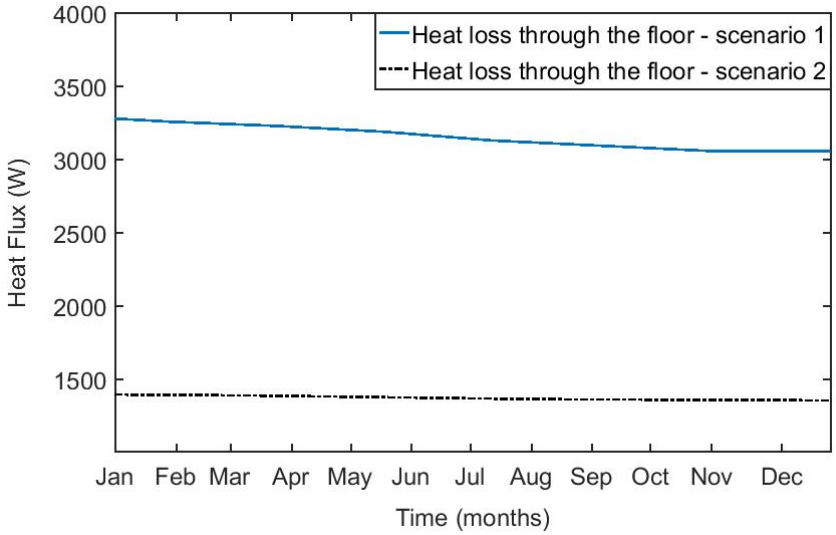

Fig. 2.13: Monthly heat flux through the SPEB basement's floor simulated within Scenario 1 and Scenario 2.

slab which clearly shows the necessity of a promising insulation for the below-grade envelope of the building in a cold region such as Winnipeg.

2.4.2 Mitigation Strategies for Alleviating the Energy Performance of the Below-Grade Envelope

Additional Horizontal Insulation Layer

Fig.2.14 presents the temperature profile of the soil adjacent to one of the external walls of the basement. Comparing the temperature profiles provided in Fig.2.14a and Fig.2.14b, the horizontal insulation layer efficiently lessens the impact of the seasonal temperature variation on the ground temperature which further improves the building's energy loss through the basement walls.

Based on the magnitude of the energy leakage obtained from Scenarios 2 and 3 (Table 2.6 and Fig. 2.15), the annual energy loss through the basement walls decreased by almost 23% using an additional horizontal insulation layer (Scenario 3) comparing the heat loss through the walls obtained from Scenario 2. However, according to Table 2.6, the changes in the annual energy loss through the floor were negligible since the main purpose of the additional insulation layer is decreasing the impacts of air temperature drop on the ground during winter months. However, soils at shallower levels are more susceptible to freezing and seasonal temperature decrease. therefore, the major impact of the horizontal insulation layer is posed to the heat loss through the wall (Table 2.6).

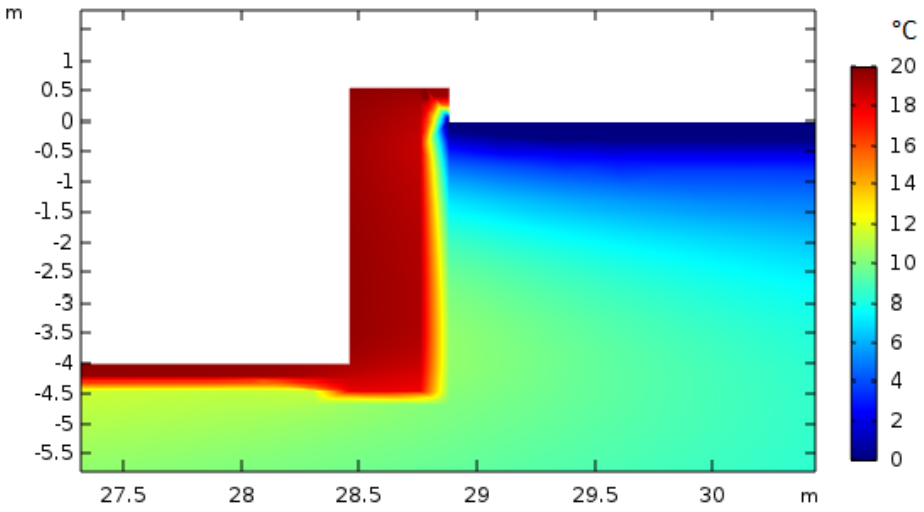

(a) Temperature profile of the basement enclosure after 8760 h - Scenario 2.

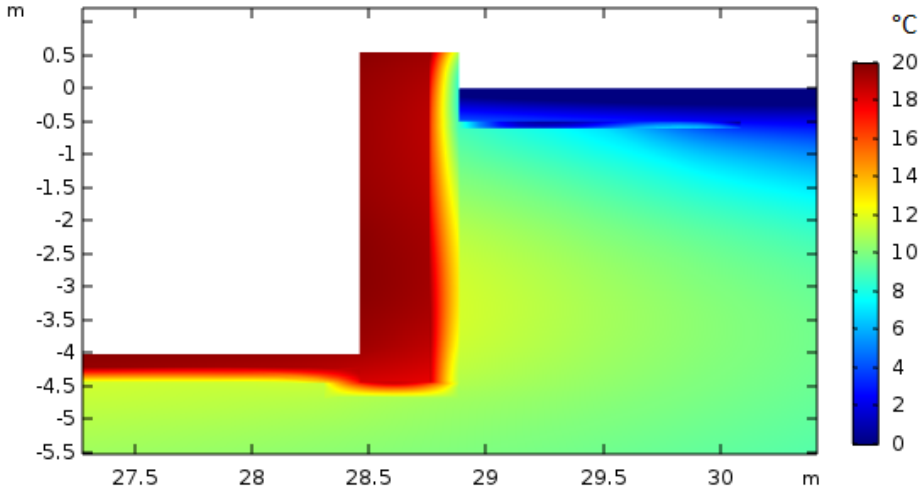

(b) Temperature profile of the basement enclosure after 8760 h - Scenario 3.

Fig. 2.14: Temperature variation contours of a cut-plane of the geometry of the model representing the effect of the additional horizontal insulation layer on temperature profile.

Case study	Energy loss through the walls [MWh]	Energy loss through the floor [MWh]	Total [MWh]
Scenario 2	18.448	12.065	30.514
Scenario 3	13.031	12.045	25.076

Tab. 2.6: Comparison of the results of scenario 2 and scenario 3 of the thermal analysis of the SPEB's below-grade envelope.

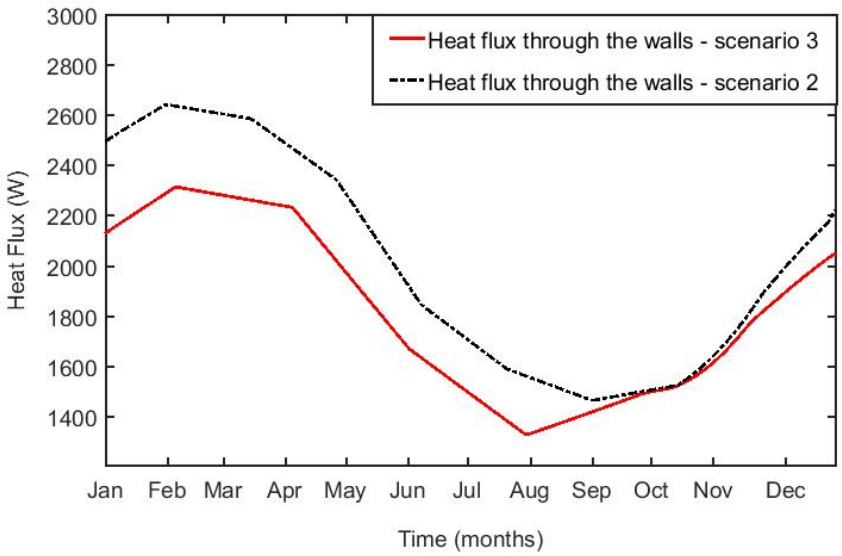

Fig. 2.15: Comparison between the heat flux through the SPEB basement's walls simulated within Scenario 2 and Scenario 3.

Impact of U-value on the Energy Loss through the Walls

Heat transfer through the walls can be estimated using the following equation:

$$q = U\ (T_s - T_{in}) \tag{2.10}$$

where, q is the heat flux through the walls (W), U denotes the heat transfer coefficient of the wall, T_s represents the ambient soil temperature [°C] and T_{in} is the indoor air temperature of the basement [°C].

Based on Eq. 2.10, heat flux through the walls is highly dependent on the thermal property of the insulating material (U-value) as well as the thickness of the insulation layer surrounding the walls. In fact, the variation of the two mentioned parameters impact the heat exchange rate through the walls by changing the walls thermal resistance (R_{wall}). Thus, in this section, the sensitivity of the basement's heat loss through the walls to the thickness of the insulation layer which further changes the U-value ($U = 1/R_{wall}$) is estimated. To this end, the thickness of the insulation layer surrounding the basement structure has been changed from 125 mm to 150 mm with 5 mm steps and the corresponding U-value is calculated. Fig. 2.16 shows the variation of the energy loss through the walls with U-value. Results signify that walls U-value is inversely correlated with the heat flux. In other words, changing the U-value of the wall by 15% can decrease the energy loss by 26% comparing to the results obtained from Scenario 2, which contains the original design of the walls insulation. Therefore, if the application of a thicker layer of insulation is justified from the structural point of view, it can be proposed as a solution for alleviating the building's energy loss through the below-grade envelope.

2.4.3 Comparison of the 2-D and 3-D Analyses

In this section, the 3-D analysis whose results have been presented in section 2.4.1 and section 2.4.2 are compared with the results of the equivalent 2-D numerical analysis whose general geometry and mesh set up have been explained in section 2.3.3.

To make sure that initial temperature imposed on the soil domain has the least impacts on the results, the 2-D analysis has been conducted over a period of eleven years although only the results of the last year have been presented in detail. Table 2.7 summarizes the estimated annual energy loss through the basement of the SPEB using the 2-D and 3-D analyses.

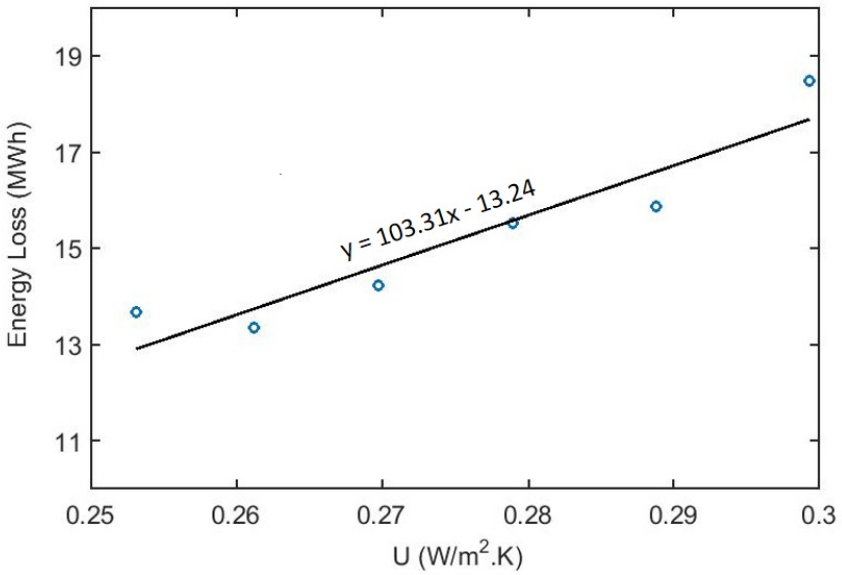

Fig. 2.16: Variation of the energy loss through the basement's walls with U-value of the wall (R^2 = 0.884).

Total energy loss [MWh]	2-D analysis	3-D analysis
Scenario 1	94.637	77.854
Scenario 2	35.425	29.693
Scenario 3	27.305	25.076
Scenario 4	33.295	27.475

Tab. 2.7: Comparison of the results obtained from the 2-D and 3-D analyses of thermal performance of the SPEB's below-grade envelope.

According to Table 2.7, a discrepancy can be observed between the results of the 2-D and 3-D models regarding the building's energy loss. The annual energy loss estimated using the 2-D analysis is 8%–18% higher than the results of the 3-D study within Scenarios 1–4. This is speculated to happen due to three main reasons as listed below:

- In the 2-D analysis, the axisymmetric boundary condition has been applied at the centerline of the soil domain. However, as shown in Fig.2.1 the basement's plan is not fully

symmetric. Consequently, the basement floor area and the corresponding heat loss cannot be estimated accurately.

- The 2-D analysis implicitly yields a plain strain condition to the model. However, the building's geometry spreads over a specific area in each direction which contradicts with plain strain condition.

- Based on the literature [72, 73, 71, 79], the energy loss through the building basement can be estimated by three-dimensional model more accurately rather than the two-dimensional analysis. The reason is speculated to be the accurate modeling of the basement corners where most of the heat loss through slab and walls occurs due to the thermal bridge.

Given the above-mentioned reasons, authors believe that three-dimensional study can better estimate the building's heat loss. However, in case of mathematical complexities of 3-D analysis, 2-D simulations can be applied while potential overestimation is taken into account.

2.4.4 Cost Analysis

In this section, the economical aspect of thermal performance of the SPEB below-grade enclosure is assessed. To encourage the application of a more efficient thermal insulation design in any project, visualizing the savings made in the budget is one of the most convincing approaches. Therefore, a cost analysis has been done using the commercial rates provided by Manitoba Hydro [102]. Results regarding the heat loss rates have been summarized in Fig. 5.2.

Based on the 2D analysis results, the uninsulated basement has a significant heat loss (10,145$ annually) which is almost three times higher than the case in which the below-grade enclosure

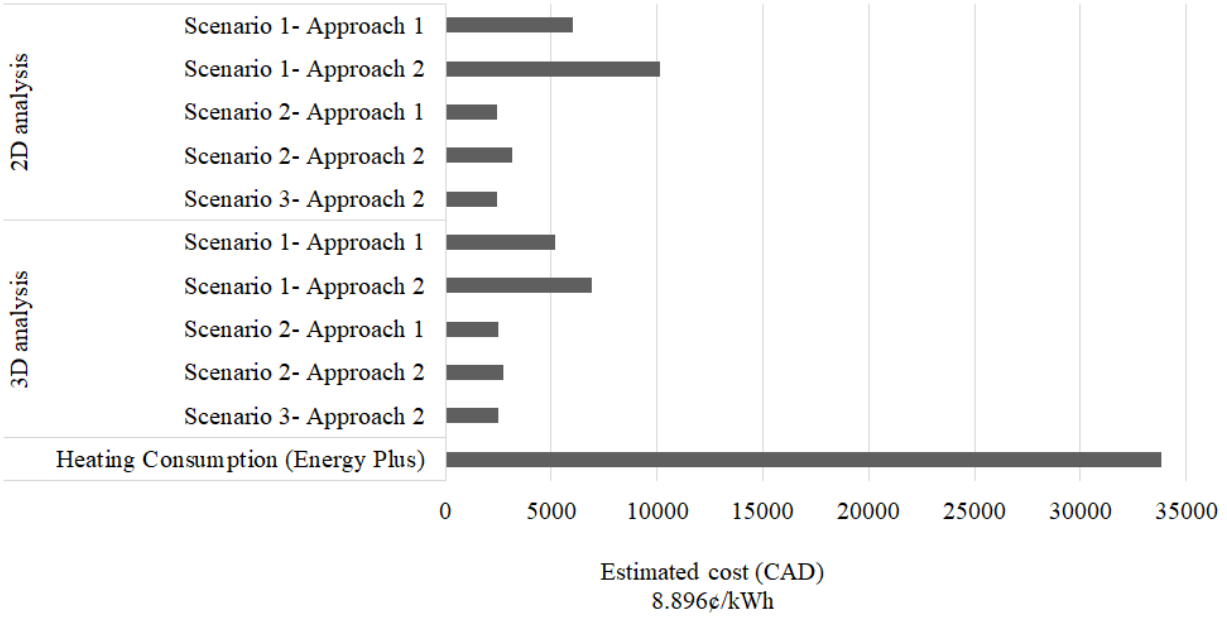

Fig. 2.17: Estimated cost of the energy loss through the SPEB below-grade enclosure using different analyses.

is insulated using extruded polystyrene. Although comparing to 2D analysis, the recorded heat loss from the uninsulated basement and the corresponding budget waste is 30% lower for the 3D analysis (i.e. 6,990$ annually for the uninsulated basement).

The annual energy consumption of the SPEB required for heating has been estimated to be 380 MWh [68] which costs 33,804$ each year. However, depending on the estimation method (i.e. 2D or 3D analysis within Approach 1 or 2), 20–30% of this budget is wasted through heat leakage from the basement if no insulation is applied on the walls and slab of the basement. Even in case of insulating the building according to the SPEB design, 8.2–9.3 % of the total energy consumption of the building in terms of heating leaks to the ground yet. Such great heat dissipation to the ground contributes to significant amount of budget loss. This necessi-

tates application of the provided mitigation methods such as additional insulation all around perimeter of the building.

2.5 Conclusion

The energy performance of the below-grade envelope of the SPEB located in the Fort-Garry campus of the University of Manitoba, Winnipeg, Canada has been investigated in this study.

During the first stage of the simulation, the annual energy loss of the building through the basement is estimated within the above-mentioned approaches for a Scenario in which the below-grade enclosure is not insulated. In the second scenario the annual energy loss of the basement through the walls and the floor slab is estimated when an insulation is applied. After estimation of the annual energy dissipation from the building to the ground within Scenario 2, authors provided the potential solutions for decreasing the heat leakage from the basement to the ground. Based on the results, the following conclusions can be drawn:

- Minimizing the thermal gradient between the interior and exterior surfaces of the basement walls was proved to be one of the approaches for mitigating the energy loss through the basement.

- the 2-D analysis overestimated the energy leakage from the basement compared to the 3-D analysis due to less accurate modeling of the basement corners where most of the heat loss through slab and walls happens due to the thermal bridge. In addition, the axisymmetric boundary condition and plain strain condition of the 2-D model causes overestimation of the annual energy loss through the sub-grade envelope.

3

Thermal Imbalance Due to Application of Geothermal Energy Piles and Mitigation Strategies for Sustainable Development in Cold Regions: A Review [1]

Abstract

Due to population growth and increasing energy demand all over the world, geothermal energy, which can be extracted from both deep and shallow geothermal resources, has been widely applied recently. In the current paper, the application of shallow geothermal energy by means of ground source heat pump (GSHP) system as well as different elements of this system are widely investigated. Furthermore, geothermal energy piles, one of the most popular ground heat exchangers (GHEs) which serves two purposes of supporting the building and providing heat to the building, has been reviewed. Thermal imbalance, which is encountered while using geothermal energy, is discussed and its potential solutions are reviewed. These solutions

[1] **Saaly M.,** Maghoul P., 2019. Thermal Imbalance Due to Application of Geothermal Energy Piles and Mitigation Strategies for Sustainable Development in Cold Regions: A Review, *Innovative Infrastructure Solutions*, 4: 39. DOI: 10.1007/s41062-019-0224-1.

are devided into two major categories of GHE modification and application of auxilary heating/cooling units. If feasibility of these solutions be justified, they can effectively reduce the underground thermal imbalance.

3.1 Introduction

The application of renewable energy resources has been extensively developed all over the world in recent years. The main reason for such investment is to mitigate the adverse effects of climate change and CO2 emission due to the application of fossil fuels for supplying the increasing energy demand. One of the promising renewable energy resources in response to this increasing energy demand is the geothermal energy [90]. Geothermal energy relies on the fact that the ground temperature at a certain depth is not affected by the seasonal temperature changes and is warmer and cooler than the outdoor air in winter and summer, respectively. Therefore, the ground can be treated as an energy source and heat can be extracted from the ground in winter and rejected to it in summer. This technology has been broadly used in different places such as Europe, Australia, China and the USA [164].

The geothermal energy can be divided into shallow and deep categories according to the depths of heat extraction. The depth of heat extraction depends on the temperature of the geothermal resource. For example, deep geothermal energy can be extracted from high temperature reservoir (T higher than 150°C), intermediate geothermal resource (90°C ≤ T ≤ 150°C) or low temperature reservoir (25°C ≤ T ≤ 90°C) [36]. However, shallow geothermal energy is usually harvested from the depths of the ground having a temperature less than the low temperature resource. Also, the thermodynamic function of the shallow ground source is not like a resource but only a source since the ground experiences both processes of heating (during summers)

and cooling (during winters) [36]. To extract deep geothermal energy, aquifers at depths more than 400 m and temperature more than 20°C are only considered as deep geothermal energy resources.

The production of deep geothermal energy can be operated by means of hydrothermal and/or petrothermal systems. The hydrothermal system exploits hot water of deep aquifers by means of a production well to pump the hot water to the surface and a reinjection well for water disposal. It is worth mentioning that minerals and other contaminants existing in aquifers may adversely affect the geothermal system therefore there might be a need for filtration equipment or secondary heat exchanger. Unlike the hydrothermal system, the petrothermal system uses the thermal energy stored in deep rocks [3]. Thus, utilizing the deep geothermal energy needs a great investigation into geological conditions of deep subsurface.

Unlike deep geothermal energy, shallow geothermal energy needs a heat pump to raise the temperature since its energy output is not high enough to be used directly.

As such, this paper aims to investigate thoroughly the application of shallow geothermal energy using ground source heat pump system (GSHPs). Due to the high capital cost of drilling trenches for the harvest of geothermal energy, geothermal energy piles that serve two purposes of supporting the building as well as operating as geo-heat exchangers of the GSHP system gained popularity in recent years.

Although GSHPs and more specifically application of geothermal energy pile is one of the fastest growing application of renewable energy all over the world, there are some impediments for broad application of them especially in cold regions having long and cold winters. One of the common problems, underground thermal imbalance, which is caused by the unbalanced

extraction/injection of heat from/to the ground is addressed in this paper. As the energy harvest from the ground exceeds the heat injection over the operation time of the GSHPs, subsurface temperature decreases gradually which further leads to failure of GSHPs. As such, some strategies applied to mitigate the occurrence of thermal imbalance are investigated. The structure of this paper is as follows. First, the tools and the system by which geothermal energy can be extracted are introduced. Then, the underground thermal imbalance and the potential reasons for its occurrence are presented. Finally, the mitigation methods and the systems that were applied for meeting the thermal balance of the ground are proposed.

3.2 Geothermal Heat Pump Systems (GHPS)

Heat pumps, in general, are intended for reversing the natural flow of water from cold to hot by consuming the electrical energy. GSHP systems extract heat from the ground, ground water or less commonly ponds and shallow aquifers. In fact, shallow ground, ground water and surface water whose temperature a few feet below the surface does not fluctuate significantly over a day or a year can be used as a reservoir for extracting energy by means of geothermal heat pump systems (GSHP). They are applicable for a wide range of buildings and are commonly installed using shallow trenches and boreholes [116]. GSHP system's functionality is based on circulating a fluid between the heat pump and heat exchange elements in the ground by which warmer ground gives energy to the cooler fluid. Although GSHP works the best with a heating system, they can be applied as a cooling system in summer in which heat is taken from the building and is delivered to the ground. The required energy for the operation of GSHP is provided by electricity power and is less than the primary energy that conventional heating systems need. Depending on the system and climatic and geological conditions, this energy is three or more than three times less than the thermal energy that GSHP provides [160, 123]. Although the

GSHP system is a very economical approach for providing energy, its capital cost, including trenching cost, is significantly high. Therefore, the capacity of a GSHP system, which directly depends on the energy demand of the building, should be well assessed before its construction.

3.2.1 GSHP Components

A GSHP system is composed of three components: 1) ground heat exchanger 2) heat pump and 3) heat distribution system [116].

The performance of a GSHP system depends not only on its components but also many other factors such as heat transfer fluid, heat transfer fluid flow rate and the soil type. The ground heat exchanger can be an open-loop or a closed-loop system and its selection depends on different parameters affecting the feasibility of the project [160]. For example, in application of an open-loop system, the quality of available groundwater is important since direct contact of water and the refrigerant may cause fouling and corrosion of the heat exchanger. The interest toward application of the open-loop systems as the ground heat exchanger is growing due to its simple design and better thermodynamic performance than closed-loop systems since trenches transfer the groundwater at the ground temperature directly rather than as a heat exchanger which transfers fluid having a temperature other than temperature of the ground. Also, if the open-loop system can be used also for other purposes such as supplying the potable water, it can be economically beneficial.

Although the installation of an open-loop system is readily possible where groundwater is abundant, the environmental regulations have restricted the application of open-loop systems since the underground water temperature would be manipulated when the system is working. Therefore, the ground heat exchanger is usually a closed-loop system which can be a vertical

borehole or straight or spiral horizontal pipes. In all these cases, the heat exchanger system consists of a set of pipes buried in the ground which is filled with water or mixture of water and an antifreeze liquid as the heat carrier fluid [160].

Closed-loop systems can be installed either horizontally (straightly horizontal or spirally horizontal) or vertically depending on the feasibility of the project. In both configurations, the heat exchanger fluid circulates along the loop and exchanges heat with the ground. The utilization of the antifreeze component in the heat carrier fluid depends on the mean temperature of the heat pump that, on average, should be 5°C above the freezing point of the heat carrier fluid. It is worth noting that in horizontal closed loop systems, the application of antifreeze in heat carrier fluid increases the viscosity which increases the pumping energy and therefore reduces the overall efficiency of the heat pump [123].

In horizontal closed-loop systems, the installation process comprises of removing the top 0.9 to 3 m of the ground, depending on the frost depth in the ground in cold regions, installing the horizontal loop in series or parallel and then filling the excavated area with the soil. In this type of closed-loop systems, the temperature extracted from the soil is mainly recharged by solar energy. Therefore, unlike vertical closed-loops, the temperature of the covering soil is sensitive to seasonal temperature variations at shallow depths due to the installation of the horizontal loops in relatively shallow trenches. Although the trenching costs for the application of horizontal loops are significantly lower than trenching boreholes for installing a vertical loop, in cases with less land available horizontal loops are not the best option. Aside from larger available areas, horizontal loops need longer pipe length than vertical loops which increases the capital cost of that.

Unlike horizontal loops, vertical loops are specifically recommended for buildings with high energy demand and less available land. Also, in the case of presence of hard rocks near the soil surface, the application of horizontal loops may not be feasible. Boreholes excavated for the installation of vertical loops are between 15 m to 120 m length which is more than the neutral zone, the depth in which the thermal profile of the ground remains constant [160, 123]. These boreholes are then equipped with polyethylene pipes (U-tube, pipe-in-pipe and concentric tube) whose diameter varies based on soil condition and temperature and the surrounding room in the borehole is then filled. Aside from the high trenching cost of the vertical closed-loop, they need the least pumping energy and the least surface land. As such, decreasing the trenching costs of the vertical loops initiated the idea of merging the GHE with the structural elements of the buildings. In this regard, geothermal energy foundations are proposed to structurally support the building as well as exchanging heat between the ground and the heat exchanger fluid. In the next section, buildings' pile foundations equipped with U-shape pipes, geothermal energy piles, will be discussed thoroughly.

3.3 Application of Geothermal Energy Piles

Geothermal energy piles are new systems that harvest shallow geothermal energy underneath the building. The most significant feature of this system is the application of structural elements as a heat exchnager element to provide energy to the building. As mentioned before, the capital cost of GSHP systems is significantly high due to the cost of boreholes excavation and installation process. However, the application of geothermal energy piles would decrease the capital cost of GSHP since for achieving two objectives (building foundation and heat exchanger), only one drilling cost needs to be paid. In fact, the added costs of applying geothermal pipe loops to the pile that structurally support the building is significantly small compared to the installation

cost of vertical closed loop geothermal systems separately [24, 51]. The heat exchange system is based on injecting and harvesting geothermal energy stored in the ground to/ from the building via heat carrier fluid circulating through the pipes embedded in the geothermal piles. The materials that have ever been used in construction of geothermal energy piles could be precast or cast-in-place reinforced concrete and steel [39]. However, the most common material used in construction of geothermal energy piles is concrete due to its high thermal storage capacity and high thermal conductivity [58]. The heat exchanger pipes, which are usually made of high density polyethylene, are then installed by being fixed to the reinforcement cage of the reinforced concrete pile. Pipe configuration inside the geothermal energy pile, which can be either single, double or triple U-shaped pipes, W-shaped pipes or spiral, is significantly important since it affects the efficiency of the geothermal pile. Based on the literature [93, 58, 57, 59, 128], as the length of the pipe increases, the overall heat exchange will increase as well. In other words, spiral and W-shaped pipe configuration have higher efficiency than U-shaped pipe under absolute same flow rate although their installation cost is relatively higher than U-shaped pipe.

3.3.1 Mechanical Behavior of Geothermal Energy Piles

Aside from the feasibility of energy piles from cost-efficiency and environmental point of views, their geotechnical aspect needs to be studied as well.

The thermo-mechanical behavior of geothermal energy piles which are subjected to both structural loading and heating/cooling cycles (thermal loading) is of the greatest importance during the service life of such piles. In fact, heating and cooling cycles may change the behavior

of soil-pile interaction contributing to additional building settlement or additional tensile stresses in the pile.

Geothermal piles can be designed for both extracting and rejecting heat from/into the ground. In cold regions, the geothermal energy is commonly applied for providing heat to the residential and constitutional building. Therefore, special care should be taken while using geothermal piles in regions with harsh winters to prevent the soil-pile interface from freezing and its following problematic issues by constant monitoring the thermal system. Similarly , such systems in warm region such as Australia, Southern China and some parts of USA may also need an accurate monitoring system and considerations during their design process. In fact, in these regions, the annual cooling demand of residential and institutional buildings is much higher than their heating demand. According to the literature [155, 77], soil temperature in warm regions where the ground is treated as a heat sink increases which further leads to volumetric strains in the soil that contributes to pile heave or settlement. This would further affects the serviceability of the geothermal pile which necessitates additional considerations in the design of such systems [115].

Three of the most important studies investigating the geotechnical behavior of geothermal piles through in-situ tests have been done in London (UK), Lausanne (Switzerland), and Bad Schallerbach (Austria).

The London case situated in the Clapham Centre of Lambeth College in South London where Amis et al. [7] and Bourne-Webb et al. [20] conducted the in-situ tests on a test pile and a heat sink pile over a 53-day span. To assess the effects of thermal cycles on mechanical behavior of the pile under compressive loading, the temperature and strain profiles of the pile were monitored. It should be noted that the tested piles experienced very extreme temperatures in

thermal cycles (maximum cooling -6 and maximum heating +40) which is above the normal range of heat pumps [7]. It was reported that the thermal cycles posed no serious detrimental impact on the behavior of the geothermal energy pile since the results signified that after the cooling cycle, the pile settlement that increased by 2 mm was almost fully recovered during the heating cycle. However, the results of this study cannot be generalized to other geothermal piles because the applied thermal cycles in these in-situ tests were shorter in period and extremer in temperature than the actual cycles implemented on real application of geothermal piles.

In another work situated in École Polytechnique Fédérale de Lausanne (EPFL), one of the 97 piles of a four storey building having bi-functional role has been studied. This pile was equipped with a U-shape pipe for exchanging heat by means of a heat carrier fluid. In order to investigate the effects of thermo-mechanical loading on the pile, it was subjected to mechanical loads caused by the dead weight of the building and thermal loads applied at the end of construction of each storey. The thermal loads consisted of thermal cycles each lasted 28 days [82, 81]. Results signifies that while a geothermal pile is subjected to thermal cycles, the direction of strain due to the thermal load and the mechanical load is upward and downward, respectively. Therefore, the friction resistance is not affected and a relief of side friction mobilization can be seen which affects the capacity of the pile.

Through another in-situ study located in Bad Schallerbach, Austria, a geothermal pile which is a part of an operational GSHP system was installed and tested. This study evaluated the response of the pile in both conditions with or without mechanical loadings. According to Brandl [22], when the pile is in a heating cycle and is not subjected to a mechanical load, it will expand freely. While a pile is embedded in the ground, the friction between the pile and the ground does not let the pile expand freely. Therefore, the measured strain change is less

than the free strain change. The difference between the free strain and the measured strain change generates thermal stress into the pile and should be considered in the structural design. According to the results, the thermally-induced axial stress emerged in the pile highly relies on the end restrained of the pile which is influenced by many factors such as the quality of the soil layer at the pile toe or the loading at the pile head. Therefore, according to Murphy et al. [111], it relies on the geological conditions and the depth of bedrock of the location where the pile is embedded. However, Bourne-Webb et al. [20] suggested that the effects of thermal stress should be carefully considered since in some cases that stress of the pile is close to the structural limit imposed by codes, it may contribute to detrimental effects [6].

One of the factors which affects the accuracy of the above explained in-situ tests is the time interval in which the experiments have been conducted. Although Bad Schallerbach test had been done in a year interval, both London and Lausanne in-situ tests had been done over fairly short time intervals which may affect the test results. Therefore, special care should be taken while using the results of the aforementioned studies.

In addition to the in-situ experiments conducted in Europe, Murphy et al. [111] and Akrouch et al. [4] investigated into foundations of a new building at US air force academy and NGES at Texas A&M University, Riverside campus, respectively. NGES has two sites one of which is mainly consist of clay and is subjected to the in-situ tests conducted in the above-mentioned study. In fact, the main purpose of the mentioned study was to evaluate the thermo-mechanical behavior of energy piles in clay soils. In this regard, a group of eight piles, having a length of 5.5 m and a diameter of 0.18 m, embedded in the NGES clay site were studied. Two of these piles were geothermal piles and six other ones were used to assess the pile behavior under mechanical loadings. The piles were instrumented with six thermocouples in order to monitor

the temperature changes in the piles. In this study, the Thermal Response Tests (TRTs) were applied to determine the thermal properties of the subsurface and the geothermal pile system. The instruction of these tests is as follows:

- Circulate water through the heat exchanger pile and supply a constant amount of power to it.
- Control the temperature of the fluid while entering and exiting the pile foundation.
- By the following equation calculate the input heat flux in Watts:

$$Q = \Delta T_{fluid}\, \dot{V}\, \rho_{fluid}\, C_{fluid} \tag{3.1}$$

  where, ΔT_{fluid} is the difference between the entering and exiting temperature of the heat carrier fluid, $\dot{V}$ is the fluid flow rate (m^3/s), ρ_{fluid} is the density of the fluid (kg/m^3), C_{fluid} is the specific heat capacity of the fluid ($J/(kg.K)$).

- Divide the heat flux value by the cross sectional area of the pile so that the heat flux density can be obtained.

The aforementioned tests (TRTs) were performed at the head of the pile before construction of the building. Murphy et al. [111] applied seven test stages in order to determine the thermal response of the components of the geothermal energy piles. These stages are designed to avoid heating the pile rapidly and taking any biased results. While in the NGES study done by Akrouch et al. [4], five tension load tests were performed on the tested piles. The procedure of each test consisted of applying mechanical loads for 1 hour and then turning on the water pump and starting the circulation of water into the heat exchanger pipes for 4 hours. While the water was

circulating into the piles, its temperature increased by 10-15°C. In all stages, the axial strain and temperature of both piles and soil were monitored. According to the results, in the air force academy experiment, some of the test piles showed a uniform change in temperature with depth which is in compliance with the temperature variation with depth in Akrouch et al. [4] study. However, it is worth to be noted that the pile temperature in some cases did not vary uniformly with depth. Based on these two experiments, it is better to locate geothermal piles under the building uniformly in order to minimize the distortion caused by the deformation of such piles since the settlement of the geothermal piles is inevitable and its relative magnitude increases by time. In addition, Akrouch et al. [4] believes that minimizing the initial settlement of the piles can be one of the solutions for decreasing the magnitude of long-term displacement of the geothermal piles. In US air force academy test, the effects of end restraint boundary condition have been assessed and results represent that thermal axial stress decreases as the head stiffness of the pile becomes lower. By interpreting the staged tests, Murphy et al. [111] realized that the efficiency of a geothermal energy pile to a great extend depends on the heat transfer through the the loop. It is worth mentioning that although these two experiments were conducted on a group of piles, in none of these experiments all of the piles in the group were all geothermal piles. Therefore, generalizing the results obtained from these studies to evaluate an actual group of geothermal piles needs more investigation and considerations due to potential problems caused by improper design of geothermal energy piles. One of the common problems is the underground thermal imbalance which is caused by the unbalanced heat extraction and rejection from/into the ground by the GSHP system. In the next section, a review of the studies that have investigated this problem is presented.

3.4 Thermal Imbalance

Long-term efficient operation of GSHPs necessitates underground thermal balance, which means that the annual heat injected into the soil is equal to the annual heat extracted from the soil [148]. One of the main reasons of GSHPs failure in cold regions is the occurrence of thermal imbalance [157]. As mentioned before, the application of GSHPs in cold regions attracted attention during past few years. In these regions, heat extracted from the ground is more than heat rejected into it which contributes to a gradual decrease in soil temperature [162, 153, 100, 66]. Therefore, the outlet temperature of the ground heat exchanger will decrease gradually. Decrease in the outlet temperature of the ground heat exchanger (GHE) contributes to a decrease in efficiency of GCHP and deterioration of heating performance of the system. The aforementioned problem is more serious in projects that the GSHPs functions only for supplying heating demand of a building, where heat pump only extracts heat from the soil without rejecting heat back to the ground [144, 31].

In order to be able to quantify the level of underground thermal imbalance, the Thermal Imbalance Ratio (TIR) can be used [157, 159]. This factor is defined as follows:

$$TIR = \frac{Q_{AHR} - Q_{AEH}}{\max(Q_{AHR}, Q_{AEH})} \tag{3.2}$$

where Q_{AEH} is the accumulated extracted heat from the soil during the heating period and Q_{AHR} is the accumulated rejected heat into the soil during the cooling period. Positive values of TIR represent larger heat extracted from the soil than the heat rejected into the soil and negative TIR represents higher level of heat rejection than heat extraction into/from the soil.

Maintaining the efficiency of GSHPs during its service life necessitates TIR of zero or close to zero meaning that the underground thermal balance is met.

3.4.1 Problems Caused by Underground Thermal Imbalance

Underground thermal imbalance can be categorized into long-term and short-term. The operation of GSHPs after a few years may contribute to the variation of soil temperature. This leads to long-term underground thermal imbalance. In this regard, Li et al. [92] studied the performance of a GSHP system and ground temperature field. Two simulations have been done in this study in which GSHP operates in both double-season mode and only heating mode. Based on a 30-year time span simulation of the double-season mode, the underground thermal balance has been met since the total heat extracted and rejected from/to the ground were equal. However, if the system operates within the only heating mode for 5 years and 13 years, the underground soil temperature can drop by 6°C and 13°C which signifies the occurrence of thermal imbalance. In another study, Li et al. [91] investigated the operation of GSHP system over summer. The system operated 12h every day and over 90 days in a year to provide space cooling in summer. After the 7th summer, the temperature of the soil observed to increase by 2°C.

In order to assess the impacts of different operational strategies on the performance of GSHPs and intensity of thermal imbalance, Qian and Wang [121] applied four different scenarios for GSHPs operation as follows:

- Scenario 1: The GSHPs operates only during summer and cooling load is 50 kW.
- Scenario 2: The system functions in summer with cooling load of 50 kW and in winter with heating load of 40 kW.

- Scenario 3: The system operates in the summer with cooling load of 40 kW and in winter with heating load of 50 kW.
- Scenario 4: The GSHPs only works in winter with heating load of 50 kW.

Based on the results, the thermal loads of scenario 1 and scenario 4 contributed to heat and cold accumulation in the ground, respectively. After a 10-year interval, the ground temperature for scenario 1 increased by 21.5 °C and for scenario 4 decreased by 10.7 °C. It is worth mentioning that in case of applying scenarios 1 and 4 for a longer period to the GSHPs, changes in soil temperature would be more severe.

Based on another study, Yu et al. [161] reported a 3°C drop in the soil temperature after 10 years of continuous operation of GSHPs designed for supplying the energy demand of a building in Beijing and Chang and Kim [28] reported an increase of 1.7°C of soil temperature after 8 days of operation of GSHPs.

Liu et al. [98] conducted an investigation into the performance of GSHPs in three cities located in cold climate zone over a 10-year span of time. Based on the results, the soil temperature in two of these cities was recorded to decline year by year due to the higher heating load than cooling load. However, in one of these cities the GSHP system was more stable and showed a greater average COP. Kharseh et al. [74] and Wan et al. [139] previously asserted that such exceptions occur due to the great impacts of meteorological parameters and building envelope thermal characteristic. You et al. [157] simulated the operation of GSHP used for just heating and for both heating and cooling of a single office building in four typical cities. The temperature of the heat exchanger fluid circulating around a single U-tube while heating and cooling the building was 7°C and 40°C, respectively. Based on the results, the soil temperature

decreased significantly while the system is only-heating mode. However, the system operating within both heating and cooling modes caused an increase in soil temperature in two of the cities and a decrease in the other two ones. Like previous studies, meteorological parameters known to be the reason of such difference in the temperature variation of the soil while GSHP is working.

In some cases, the ground temperature decreases in heat extraction period and increases in heat rejection cycle. This can adversely affect the performance of the GSHP system. The mentioned phenomenon leads to short-term thermal imbalance in which soil temperature drops significantly before the end of the heat extraction period. This causes the soil at the interface with the geothermal pile temporarily freeze which leads to an increase in the bearing capacity of the concrete pile during the cold season. Once the system starts rejecting heat into the ground during spring and summer, thawing occurs that leads to drastic decrease in the bearing capacity of the pile foundation. This will drastically impact the structural integrity as well as energy integrity of such system. In this regard, Lu and Chen [99] studied an office building located in Shanghai equipped with a GSHP system. While the system is in cooling mode (heat injection to the ground), the underground soil temperature has been reported to increase by 3.5°C after 10 hours operation of the GSHP system. This contributes to lower heat transfer from the building to the soil and therefore a decrease in COP of the system. Shang et al. [129] studied soil temperature variations due to different modes of intermittent operation of a vertical GSHP system. The studied modes are as follows:

- Mode 1: 12h heat extraction using the GSHP system and 6h downtime.
- Mode 2: 12h heat extraction using the GSHP system and 8h downtime.

- Mode 3: 12h heat extraction using the GSHP system and 10h downtime.
- Mode 4: 12h heat extraction using the GSHP system and 12h downtime.

According to the results, when the heat pump starts working, COP decreases and the compressor power increases due to a constant decrease of ground thermal energy. This occurs due to an insufficient temperature recovery time of the soil which is the time required for the soil to reaches its initial condition. The difference between the initial and recovered soil temperatures was recorded to be 1.2°C for the first mode. Results signify that under modes 3 and 4, soil temperature almost fully recovered and therefore can be reported as the optimum intermittent time in which the system can operate.

Due to the great tendency toward expanding the application of GSHP systems all over the world, potential problems inhibiting the effective operation of this system need to be solved. Therefore, the existing mitigation strategies to meet the thermal balance of the ground in cold regions need to be investigated. In the following section, some solutions provided in the literature to underground thermal imbalance are thoroughly reviewed. Finally, some suggestions are proposed which pave the way for further research and efficient application of GSHP systems in cold regions.

3.5 Mitigation Strategies for Ground Thermal Imbalance Due to Application of GSHPs in Cold Regions

3.5.1 GHE Configuration Modification Approach

GHE has a great impact on the performance of GSHP. Modification of GHE configuration is considered as one of the solutions to alleviate less severe underground thermal imbalance as a result of the application of GSHP system. This approach makes no change in the system's configuration but just improves the spacing between boreholes, boreholes length, boreholes layout or in some cases improves the thermal properties of the soil. In this section, the aforementioned changes in the GHE configuration will be discussed.

The space between boreholes is an important factor in the design of GHE due to the impact of the boreholes on each other. To minimize this impact, the spacing between the trenches is required to be increased which is not feasible in many construction sites [103]. The number of boreholes is another important parameter in the overall heat supply of the ground by GSHPs which is constrained by the land available for installation of GHE [129]. Therefore, the efficiency of the GSHP system is highly dependent on the number of boreholes and the spacing between boreholes since the soil temperature recovers easier as the space between boreholes increases. In this regard, since the selection of optimum boreholes configuration necessitates considering several parameters, Jeong et al. [69] used GLHEpro, a ground loop heat exchanger design software, for designing the boreholes arrangement.

Qian and Wang [121] compared four different scenarios in which the space between boreholes assumed to be different. In scenario 1 the space between the boreholes is 5m, in scenario 2 this space changed to 1m, in scenario 3 the space between the boreholes increased to 3m and in scenario 4 the space between the boreholes is 7m.

Other conditions are the same in all scenarios. Results showed that for the GHE with 1 m spacing between boreholes, the average soil temperature increased by 46.2°C in 30 days which caused inefficient function and lower COP of the GSHP system. However, increasing the space between boreholes leaded to an increase in COP of the system which shows that increasing the space between boreholes helps the soil to recover its temperature quickly and the GSHP to function efficiently.

In another study, Dehghan et al. [41] optimized the distance between boreholes. In this regard, GHE was designed to consist of 2, 3 and 5 boreholes whose distance represented by a variable d. Then, the performance loss for critical GHE based on different values of d is determined which leads to estimate the optimum borehole spacing.

Bai and Che [11] showed that boreholes spacing has a great impact on the soil temperature and reasonable layout of boreholes can improve the efficiency of GSHP systems. It was concluded that as the borehole spacing increases, the heat flux declines less over time which favorably affects long-term efficiency of GSHP system (Fig.3.1).

It is worth mentioning that the above-mentioned studies investigated the spacing between boreholes in order to minimize the underground thermal imbalance. However, in the case of designing the space between geothermal piles instead of heat exchanger boreholes, further investigation is required so that the structural load demand of the building can be fulfilled as well.

Aside from the space between the boreholes, the configuration and layout of a group of boreholes have a great impact on the long-term underground temperature changes. This occurs due to the reason that soil temperature variation is highly dependent on soil temperature

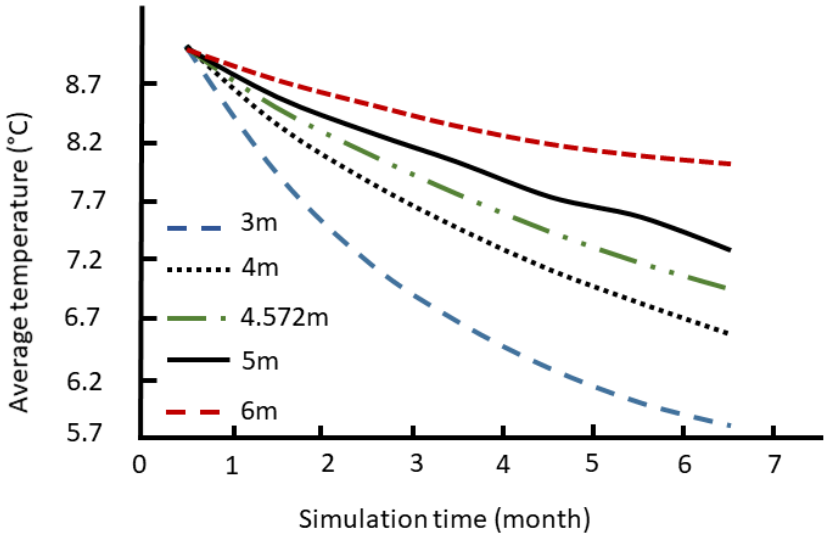

Fig. 3.1: Soil average temperature variation vs time for different borehole spacing [11]

recovery which is affected by boreholes layout. In another study Kurevija et al. [78] showed the influence of geometric array of multiple boreholes of GHE through a series of simulations based on two numerical models of "ASHRAE/Kavanaugh model" and "Lund/Eskilson model". Two borehole arrays of 2×21 and 6×7 are compared while borehole spacing also varies from 4 m to 9 m. Results showed that the borehole wall temperature and further their surrounding soil temperature for the 2×21 borehole array declines less severely over time than the 6×7 borehole array (Fig.3.2 and Fig.3.3).

In projects lacking available land, increasing the borehole length proposed as a more feasible solution for decreasing the intensity of underground thermal imbalance. As the boreholes length increases, the enlarged contact area with the surrounding soil leads to extracting heat from a greater volume of the soil and will contribute to a decrease in thermal imbalance. Gehlin et al. [60] also asserted that the interest toward deeper boreholes is growing year by year due to

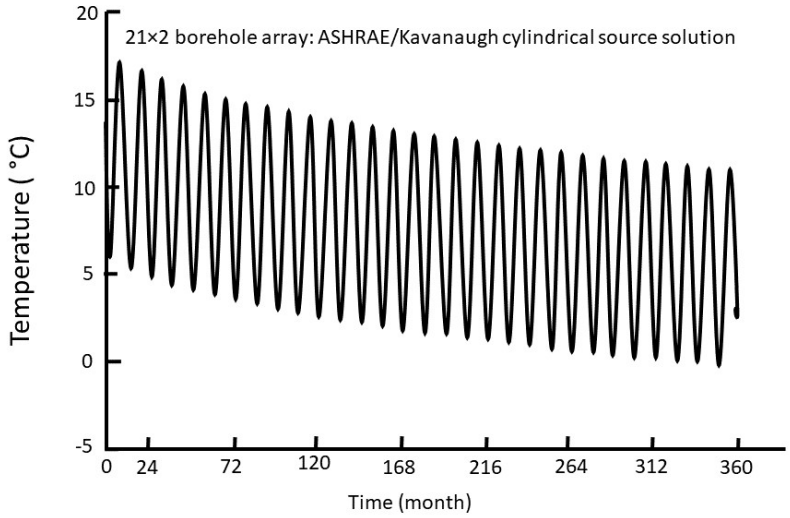

(a) Average borewall temperature for 21 × 2 borehole array

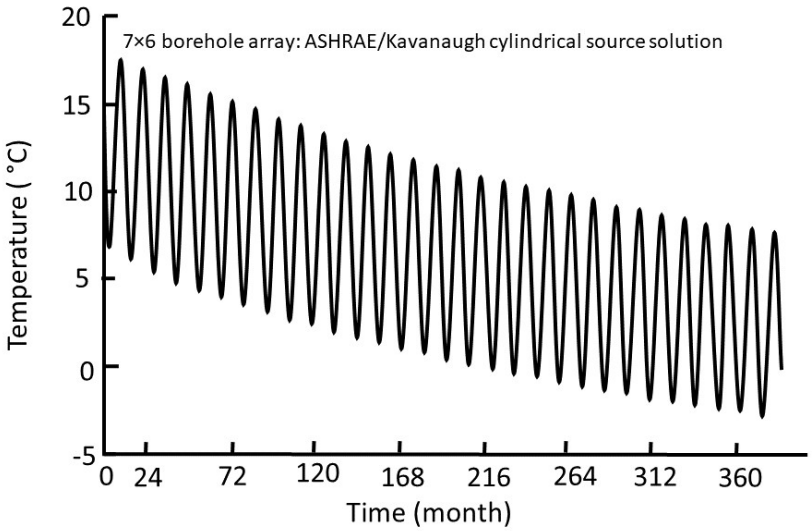

(b) Average borewall temperature for 6 × 7 borehole array

Fig. 3.2: Mean borewall temperatures over 30 year operation of GSHP system for ASHRAE/Kavanaugh solution [78]

limited available land for drilling, pre-existing boreholes on neighboring properties and deep unusual or unconsolidated soil layers.

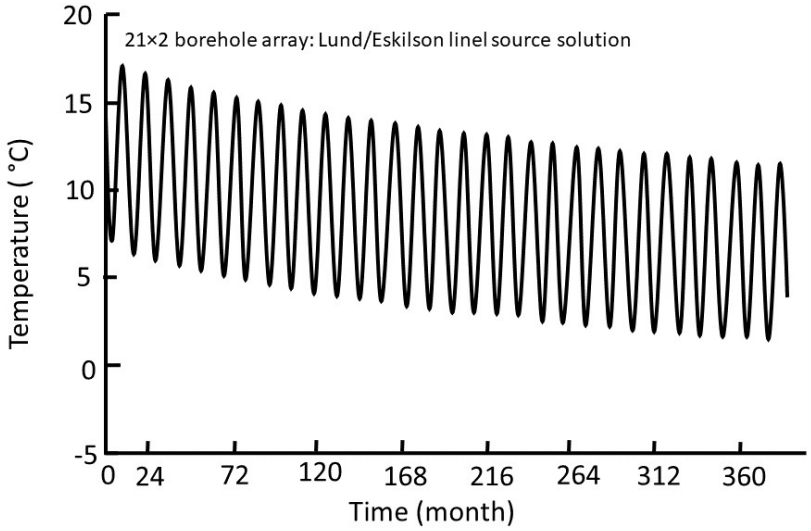

(a) Average borewall temperature for 21 × 2 borehole array

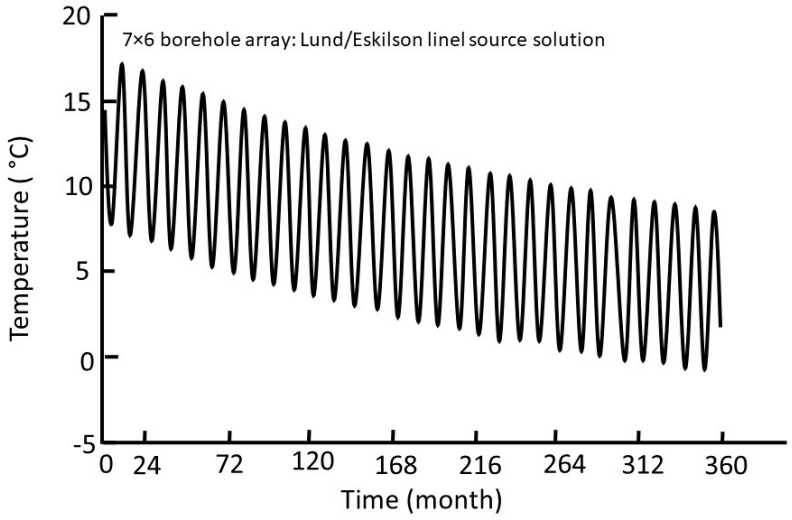

(b) Average borewall temperature for 6 × 7 borehole array

Fig. 3.3: Mean borewall temperatures over 30 year operation of GSHP system for Lund/Eskilson solution [78]

Yang et al. [147] conducted a numerical study by simulating a proposed GSHP system and changing the boreholes length while the energy demand of the system is constant. Results

showed that the efficiency of GSHP system increased as deeper boreholes were designed for exchanging heat with the ground.

The occurrence of underground thermal imbalance is mainly caused by slow heat recovery of the soil [33]. According to Shang et al. [129], a higher soil thermal conductivity leads to a faster heat transfer. If the soil temperature recovery time is insufficient, a rapid decline in the heat pump performance and soil temperature will be observed. Therefore, improving thermal properties of grout and surrounding soil, as a solution for alleviating thermal imbalance, can increase the heat exchange rate of GHE and accelerate the heat recovery time of the soil. Through a numerical study Leong et al. [88] investigated the performance of GSHP system for three types of soil having five different degrees of saturation. Results showed that decrease in the soil moisture content deteriorates the performance of GSHPs and further contributes to a more severe underground thermal imbalance and affects COP of the system.

Through another study, Yang et al. [149] observed that higher soil moisture content contributes to slower soil temperature decline as a result of heat extraction. Also, Yang et al. [149] investigated the effects of soil type on soil temperature variation and long-term underground thermal imbalance. Based on the results, it is believed that GSHP systems operate more efficiently in sandstone than sand and clay since the temperature of sandstone decreases slowly and recovers quickly that further leads to alleviating the underground thermal imbalance. It needs to be mentioned that the feasibility of any changes in the soil thermal properties and moisture content needs to be assessed thoroughly since some of these changes may affect mechanical properties of the soil and in case of using thermal piles may adversely affect their structural integrity.

3.5.2 Improving the Thermal Resistance of Heat Exchanger Boreholes

Thermal properties of the grout backfilling borehole and the heat exchange pipes directly impacts the heat exchange between the ground and the heat pump system [34, 96, 130]. In this regard, improving the thermal conductivity of the grout materiel is speculated to be one of the methods for meeting the required heat extraction/rejection from/into the ground with lower temperature change of the soil. Various numerical, empirical and analytical studies have been conducted to investigate the impact of grout thermal conductivity and heat capacity on the heat-exchange performance of borehole heat exchanger [163, 135, 34, 126, 14]. In this section, the proposed methods for improvement of grout thermal properties is aimed to be discussed.

Through an experimental study Lee et al. [84] investigated the thermal conductivity and viscosity of different mixtures of bentonite grout whose thermal conductivity was enhanced by adding silica sand and graphite. Results signified that at each 10% increase of the graphite and silica sand content, the thermal conductivity of the grout increased by 0.08–0.12 and 0.49–1.22 W/m.K, respectively. Given that, silica additive doesn't enhance the thermal conductivity of the grout significantly comparing to the same content of graphite.

In another work, Delaleux et al. [42] investigated the improvement of the thermal conductivity of the bentonite-graphite composite grout. However, the mentioned study was intended to optimize the content of graphite by usage of ground Compressed Expanded Natural Graphite (CENGg) instead of graphite flakes. Based on the results, using CENGg, thermal conductivity of 5 W/m.K can be obtained while dreducing the graphite content by 5%. In another study Tiedje and Guo [135] optimized the thermal enhancement of bentonite grout by evaluating the efficiency of different types of carbon fibers due to their high thermal conductivity and corrosion resistance. It was shown that a mixture of bentonite with carbon fibre could increase

the effective thermal conductivity of the grout up to twice as effective thermal conductivity of bentonite grout with graphite additive.

In an experimental study Lee et al. [85] showed that the effective thermal conductivity of the boreholes grouted with bentonite mixed with both graphite and silica sand additive increased up to 9.1% comparing to the borehole grouted with bentonite mixture containing only silica sand additive. Care must be taken in using additives for enhancement of bentonite grout's thermal conductivity. For example, adding graphite may adversely affect the mechanical behavior of the grout mixture and decrease its compression strength [42, 86]. It is also worth mentioning that the methods for increasing the grout thermal conductivity proposed in this section are only applicable for bentonite mixture. For the cement grout, the overall thermal conductivity is higher than the bentonite grout with some additives [85].

3.5.3 Integrated-Systems Approach

GSHP Integrated with Solar Energy

Solar energy which is one of the most widely used renewable energies has long been considered as one of the most applicable energy sources assisting GSHP systems. This integrated system works the best in regions receiving abundant solar radiation since the excess solar energy is injected into the soil, recharges the soil's heating capacity and increases COP of the GSHP system. The idea of using solar collectors and the earth as the energy source and forming solar assisted ground-source heat pump (SAGSHP) initiated by Metz [104] after energy crisis of 1980s. However, in recent decades it is widely used for heating and providing domestic hot water (DHW) for residential buildings.

Chen et al. [31] investigated the operation of a SAGSHP system through a long-term simulation in order to study the advantages of this system over conventional GSHP system. After running the simulation for a 20-year span, it was observed that COP of SAGSHP system increased by 26.3% with respect to the conventional GSHP. It was also reported that by application of 1 m^2 solar collector, 3.67 m of boreholes length can be saved. The application of SAGSHP not only leads to the production of more heat, but also the consumption of less electrical power. Based on the results, over one-year operation of SAGSHP, the consumption of electrical energy decreased by 5.2 GJ. It is worthwhile to mention that a higher heating demand during wintertime in cold regions necessitates enlarging the total area of solar collectors.

Through another study, Ozgener and Hepbasli [117] investigated the energy performance of a SAGSHP constructed in Solar Energy Institute of Ege University in Turkey. The system consists of three main circuits as follows:

- The ground coupling system with solar collector
- The refrigerant circuit
- The fan-coil circuit for heating the building (water circuit)

In order to assess the efficiency of the solar collector in providing energy for the SAGSHP system, the following equation was proposed:

$$\epsilon_c = \frac{\text{Useful energy delivered}}{\text{Energy absorbed by the solar collector}} \tag{3.3}$$

Based on the observations, the energy efficiency of the system was reported to be 67.7%. Considering the great efficiency of this hybrid system, it is observed that energy demand of the

building cannot be supplied by the GSHP system operating monovalently (i.e. independent of solar energy collectors).

In an experimental study, the performance of a GSHP system combined with solar collectors is studied [136]. The solar energy collectors were used for providing DHW and the excess solar heat was injected to the ground to facilitate meeting its thermal balance. It is observed that after 11 months operation of SAGSHP system, COP of the system is constant and equal to 3.75. Results signified that 34% of the total heat extracted from the ground was recovered by means of the solar collectors. This contributed to the uniform performance of the system as a result of underground thermal balance.

Wang and Qi [142] analyzed the performance and thermal storage capacity of a SAGSHP system experimentally and numerically. Solar radiation, which is a determining factor in efficiency of the system, is connected to a water storage tank in which the absorbed solar energy is stored and further transferred to the ground. However, the time required for the stored water to transfer to the ground is fairly high. This will rise a lag with the time that the heat actually needs to be rejected into the soil. Therefore, it is believed that the solar collector area and volume of the water tank should be matched. Through an optimization, the values between 20-40 l/m^2 is offered for the ratio between water tank volume and solar collector area.

Through a numerical simulation, Han et al. [65] worked on operation characteristics of a SAGSHP system in Harbin, where is a region in china with severe cold climate. It was observed that the application of a latent heat storage tank contributed to an increase in solar energy supply fraction. In specific time intervals especially during nights, the latent heat storage tank recharges the soil which further improves the COP of the system.

Dikici and Akbulut [47] conducted an energy analysis on a SAGSHP system in Turkey. It has been concluded that the performance of a heat pump system is highly sensitive to the capacity of the evaporator and solar heat exchanger. Also, the hybrid system operates more efficiently comparing to a conventional GSHP system since COP of the SAGSHP system was estimated to be 3.35 while an equivalent GSHP system operated with COP of 2.95.

In another numerical study, Kjellsson et al. [75] studied in TRNSYS the performance of a SAGSHP system which works within four different operation strategies as below:

- system 1: The system operates without solar energy assistance.
- system 2: Solar energy is used for recharging the borehole.
- system 3: Solar energy is used for supplying DHW.
- system 4: From November to February, solar energy recharges the borehole and provides DHW during the rest of the year.

Based on the obtained results, if the system is designed properly, the most efficient use of solar energy can be achieved by the system that provides DHW during summer and recharges the borehole during winter.

Wang et al. [143] evaluated the performance of a SAGSHP system designed for supporting the heat demand of a house in Harbin, China. Through this experimental study, soil was the cold source for the building during the summer and a combination of solar energy and underground heat was applied for providing heat during the winter. Results signified that 49.7% of the heat demand of the building can be directly provided by the solar collectors which leads to a great saving in electricity and an increase in COP of the system.

In an experimental study, Bakirci et al. [12] investigated the performance of a solar-ground source heat pump system in Erzurum, Turkey. In a cycle, the heat carrier fluid first comes from the solar energy collector and then goes to the water-source evaporator of the heat pump where it releases some parts of its energy. Then, the fluid enters GHE to release the remaining part of its energy into the ground and using a water circulating pump goes back to the solar collector. The aforementioned cycle alleviates soil temperature recovery and lessens the severity of the underground thermal imbalance which contributes to the greater COP of the system.

In another numerical study, Chen and Yang [32] studied the performance of a SGSHP system intended to provide both space heating and DHW over a 20-year span in Beijing. One of the five main modules of the provided system was reversible heat pump subsystem that modified the system for cooling purposes. The main subsystems of this SGSHP system are listed below:

- Solar collecting subsystem
- DHW supply subsystem
- Close-loop GHE subsystem
- Reversible heat pump subsystem
- indoor heat exchanging subsystem

Using TRNSYS, the influence of the solar collector area on the total borehole length and performance of the system was investigated. The system was designed to maximize the application of solar energy and further increase the efficiency of the system. According to Fig.3.4, as the area of the solar collector increases, the required borehole depth for providing a specific amount of energy decreases and the efficiency of the system increases as well (Fig.3.5).

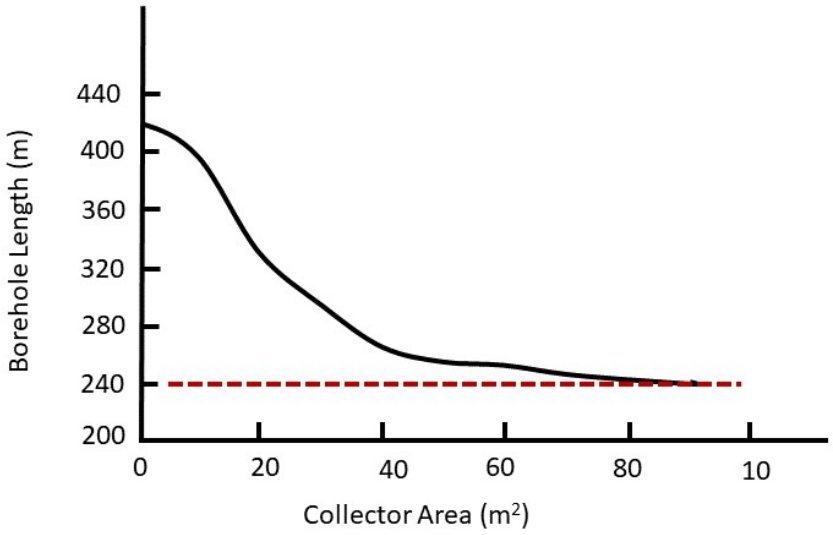

Fig. 3.4: Variation of the required boreholes length with the solar collector areas [32]

Through another phase of this study, Chen and Yang [32] evaluated the feasibility of using the proposed SAGSHP system in cold regions. Therefore, the operation of the system was evaluated in Harbin, China. Results signified that thermal balance would be kept in this region if the system works with COP of 2.8 which is significantly lower than COP of the system working in Beijing.

Si et al. [131] simulated two types of SAGSHP system designed for supplying heat and cold demand of an office building in Beijing by TRNSYS 17 as follows:

- SAGSHP(s): Solar collectors and GHE are installed in series and operate within two different modes:

  a) Heat carrier fluid first flows into the GHE and then enters the solar collector to reheat. At the beginning of the operation of the system in this mode, COP of the system increases

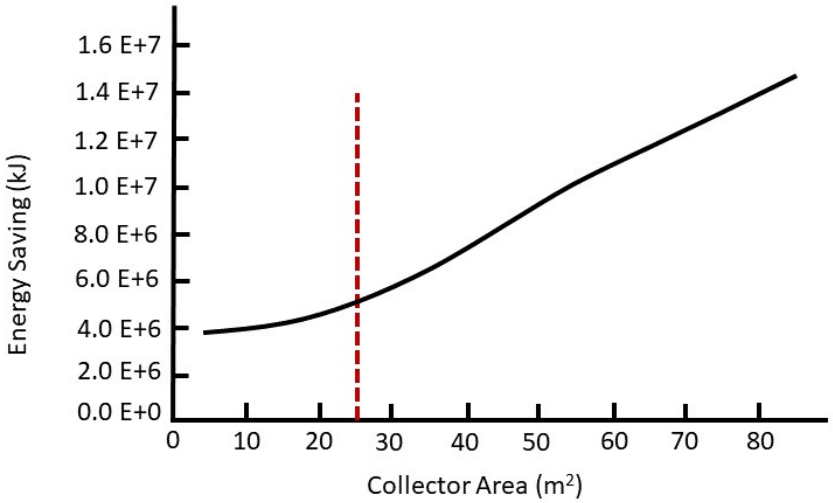

Fig. 3.5: The amount of the energy saved as the solar collector area varies [32]

although the heat load on the soil is too much that causes the COP of the system to drop after a short time.

b) Heat carrier fluid first flows into the solar collector and then flows into the GHE. Therefore, the excess solar energy is rejected into the soil and alleviates heat recovery of it which further contributes to meeting underground thermal balance. The drawback of operation of the system in this mode over mode (a) is a lower COP of the system.

- SGSHPS(r): Solar collector receives surplus solar energy and stores it in a tank during the days and applies this energy to recharge the lost heat of the soil during the nights.

Based on the results, the COP of the SAGSHP(s) was reported to be the highest among the simulated systems (Fig.3.6). Also, SAGSHP(s) was observed to meet the thermal balance of the

soil better than SAGSHP(r), since the soil temperature decreased by 0.8°C and 1.6°C after 10 years operation of the SAGSHP(s) and SAGSHP(r) systems, respectively.

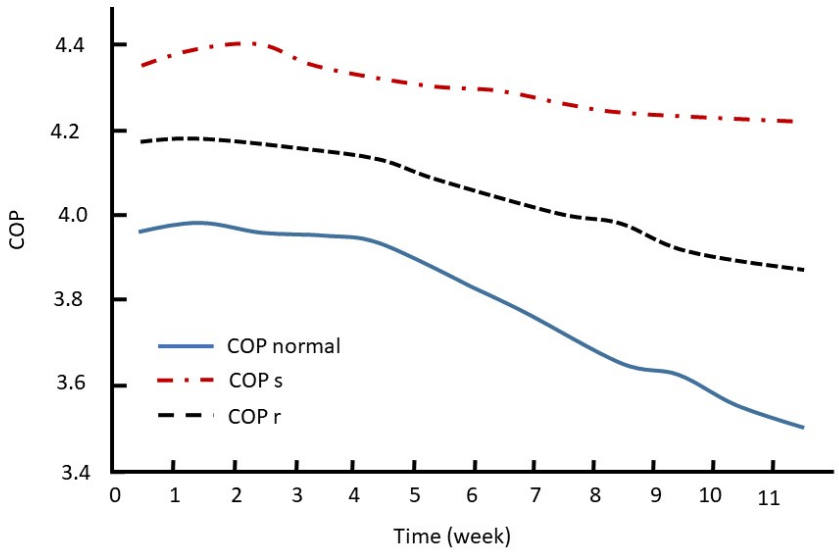

Fig. 3.6: COP of the heat pump in heating season [131]

Yang et al. [152] studied a SAGSHP system through an experimental and numerical analysis. The system was defined to work in four different operation modes in winter season. These modes included only working by GSHP, combined system of GSHP with solar collectors, day and night alternate operation mode and solar U-tube alternate operation mode. According to the results, the system operated the best within the coupled system mode in which a COP of 2.69 could be achieved. Furthermore, the soil temperature showed the least decline while working in the combined operation mode (Fig.3.7).

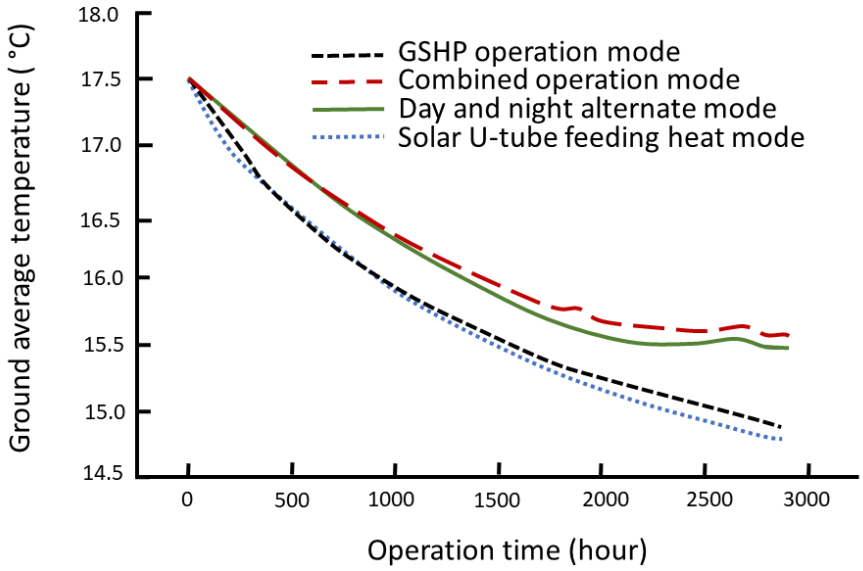

Fig. 3.7: Variations of the average soil temperature with operation time for different operation modes [152]

In another experimental study, Cite et al. [37] investigated the performance of SAGSHP system. According to the observations, the solar heat can significantly increase the performance of the GSHP due to accelerating the soil heat recovery. It is believed that recharging boreholes by solar energy could be a solution for underground thermal imbalance only if the duration of recharging be optimized to avoid wasting collected energy. Moreover, the application of storage water tank is highly recommended since it contributes to a stable performance of the system. In fact, the surplus collected solar energy is stored during the day and can be applied during the night. Therefore, the solar fraction of SAGSHPs would be constant during the operation of the system.

According to the above-mentioned literature, solar collectors can significantly increase the performance of GSHP systems and alleviate underground thermal imbalance in cold regions. However, coupling solar energy with ground source heat pump significantly increases the capital cost of the system. Moreover, solar collectors need enough space in order to supply enough heat for the system which is not possible in dense rural areas.

GSHP Integrated with Air-Source Units

One of the other most common heat compensation technologies coupled with GSHP is the system using ambient air temperature, since in some stages of GSHP system operation, the ambient air temperature is higher than the underground temperature.

According to Urchueguía et al. [138], one of the solutions for increasing the efficiency of GSHP is combining an air-to-water heat pump (AWHP) with a ground coupled heat pump equipped with a thermal storage device. The operation strategy of the system is based on supplying the building energy demand mainly by the GSHP system and once the thermal demand reaches to the capacity of the ground source heat pump, AWHP is switched on and supplies energy for the building. The mentioned coupled system proved to be around 43% and 37% more efficient in term of saving the primary energy consumed by the system when operating in heating mode and cooling mode, respectively. Pardo et al. [119] also conducted a numerical study on the GSHP coupled with AWHP and according to the results, the coupled system has around 20% less electricity consumption comparing to the conventional GSHP system.

Through another study, using an auxiliary heat/cold unit in a GSHP system functioning with an open loop heat exchanger was investigated [112]. The air/water-to-water hybrid heat

pump system switches between the groundwater and ambient air as a heat source/sink which contributes to a higher efficiency of the system comparing to the system using the groundwater as the only heat source/sink.

You et al. [157] proposed a new heat compensation unit with thermosyphone (HCUT) which uses a combination of air-source heat pump and air-source thermosyphone to transfer ambient air's heat to the ground. The coupled system, whose performance was simulated over 10 years, provides space heating and cooling for a building located in Harbin, China. The operation of the system is founded on providing heat by GSHP unit during winter and once the ambient temperature becomes higher in summer, the HCUT unit transfers heat from the ambient air via the heat carrier fluid to the ground. Thus, the heat extracted from the soil during winter can be as much as the heat rejected to the soil plus the heat transferred to the ground by HCUT unit during the non-heating season. The mentioned cycle leads to meeting the thermal balance of the soil and avoiding the degradation of the system due to a decrease in underground annual temperature.

In another work, You et al. [156] proposed a new air-source heat compensator (AHC) integrated with a GSHP system which can provides heat for space heating and DHW as well as heat for compensating the underground thermal imbalance. At the beginning of the heating season, when the ambient air temperature is not too low, AHC provides heat for space heating. Fig.3.8 compares the average soil temperature variation while the ground coupled system and the hybrid system are operating. As can be observed, the hybrid system can efficiently meet the underground thermal balance.

Allaerts et al. [5] presented a novel hybrid ground-source heat pump system with active air source regeneration. The principle of this hybrid system is the independent and simultaneous

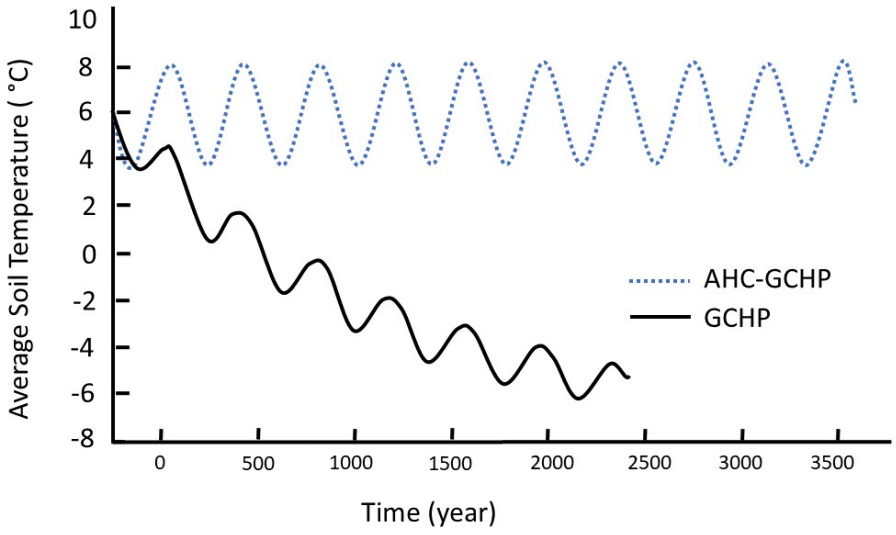

Fig. 3.8: Average soil temperature during operation of the AHC-GCHP and GCHP systems [156]

operation of a heat pump and a dry-cooler (additional heat rejecter). The system operation is based on storing seasonal energy into two separate warm and cold borefields. In winter, when the ambient air temperature is relatively low, warm borefield supplies heat for the heat pump and the dry-cooler extracts heat from the cold borefield. Likewise in summer, when the ambient temperature is high, the dry-cooler extracts heat from the air and rejects heat into the warm borefiels while the cold borefield is used to supply cold demand of the building. It has been observed that using two borefiels regenerating heat by the ambient air enables 47% reduction in the size of the borefileds comparing to the single borefield heat pump system.

GSHP Integrated with Fossil Fuels

In order to supply the portion of heat/cold demand which is beyond the capacity of a ground source heat pump, boiler and cooler towers are frequently used in heating dominated and cooling dominated systems, respectively. In fact, the GSHP provides the base load of the building and the supplementing system supplies energy during the peak load. Therefore, in the case of less severe underground thermal imbalance adding a boiling or cooling tower to the system is economically feasible due to its low initial investment.

Hackel and Pertzborn [63] investigated the thermal performance of three hybrid ground source heat pumps (HGSHP) used in three different buildings located in cooling-dominated and heating-dominated locations. In order to satisfy the peak heat demand of these buildings, boiler and heater towers are used in the heating-dominated system and the cooling-dominated one. It is believed that if the system is implemented correctly, using a hybrid system can be cost effective especially in regions experiencing severe underground thermal imbalance due to operation of GSHP system. Michopoulos et al. [106] also developed a HGSHP which uses an auxiliary heating unit. The primary energy supplier of the building is a GSHP wich is coupled with a 120 kW oil-fired boiler used as a backup for GHE.

In order to increase the energy-saving feature of the GSHP system and satisfy the energy demand of the building in which the system is used, Ni et al. [114] presented a coupled GSHP system that operates with a gas boiler as an auxiliary heat source. Based on a cost analysis done between different heat load distributions between the GSHP and the boiler, the optimum operation of the system can be reached when 60% and 40% of the heat load is supported by the GSHP and gas boiler, respectively. Based on another study conducted by Alavy, the operation costs of the

GSHPs that uses boiler tower as an auxiliary heat source will be less if the capacity of GSHP is higher.

GSHP Integrated with Waste Heat

Waste heat can be effectively used for water and space heating. Integrating GSHP with waste heat can compensate for the imbalance between heat extraction and rejection from/into the soil. However, waste heat is usually not high enough and needs to be connected to a heat pump to be efficient. Using waste heat as an auxiliary heat source for recharging the ground heat in cold regions can be considered as a solution for underground thermal imbalance. According to Chai et al. [27], one of the great sources of waste heat are subways whose temperature specifically in tunnels are significantly high that leads to consumption of additional power by ventilation and air conditioning system to exclude this excess heat. However, by means of a waste heat recovery system, this heat can be delivered to stakeholders using air/water heat pumps.

Liu et al. [97] proposed a hybrid system combining subway exhaust heat with GSHP. Subway heat is utilized as an auxiliary heat source in winter and increases the efficiency of GSHP. According to the results, this combined system can operate with COP of 3.31.

Fang et al. [54] also conducted an investigation into the coupled system in which industrial waste heat is rejected into the ground in summer and the stored heat is then utilized by a GSHP in winter.

In another study, Li et al. [89] presented a hybrid system in which a combined heat and power (CHP) system utilizing waste heat of flue gas is integrated with a GSHP system. Based on the

results, the system is highly efficient and COP of GSHP system reported to be 5.3 and asserted to be helpful in the case of using any other waste heat resources.

3.6 Conclusion

Geothermal energy has recently gained popularity all over the world specially in the regions with cold climate and longer winters. However, in these regions the heating demand of buildings is most commonly higher that the cooling demand during the year. Therefore, the amount of heat that is needed to be extracted from the ground during winter is considerably higher than the heat rejected to the soil during summer. This excess heat extraction form the ground leads to underground long-term and short-term thermal imbalance which may contribute to deterioration in performance of GSHP system. According to the literature, solutions provided for alleviation of thermal imbalance can be categorized as follows:

- GHE modification approach which is specifically recommended for alleviating less severe underground thermal imbalance. This approach focuses on making changes in the GHE configuration. These changes include increasing the length of the boreholes, increasing the space between the boreholes and improving thermal properties of the filling materials of the boreholes and their surrounding soil. The later solution tackles the thermal imbalance problem by increasing the moisture content of the grout and the soil which further contributes to accelerating the soil heat recovery.

- Integrated-systems approach is the term used for the approach in which GSHP systems are equipped with auxiliary heating/cooling units. These auxiliary units usually utilize solar energy, fossil fuels or waste heat and support the excess energy demand that disturbs thermal balance of the soil. Based on the literature, the solar energy auxiliary units

are highly recommended in cold regions that receive abundant solar radiation. They operate either by rejecting solar heat to the soil in order to meet its thermal balance or by supporting a portion of the required energy.

Unlike solar energy, supplementary systems working by fossil fuels can be applied as auxiliary units for GSHP systems working in both cold regions and regions with intensive cooling demand. Cooling and boiling towers are the most common systems using fossil fuels can be applied for supplying energy demand in regions with excessive cooling demand and heating demand, respectively.

The application of waste heat as an auxiliary heat source is another solution proposed for supplying space and water heating. Aside from environmental advantages, this method can economically support the heating/cooling system of residential buildings.

4

Energy Performance Analysis of a Proposed Geothermal Pile System for Heating and Cooling Energy Demand for a Building in Cold Regions [1]

Abstract

In this chapter, the performance of a proposed geothermal energy pile system for the energy demand of an institutional building is investigated. The building studied in this research is situated in the Fort-Garry campus of the University of Manitoba in the southernmost portion of Winnipeg (MB) in Canada. In an urban area, underground temperatures are substantially higher than the surrounding rural areas due to the buildings heat leakage to their underneath ground. In this study, this heat loss is harvested through geothermal piles and rejected to the building for the HVAC system utilization. The underground thermal imbalance, which is the most common problem encountered while utilizing the geothermal energy in cold regions, is extensively studied. It is concluded that despite the heat leakage through the basement

[1] **Saaly M.,** Maghoul P., Kavgic M., Polyzois D., 2019. Performance Analysis of a Proposed Geothermal Pile System for Heating and Cooling Energy Demand for a Building in Cold Regions, *Sustainable Cities and Societies*, 45, pp: 669–682.

enclosure, thermal balance of the soil, in case of supporting the total energy demand of the building by geothermal piles, cannot be met. The application of some auxiliary heat sources is proposed. Finally, the amount of energy harvested from the ground is calculated by maintaining the thermal balance of the soil and preventing the freezing at the soil-pile interface which affects adversely the structural performance of geothermal piles.

4.1 Introduction

As the living conditions and housing standards are improving, energy demand all over the world is increasing as well. As such, sustainable buildings design that offers methods for reducing the energy demand, increasing the energy efficiency and usage of alternative renewable sources of energy has become widespread [62, 76]. A significant component of total global energy demand relates to the energy used to heat and cool buildings. For example, in Canada in 2009, 49% of all institutional energy use was for space heating (NRC, 2011). In order to reduce the greenhouse emissions due to indoor temperature regulation, technologies that use alternative and renewable sources of energy must be developed and applied. Among different sources of renewable energies, Ground Source Heat Pump systems (GSHPs), also known as geo-exchange systems, are a promising source of energy for heating and cooling buildings [140, 15, 116]. Such systems extract heat from the ground during the cold seasons or inject heat to the ground during the warm seasons by circulating a heat carrier fluid between a heat pump and a ground loop system through heat exchanger pipes. The ground loop system can be vertical boreholes or horizontal trenches.

Geothermal energy piles, whose application has become popular in recent years, have the similar operation principle as vertical trenches [53, 82]. In fact, to reduce additional costs of

drilling and installing the conventional borehole heat exchangers and to take advantage of the fact that piles are needed to support superstructures, heat exchanger pipes are installed directly inside the pile foundation. Higher temperature of surrounding soils is transferred to the heat carrier fluid through the large surface of a concrete pile. In fact, since concrete has a high thermal storage capacity and thermal conductivity, it works well as an energy absorber. According to Lee et al. [87], due to relatively high drilling costs of ground heat exchanger (GHE) of conventional GSHP systems, merging GHE into the piles supporting structural load of a building can reduce the installation costs by 83.7%.

Using pile foundations as ground heat exchangers is a relatively new engineering technology. The design of a geothermal pile system needs to consider the local geology, groundwater, and climatic conditions. Geothermal piles are subjected to both thermal and mechanical loading, which make the interaction between the thermal piles and soil more complex. However, their behavior is still poorly understood, especially in cold regions, mainly due to the absence of reliable technical assessments and guarantees.

The application of geothermal energy piles or geothermal geo-structures is more established in Europe. Since 1980s, the geothermal energy has been harvested using buildings foundation elements in Austria and Switzerland [22]. One of the buildings in which the geothermal piles have been used for supplying the energy demand is the terminal E of Zürich airport [118]. The building's foundation consists of 440 piles and 300 of those are geothermal energy piles. The GSHP system of the building was designed to supply 85% of the annual heating demand of the building using a heat pump having a capacity of 630 kW. Also, the cooling demand of the building is supported by geo-cooling system where the thermal loads obtained during the cooling distribution are rejected directly into the ground through the geothermal energy piles.

The application of geothermal energy piles in the USA has also gained popularity in the last few years. In an experimental study, Akrouch et al. [4] investigated the thermo-mechanical behavior of a geothermal energy pile in the National Geotechnical Experimentation Site (NGES) of the Texas A&M University. The effects of thermal cycles on the mechanical behavior of the pile were investigated by circulating hot water through the GHE at different levels of mechanical loadings. Based on the results, although the thermal cycles created thermal stresses and strains in the pile, the thermally induced stress in the pile was negligible. In another study Murphy et al. [111] studied the thermo-mechanical behavior of eight geothermal energy foundations of a building at the US Air Force Academy. Results indicated that for a 18°C increase in temperature of the piles, the thermal axial stress and maximum upward displacement of 4–5.1 MPa and 1.4–1.7 mm, respectively, were generated in the piles. This necessitates further consideration in the design of geothermal energy piles.

Although the use of geothermal energy piles has also been recently expanded in Canada, the adoption rate of such systems is still low in comparison to European countries and the USA. One of the main problems facing the adoption of thermal piles in cold regions is unbalanced heating/cooling load profiles. A thermal imbalance may develop in the ground when the amount of heat extracted from the ground over the winter varies greatly from the amount of heat injected into the ground [157, 37].

For example, the thermal imbalance and excessive heat extraction from the ground during the cold season can cause the ground temperature to drop below the freezing point and consequently the soil surrounding the thermal piles can freeze. Freezing at the interface between the pile structure and surrounding soil due to excessive heat extraction over the winter temporarily increases the bearing capacity of thermal piles. Once the temperature in the ground slowly

rises during the spring and summer seasons, thawing occurs at the interface and the bearing capacity of such piles decreases drastically. This can lead to a system 137 failure, adversely affect the structural integrity of such systems, and cause many problems for designers and insurance companies.

According to the literature such as Kharseh et al. [74] and Liu et al. [98], the underground thermal imbalance due to the application of geothermal energy is highly sensitive to meteorological parameters as well as soil conditions and geological factors of each region. Therefore, the thermal performance of a single system can be highly different in different climates and regions. Aside from the meteorological and geological parameters, the operational strategy of a GSHP system affects the occurrence and intensity of the thermal imbalance in the ground. Li et al. [92] investigated the performance of a U-vertical ground coupled heat exchanger operating within two different strategies. Results showed that with different operational strategies, the soil temperature varies within a 29 °C interval. In an empirical study, Yang et al. [150] investigated the effect of the operational strategy on the performance of a geothermal pile equipped with a spiral coil as the GHE. Results showed that changing the operational strategy of the system could increase the rate of heat exchange between the soil and the energy pile up to 32%. There are also a number of studies that proposed auxiliary units for the GSHP system to enhance the thermal balance in the ground [117, 146, 141, 158, 110, 119, 145, 151]. These auxiliary heat sources include technologies applying solar energy, air-source units or units applying waste heat [159].

Although thermal imbalance and system failure during the operation of thermal piles has been widely observed in cold regions, there is currently no established calculation method for geotechnical and energy performance design. As such, there is a pressing need to improve

scientific knowledge and design procedures for geothermal energy piles. One of the factors which has been almost ignored in the design of such systems is the fact that in urban areas the severe decline in the soil temperature is improved due to the heat loss of the buildings through their below-grade enclosures [56]. In fact, the energy loss of buildings in urban areas can significantly change the thermal profile of the ground in shallow depths. As such, this study intends to comprehensively apply the knowledge of buildings heat loss and geothermal pile design for supplying the building energy demand. In fact, the current study is aimed at investigating a potential geothermal foundation system which can re-harvest the heat leaked form the buildings below-grade envelope into the soil.

In this chapter,the geothermal energy piles are designed and their performance is assessed for energy demand load of the SPEB. In this regard, the soil temperature variation while providing 100% of the building's heating/cooling energy demand during the winter and summer seasons considering the heat loss through the basement enclosures is estimated and the possibility of any thermal imbalance in the soil is studied. A five-year period is assumed to be sufficient for analyzing the thermal response of the ground and the results of a 3-D heat transfer simulation is presented. Based on the obtained results, some suggestions have been provided for alleviating the possible underground thermal imbalance.

In order to have a more accurate view regarding the ground capacity in providing the heat/cold energy demand of the building, it is assumed that all the geothermal piles are equipped with U-shape heat exchanger pipes. As the heat carrier fluid circulates through the pipe, it exchanges heat with the ground. The heat provided by the GHE is then compared to the heat demand of the building. Finally, a potential approach for increasing the heat supply by the GHE is provided.

determine the physical properties of soil samples such as

4.2 Modeling of Geothermal Energy Piles for Heating and Cooling Energy Demand

This section aims to assess the performance and feasibility of a hypothetical geothermal pile-based HVAC system for the Stanley Pauley building. As mentioned earlier, the implementation of such system has been discouraged due to the lack of understanding of the physical mechanism around the piles and recommendations for the design. Consequently, the outcomes of this research can give an important insight into the design and application of geothermal energy piles for the energy demand of buildings in cold regions.

In this study, it is assumed that all 119 pile foundations supporting the Stanley Pauley building act also as heat exchanger boreholes (Fig.2.1). The pile foundations have a depth of 5 m and as mentioned earlier, each group of two, three, four or six piles is supported by a concrete pile cap.

Fig.4.1 demonstrates the geometry of the model for the geothermal energy piles underneath the building. The dimension of the soil domain surrounding the piles in the model is 44 m × 34 m × 10 m.

The structural and energy integrity of the geothermal energy piles are evaluated by considering the effect of heat loss through the basement enclosure.

The heat transfer in the geothermal piles and soil is governed by thermal properties of concrete and soil, respectively, thermal properties of the insulation layer underneath the basement concrete slab and ambient air temperature. The assumptions made are as follows:

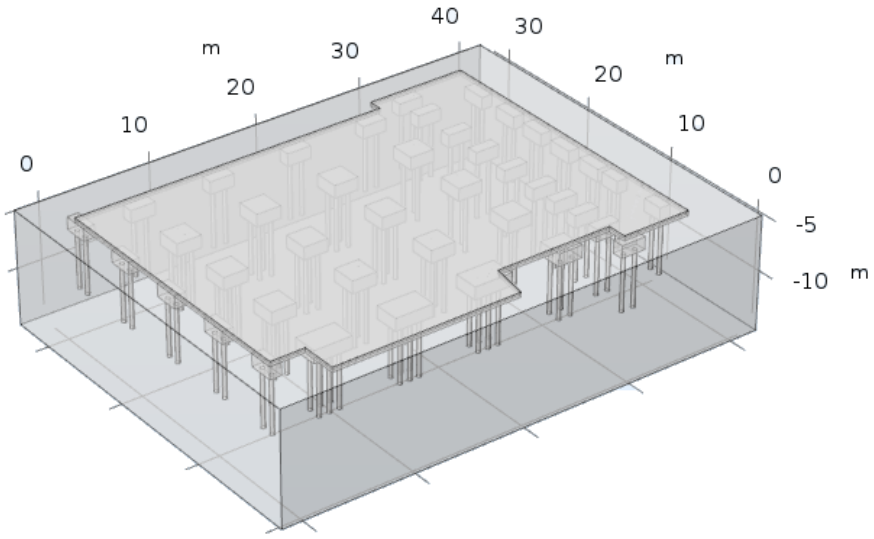

Fig. 4.1: General view of the model geometry

1. The initial temperature for geothermal piles are uniform.

2. All 119 pile foundations are geothermal piles.

3. The physical and thermal properties of the concrete used in the geothermal piles and basement slab as well as the insulation layer beneath the basement slab are constant.

4. The physical and thermal properties of the soil depend on the temperature, the latent heat of fusion, and the proportion of water and ice in the pores.

4.2.1 Governing Equations for Heat Transfer

The governing equation for heat transfer through the piles, pile caps, concrete slab and the insulation layer assumed as solid domains is described as below:

$$\rho C_p \frac{\partial T}{\partial t} + \nabla . q_c = Q \tag{4.1}$$

where ρ [kg/m^3] is the density, C_p [J/kg°C] denotes the specific heat capacity of the material, T [°C] is the temperature, t [s] denotes time, $\nabla\cdot$ is the divergence operator and Q [W/m^3] is the heat source. The heat source in Eq.4.1 and later in Eq. 4.3 represents the heat extracted and rejected from/into the soil assigned to the piles. Also, q_c [W/m^2] is the conductive heat flux through the volume as defined by Fourier's law as follows:

$$q_c = -k\nabla T \tag{4.2}$$

where, k denotes the thermal conductivity of the material and ∇ is the gradient operator.

Since the soil temperature in the current simulation may drop below the freezing temperature (T_0), heat transfer in freezing soil needs to be taken into account. This is carried out by making the following assumptions:

- The soil underneath the building assumed to be fully saturated.
- Transient heat transfer in the soil only occurs through conduction.
- The thermal conductivity of the soil is considered to be isotropic.
- Frost heave and volume change of water when freezing occurs are ignored.

$$\rho C_p \frac{\partial T}{\partial t} - L_f \rho_i \frac{\partial \theta_i}{\partial t} + \nabla . q_c = Q \tag{4.3}$$

in which L_f is the latent heat of fusion per unit mass of water (approximately 3.33×10^5 J / kg), ρ_i is the density of ice and θ_i denotes the volumetric fraction of ice in pores. In this equation, ρC_p is the volumetric heat capacity of the soil which can be estimated by the sum of the volumetric heat capacity of each constituent of a saturated freezing soil (solid skeleton, water, and ice) multiplied by its volumetric fraction as follows:

$$\rho C_p = \rho_w C_w \theta_w + \rho_i C_i \theta_i + \rho_s C_s \theta_s \tag{4.4}$$

where w, i, s subscripts denote water, ice and soil skeleton, respectively. Also, the effective thermal conductivity of a saturated freezing soil can be described as below:

$$k = k_w \theta_w + k_i \theta_i + k_s \theta_s \tag{4.5}$$

When the soil temperature drops below the freezing point, water inside pores starts freezing although some portion of pore water remains liquid even below the freezing temperature. This affects the effective thermal properties of the soil. According to Michalowski [105] the unfrozen water content fraction of the soil can be estimated as follows:

$$\theta_w = \theta_{wr} + (\theta_{w0} - \theta_{wr})\, e^{a(T - T_0)} \tag{4.6}$$

where θ_{wr} is the residual unfrozen water content which is assumed to be 0.05 in this study, θ_{w0} is the initial unfrozen water content or the porosity, a [1/°C] is a parameter that controls the curvature, taken here 0.16. Then, the volumetric fraction of ice can be expressed as below:

$$\theta_i = \theta_{w0} - \theta_w \tag{4.7}$$

The equations described above have been implemented in COMSOL Multiphysics in order to conduct the heat transfer analysis of the simulated model.

Model Parameters

The equations for heat transfer described in section 4.2.1 are implemented to estimate the subsurface temperature field and the energy capacity of the geothermal piles for providing heating and cooling energy demand of the Stanley Pauley engineering building.

Each group of two, three, four or six geothermal energy piles, made of concrete, are supported by a pile cap (900 mm) which is located underneath the two layers of extruded polyester (230 mm) and concrete slab (200 mm). The extruded polyester layer is considered as the insulation in order to control the heat loss through the basement. Table 4.1 shows thermal properties of concrete and insulation material used in this study.

Material	Thermal conductivity [W/m°C]	Heat Capacity [J/kg°C]	Density [kg/m^3]
Concrete	1.8	880	2300
Insulation	0.041	1450	34

Tab. 4.1: Thermal properties of the model materials

Based on Eqs.4.4–4.7 and considering the average values of Table 2.1, thermal properties of the three constituents of a soil are listed in Table 4.2.

Constituent	Thermal conductivity [W/m°C]	Heat Capacity [J/kg°C]	Density [kg/m^3]
Soil Skeleton	1.58	942	2560
Water	0.56	4188	1000
Ice	2.2	2117	950

Tab. 4.2: Thermal properties of the soil constituents

The boundary conditions considered in this study are presented next.

Boundary and Initial Conditions

In order to consider the effects of outdoor temperature on the subsurface temperature field, a convective heat flux q_{conv} [W/m^2], which is temperature- and time-dependent, has been assigned to the ground surface outside the building as follows,

$$q_{conv}(t) = h_{conv}\,(T_{air}(t) - T_s(t)) \tag{4.8}$$

where T_{air} (°C) is the ambient air temperature based on weather data and T_s (°C) is the temperature at the ground surface. The convection heat transfer coefficient, h_{conv}, depends mainly on conditions on the boundary layer such as wind speed and ambient temperature [67]. The average convective heat transfer coefficient for the external forced convection on a horizontal surface can be calculated as shown by Liu et al. [94].

The boundary condition considered for the top boundary of the model beneath the plan of the building representing heat loss through the basement structure is a convective heat flux q_0 [W/m^2] that has been defined as follows:

$$q_0 = h\left(T_{indoor} - T_g\right) \tag{4.9}$$

where, T_{indoor} is the temperature inside the basement which is assumed to be controlled, constant and equal to 20°C and T_g is the temperature of the soil surrounding the basement. Also, h denotes the heat transfer coefficient whose value is assumed to be 6 [W/m^2°C] [17].

According to Fergusen and Woodbury [56], underground temperature field beneath the urban areas is affected by the heat loss from the buildings. In some subsurface areas close to residential buildings in Winnipeg, groundwater temperature rises by as much as 5° C comparing to the groundwater temperature in areas far from any building [56]. This downward heat flow influence the average ground temperature and further monthly heat extracted from the soil.

In order to obtain the temperature profile of the soil underneath the Stanley Pauley building at the beginning of the building foundation construction, a heat transfer analysis has been conducted over the 30 years span of time from 1988 to 2018. The soil surface is exposed to the ambient air which significantly affects soil temperature. In order to define the ambient air temperature, the weather data provided by Environment Canada has been used. As mentioned earlier, the current analysis is conducted in an urban area where heat loss through the basement of the surrounding buildings affects the underground soil temperature. The Stanley Pauley building is surrounded by other institutional buildings from east, north-east and south-west side (Fig.**??**). These surrounding buildings have been constructed many years before construction of the Stanley Pauley building and the thermal insulation of their basement enclosure were

not necessarily respected according to the current state-of-the-art. Therefore, another analysis is made in order to obtain the impact of heat leakage of the surrounding buildings through their basement enclosure to the ground based on Eq.5.10. Also, for the surrounding open areas that are not built before, a convective heat transfer based on Eq.4.8 is assigned. Fig.4.2 shows the x-y view of the boundary conditions used for estimating the initial temperature of the soil.

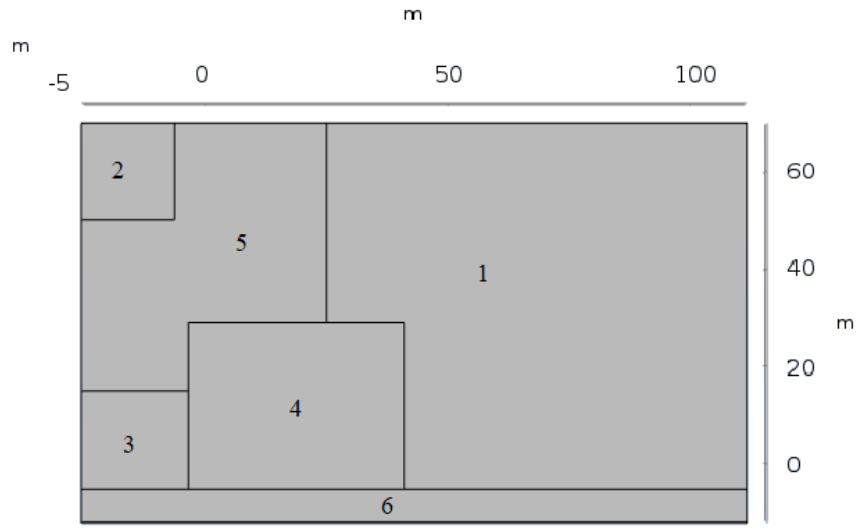

Fig. 4.2: x-y view of the 3-D model boundary conditions used for calculating the initial temperature of the soil underneath the Stanley Pauley building. Eq.5.10 is assigned to the previously constructed area (regions 1, 2 and 3) and Eq.4.8 to the open areas (regions 4, 5 and 6) where the stanley pauley soil domain is region 4.

Results obtained from the heat transfer analysis over 30 years is then applied as the initial temperature profile of the soil domain. Although the 3-D results have been used as the initial temperature of the soil, Fig. 4.3 illustrates 2-D soil temperature distribution for three representative surfaces at a 7 m distance from the east and west boundaries and at the center of the soil domain underneath the Stanley Pauley building. It can be observed that temperature of the soil close to the east boundary of the model increased the most because it has the highest mutual

boundary with the adjacent buildings and therefore it is more affected by the heat leakage through their basement.

As demonstrated in Fig.4.2, region 4 represents the Stanley Pauley building's construction site whose geometry is shown in Fig.4.1. As mentioned earlier, the depth-dependent temperature profile of this region is estimated from a thermal analysis using COMSOL Multiphysics. The obtained temperature profile is assigned as the initial temperature profile of the soil domain. To consider the effect of the adjacent buildings' heat loss, after estimating the initial temperature of the soil domain, the average temperature at each of the surrounding boundaries was calculated and assigned as a constant temperature boundary condition to the corresponding boundary. Therefore, the constant temperatures equal to 10.5°C, 15°C, 15°C, 6.7°C and 8°C were assigned to the west, north, east, south and bottom boundaries of the model, respectively. Also, a constant temperature of 15°C is set as the initial temperature of the structural material (slab and the insulation layer beneath).

4.3 Results and Discussion

In new construction practices, it is aimed to minimize the energy loss through the building envelopes. To date, most efforts to decrease the energy loss in buildings have been concentrated primarily on the above-grade envelope of buildings such as walls and roofs, since they initially posed the most substantial potential. However, it is also recognized that significant heat losses may occur due to flow of heat from inside of the building through the ground floor slab and into the foundation soils. This value might reach to the extent of 30% to 50% of the total heat loss.

As mentioned earlier, one of the challenges encountered in the application of geothermal energy piles in cold regions is underground thermal imbalance. To the best of the authors'

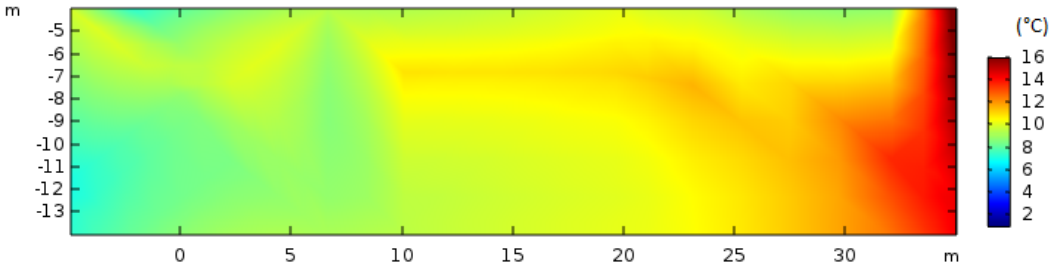

(a) Temperature profile of the soil for the depths of 4–14 m below the ground for a vertical cut-plane locating 7 m from the east boundary of the soil domain.

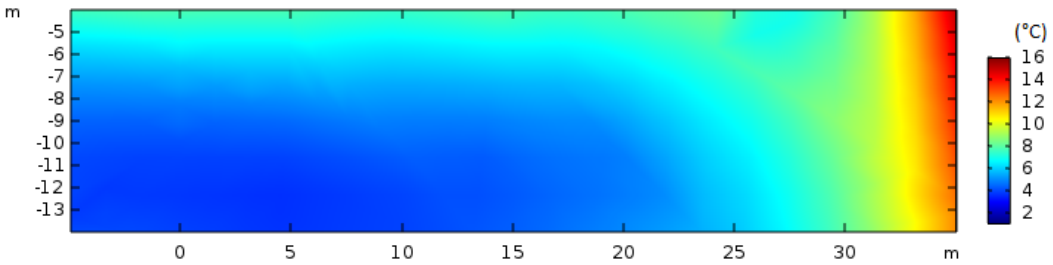

(b) Temperature profile of the soil for the depths of 4–14 m below the ground for a vertical cut-plane locating at the center of the soil domain.

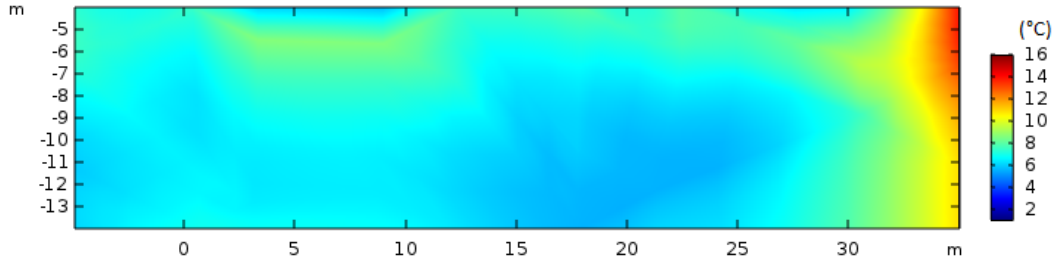

(c) Temperature profile of the soil for the depths of 4–14 m below the ground for a vertical cut-plane locating 7 m from the west boundary of the soil domain.

Fig. 4.3: Initial soil temperature profile of three cut planes beneath the basement of the Stanley Pauley engineering building.

knowledge, the effects of heat loss through the below-grade building envelope to the ground on thermal imbalance of the ground has not been well documented. Therefore, at the first stage of the simulation, the impacts of heat loss through the basement on the soil temperature underneath the Stanley Pauley building is investigated. Fig.4.4 illustrates soil temperature variation after five years construction of the building. It can be observed that soil temperature

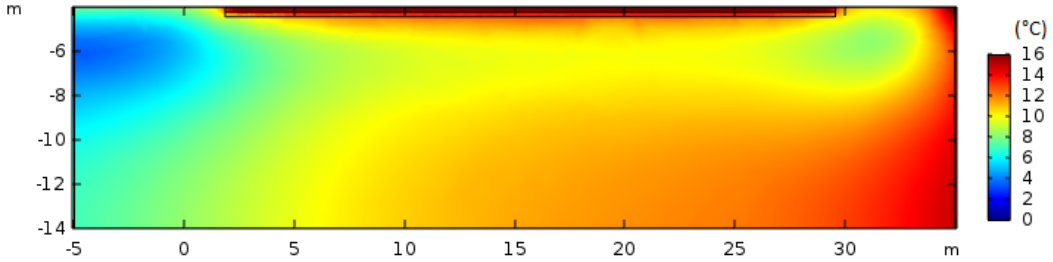

(a) Soil temperature profile beneath the basement for a plane at a distance of 6 m from the east boundary of the soil domain.

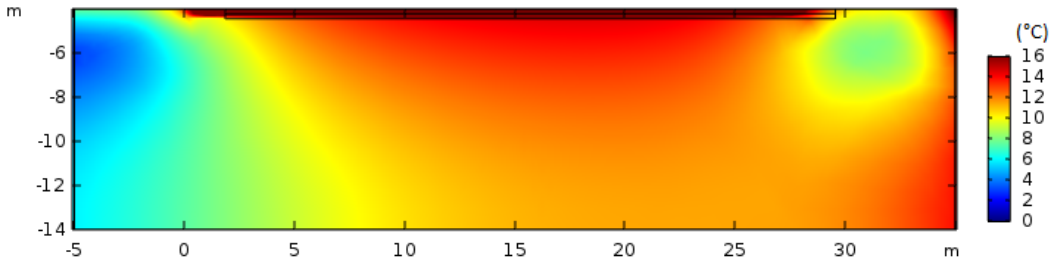

(b) Soil temperature profile beneath the basement for a plane at the center of the soil domain.

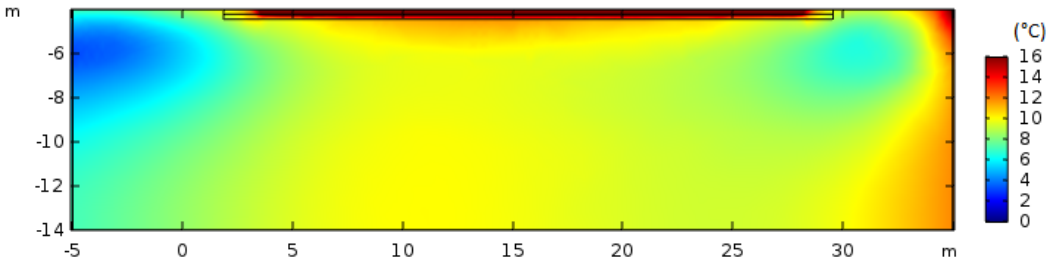

(c) Soil temperature profile beneath the basement for a plane at a distance of 6 m from the west boundary of the soil domain.

Fig. 4.4: Soil temperature distribution beneath the basement level after 5 years being affected by the building heat loss through the basement for three cut planes of the model.

is highly influenced by the heat loss through the building basement especially at shallower depths of soil. In fact, heat leaks into the ground through the basement floor despite insulating the foundation by a 230 mm layer of extruded polyester.

4.3.1 Occurrence of Thermal Imbalance

The application of geothermal energy in regions with colder climate and longer cold seasons, where annual heat extraction from the soil is higher than heat rejection into it, leads to underground thermal imbalance. The thermal imbalance of the soil is one of the biggest issues encountered by application of geothermal energy in cold regions which makes the thermal piles system non-operational in the first two to five years of its operation.

In this regard, this section intends to study the level of underground thermal imbalance after 5 years. Two scenarios are studied. In the first scenario, it is assumed that the system will be operational only during the cold months (Nov–Apr) to supply 50% of the heating demand of the Stanley Pauley building. In the second scenario, it is assumed that the system is designed to supply 100% of the heating demand of the Stanley Pauley building in 6 cold months (Nov–Apr) and supply 100% of the cooling demand in 6 hot months (May–Oct) of a year. In this case, even though the duration of heating and cooling is equal, the amount of heating and cooling loads are different (Table **??**). In order to determine the imbalance degree, the Thermal Imbalance Ratio (TIR) can be calculated as follows [157]:

$$TIR = \frac{Q_{EH} - Q_{RH}}{max(Q_{EH}, Q_{RH})} \times 100\% \tag{4.10}$$

where Q_{EH} is accumulated extracted heat during the heating season and Q_{RH} is the accumulated rejected heat into the ground during the cooling season. A higher percentage of TIR indicates a more intense thermal imbalance in the soil. Using Eq.4.10 and considering Table.**??**, TIR for the second scenario is estimated to be 38%.

To apply the heating and cooling demand of the building to the pile, it is assumed that piles are working within a GSHP system operating with a COP of 3. The heating and cooling loads according to Table **??** are then applied to the piles as heat sources whose magnitudes can be calculated as follows:

$$Q_c = Q_H \left(1 - \frac{1}{COP}\right) \tag{4.11}$$

where Q_c denotes the heat harvested from the ground by geothermal piles and Q_H is the heat supplied to the building by the heat pump, which here is equal to the demand of the building. It is worth mentioning that Q_c and Q_H for the cooling load will be represented by negative sign since heat is injected into the ground and cold is then supplied to the building. COP is assumed to be constant and equal to 3 which is a highly conservative assumption investigating the worst case scenario for the underground temperature decline. On the other hand, when thermal imbalance occurs in the soil, its capacity for providing heat will be lowered resulting in a decrease in Q_c and consequently COP.

According to Fig.4.5, illustrating results of the first scenario, soil temperature significantly declines and leads to severe underground thermal imbalance during 5 years operation of the system. It can be observed that temperature of the soil 8 m below the basement floor decreases slightly less than the soil layers at 2 m and 5 m below the basement. Since each 5 m long pile is considered as a heat source and due to extreme heat extraction along the length of piles, temperature of the soil at the depth of 2 m and 5 m decreased more severely comparing to the soil at 8 m below the basement floor. Therefore, soil temperature below 5 m is slightly less affected by the extreme heat extraction from the soil.

Results of the second scenario are illustrated in Fig.4.6. As can be observed, soil temperature decreases by almost 3.5°C after 5 years operation of the system for the soil at 8 m below the

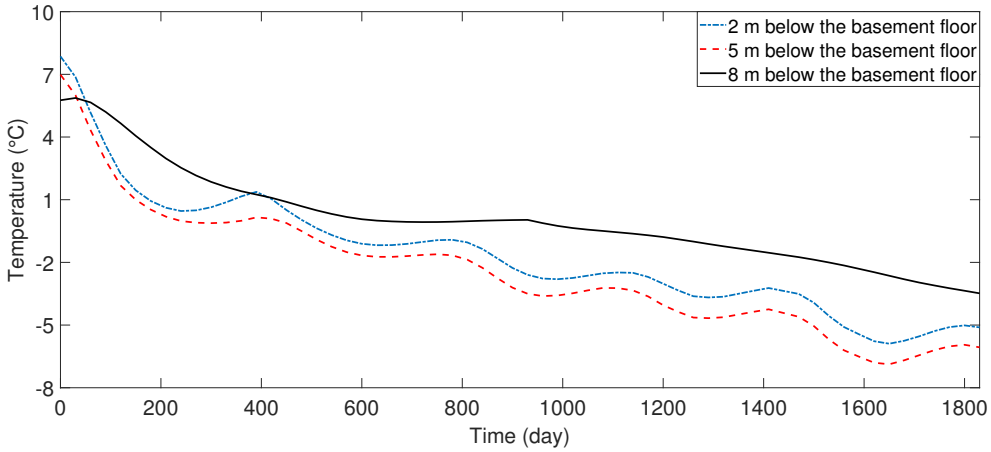

Fig. 4.5: Soil temperature variation at 2 m, 5 m and 8 m below the basement floor considering the heat leakage through the basement for scenario one.

basement floor. On the other hand, the soil temperature for the depths of 2 m below the basement level remains steady after the same operation time which signifies the contribution of heat leakage through the basement into the ground. According to Fig.4.7, the temperature variation of the soil closer to the thermal piles is more intense. Excessive heat extraction from the ground leads to freezing of the soil at the interface with concrete piles. This can temporarily increase the bearing capacity of the piles. However, thawing during the spring decreases drastically the bearing capacity of such systems. On the other hand, not only the energy integrity but also the structural integrity of such systems will be adversely affected by the excessive heat extraction. Therefore, in the next section, potential mitigation solutions will be studied in order to decrease the level of the underground thermal imbalance.

4.3.2 Impact of Increasing Pile Length on Thermal Imbalance

One of the solution for improving thermal imbalance is changing the arrangement and the length of the ground heat exchangers (GHEs). Based on the literature, as the spacing between

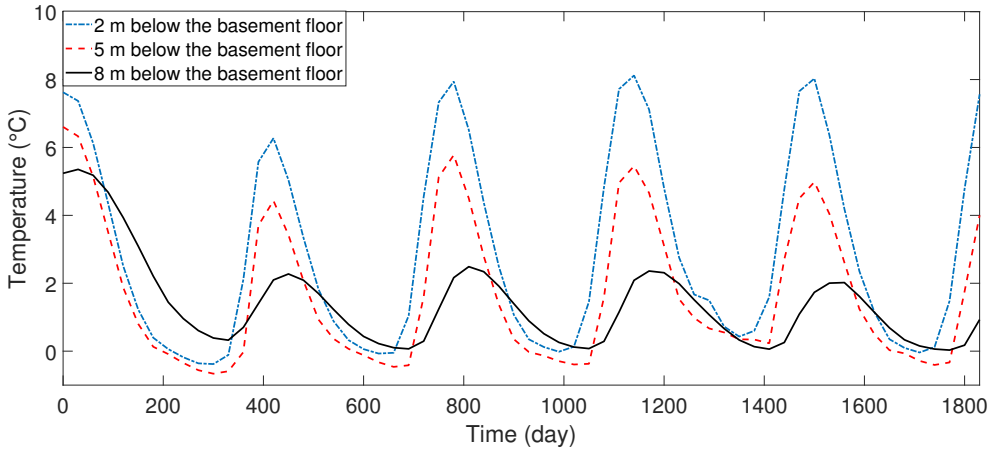

Fig. 4.6: Soil temperature variation of 2 m, 5 m and 8 m below the basement floor considering the heat leakage through the basement for scenario 2.

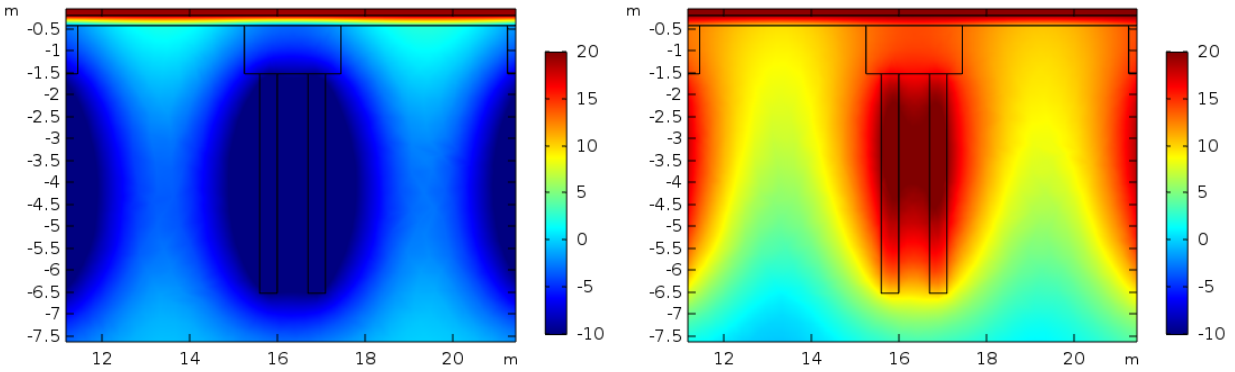

(a) Soil temperature profile at the end of the cooling season of the fifth year of operation of the system

(b) Soil temperature profile at the end of the heating season of the fifth year of operation of the system

Fig. 4.7: Temperature distribution contour for the piles located at the center of the soil domain at the end of the heating and cooling seasons of the fifth year of operation of the system

GHEs increases, soil temperature drops less severely [69, 121]. However, in the current project, increasing the spacing between the piles is not feasible due to the location of the building and land restrictions and more importantly from the structural design point of view. Therefore, increasing the length of the piles can be presented as a solution for decreasing the thermal imbalance intensity. In this regard, temperature variation of the soil surrounding two sets of

piles being 5 m and 12 m long have been compared. According to Fig.4.8, as the length of the piles increases, greater depths of soil are involved in supplying a constant energy demand comparing to the soil surrounding the shorter piles. The mentioned statement leads to a decrease in thermal gradient along the length of the pile and the soil at 8 m depth below the basement floor will be more affected by the heat extraction through the pile during the winter season, due to the higher thermal gradient, comparing to the 5 m piles.Although the rejected heat doesn't exceed the extracted heat from the ground it can be observed that maximum temperature of the soil slightly increased. This is speculated to happen due to the additional injected heat into the ground as a result of the heat loss through the below-grade enclosures of Stanley Pauley building and its surrounding buildings.

However, application of longer thermal piles necessitates a justification for its feasibility from geotechnical and structural point of view.

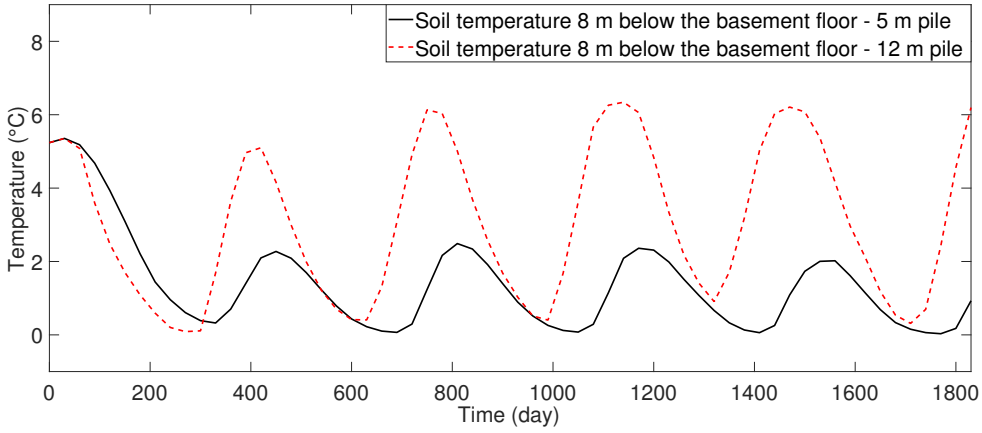

Fig. 4.8: Temperature variation of the soil at the depth of 8 m below the basement floor during 5 years operation of the system

4.3.3 Impact of Supplying Heating and Cooling Demand of the Building Simultaneously

The operation strategy of the system plays a significant role in meeting underground thermal balance. In this regard, another seasonal operation strategy is presented in this section and its impact on the soil underneath the Stanley Pauley building is studied.

In the previous sections, a heat source was assigned to each thermal pile in order to satisfy the heating demand of the building during 6 cold months of a year and supply cold demand during the other six months. According to Fig.4.6, the aforementioned trend contributed to underground thermal imbalance in the depth of soil less affected by heat leakage through the basement floor. In this section, another operation strategy is presented and its impacts on the soil temperature underneath the Stanley Pauley building is studied. In order to fully satisfy the heating and cooling demand of the building during each month, the groups of piles are divided into two subgroups of 50 and 69 piles which are in charge of rejecting or extracting heat to/from the ground simultaneously. During the 6 heating months, the larger group of piles supplies heat to the building and the smaller group satisfies the cooling demand. The aforementioned operation trend will be exactly opposite during the cooling season.

As illustrated in Fig.4.9, soil temperature at 8 m depth below the basement decreases by 4°C after 5 years operation of the system by the conventional operation strategy. However, due to the high cooling demand of the building, in the case of simultaneous cooling and heating operation strategy, soil temperature at the depth of 8 m below the basement will be almost constant after 5 years operation of the system. In fact, during the first two years of operation of the system, the soil temperature increased and then followed a steady trend. As mentioned earlier, since

the Stanley Pauley building is an educational building with data centers and laboratories, cold demand of the building during a year is relatively high comparing to residential buildings. Since this relatively equal rejected heat and extracted heat is then accompanied with heat loss through the building's basement, simultaneous heating and cooling strategy would slightly increase soil temperature. However, it is believed that the following operational strategy has different effects on soil temperature if its applied to a residential building thermal pile system.

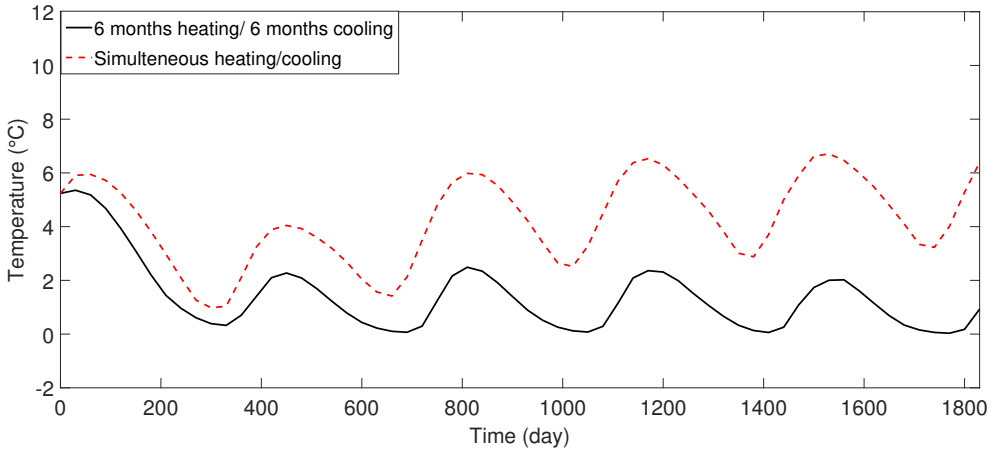

Fig. 4.9: Soil temperature variation at the depth of 8 m below the basement floor considering two different operation strategies

4.3.4 Impact of Using a Heat Compensation Unit

As mentioned earlier, an excessive heat extraction during the heating season contributes to underground thermal imbalance. In this regard, adding a heat compensation unit operating by a Solar Water Heater Thermosyphone (SWHT) is offered as an approach for maintaining the soil thermal balance. The proposed system is integrated with the GSHP system, adds additional heat to the soil during June–September and further alleviates the annual underground thermal imbalance.

The operation of SWHT is founded on entering cold water to the storage tank and since cold water has higher specific density it sinks to the bottom of the tank. Cold water flows from the bottom of the tank to the pipes embedded in heat collector panel. After circulation of water through the panel which absorbs heat from the ambient air, the water temperature increases and flows back into the storage tank. Warm water floats in the tank since the specific density of that is lower than the cold water. The heated water then flows into the pipes embedded in the ground in order to compensate for the excessive heat extracted from it.

SWHT Unit Modeling

Four SWHTs have been considered as the auxiliary heating unit for GSHP and each is assumed to operate 8 hours a day during June–September to supply the heat compensation unit with warm water. In order to estimate the outflow water temperature once exiting from the solar panel collector, a 3-D model is developed in COMSOL Multiphysics. The model simulates a 1.3 m × 2.1 m heat absorber panel made of copper which contains 22 m copper pipes carrying water. The copper used in the model has the specific heat capacity of 385 [J/(kg.K)], density of 8960 [kg/m^3] and thermal conductivity of 400 [W/(m.K)]. Fig.4.10 demonstrates a general view of the SWHT model. The temperature of the inlet water is assumed to be fixed and equal to 18°C and the initial temperature of the panel is considered to be equal to the average temperature of each month provided by the Government of Canada (Table 4.3). The bottom surface of the panel assumed to be thermally insulated. Also, a convective heat flux based on Eq.4.8 is used as the boundary condition for the top and surrounding surfaces of the panel in which T_s is temperature of the copper panel and T_{air} is the average high temperature of each month according to Table 4.3. It is worth noting that the copper panel operates during 8 warmest

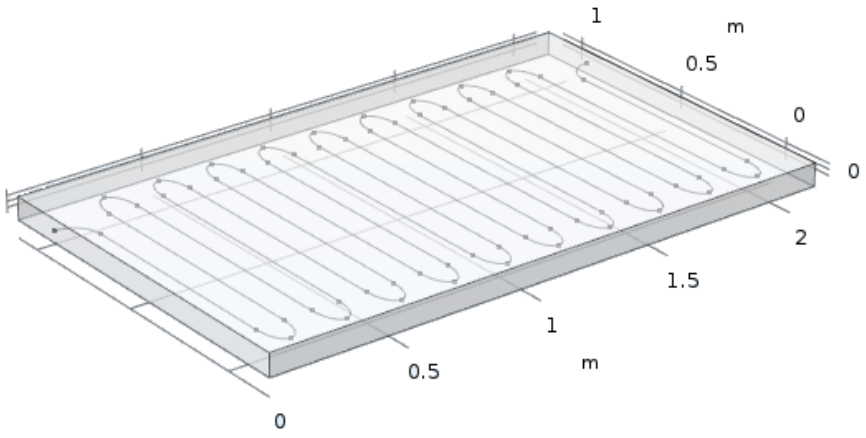

Fig. 4.10: General view of the modeled heat collector panel

hours every day during June–Sep. Based on the daily historical temperature of Winnipeg [50], at least 8 hours per day in Jun–Sep have the temperature almost equal to the daily average high temperature. Therefore, the monthly average high temperature is assigned to T_{air}.

Temperature	Months			
	Jun	Jul	Aug	Sep
Daily Average (°C)	17	19.7	18.8	12.7
Average High (°C)	23.2	25.9	25.4	19

Tab. 4.3: Winnipeg monthly temperature during Jun–Sep (source: The Government of Canada)

Subsurface Temperature Variation

According to Fig.4.11, for the system equipped with the heat compensation unit connected to four heat absorber panels, the average temperature of the soil surrounding the thermal piles remains steady after 5 years operation of the system. Therefore, the SWHT can effectively solve the problem of soil temperature decline due to the thermal imbalance.

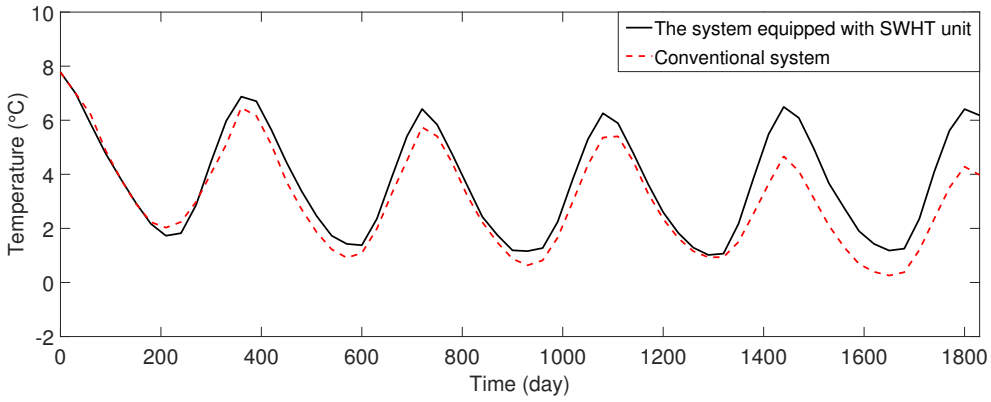

Fig. 4.11: 5 years trend of the average soil temperature variation with and without using the auxiliary SWHT heating unit

4.3.5 Simulation of Geothermal Piles Considering Pipe Flow

In previous sections, results represented the occurrence of thermal imbalance in the soil after five years of supplying the total heating and cooling demand of the Stanley Pauley building. One of the assumptions made in the previous sections is a constant COP of 3 for the GSHP system for calculation of the energy amount needed to be supplied by geothermal piles. The aforementioned assumption gives us a conservative view of the underground temperature variation and feasibility of supplying the Stanley Pauley building's total energy demand by geothermal piles. However, to investigate the actual applicability of geothermal pile for this project, the amount of heat and cold that can be supplied by geothermal piles needs to be assessed while the thermal balance of the soil is being met. The operation strategy implemented in this section is based on 6 months supplying heat and 6 months supplying cold to the building during the winter and summer seasons, respectively. In this regard, each 5 m long geothermal pile in the simulation needs to be equipped with a U-shape heat carrier pipe through which

the heat exchanger fluid (water and antifreeze) circulates and exchanges heat with the ground through the pile wall.

In order to determine the optimum inlet temperatures of the heat exchanger fluid entering the GHE, a parametric study has been conducted using COMSOL Multiphysics. Two main constraints need to be met to obtain the optimum inlet temperature: 1) maintaining thermal balance of the soil after 5 years operation of the system, and 2) preventing the soil-pile interface from freezing. Considering the mentioned constraints, the inlet temperature of the heat carrier fluid entering the closed-loop was optimized with respect to the maximum heat transfer between the pipe and the pile. Finally, the inlet temperature suggested in the simulation ranges between -1°C in winter and 20°C in summer.

In order to have a more accurate view regarding the effects of the surrounding buildings heat loss on the amount of heat extraction and rejection from/into the ground by GHE, the outlet temperatures of two representative piles located close to the east and south-west boundaries of the model are analyzed. It is worth reminding that the east boundary of the model is adjacent to a previously constructed building unlike the south-west boundary of the model where no surrounding building exists. Fig.4.12 shows the inlet and outlet heat carrier fluid temperatures during a five years operation of the system. Results signify that the difference between the inlet and outlet fluid temperatures during the winter and summer months ranges between ±5 °C for the heat exchanger fluid circulating in a pile located at a 7 m distance from the east boundary of the soil domain where the effect of surrounding buildings heat loss is more significant. However, the difference between the inlet and outlet fluid temperature changes to ±3.5 °C for the pile located at a 6 m distance from the south-west boundary of the soil domain where no adjacent building exists which further leads to less heat exchange between heat carrier fluid

and the ground. The reason is that in winter due to the adjacent buildings' heat loss, the soil temperature is higher than the soil close to the open area. This creates a higher temperature gradient and further higher heat exchange between the GHE and the ground. On the other hand, in summer, the temperature of the soil close to the open area is higher than the parts of the soil adjacent to constructed area due to direct exposure of ambient air having relatively high temperature with the soil surface.

This increases the heat extraction and rejection in winter and summer respectively due to a higher temperature gradient between the ground and heat carrier fluid caused by the presence of the built area. Fig.4.12 shows that the difference between the inlet and outlet fluid temperatures during the winter and summer seasons for each year is almost equal which signifies that a relative steady heat exchange occurs between the ground and the building during the heating and cooling seasons.

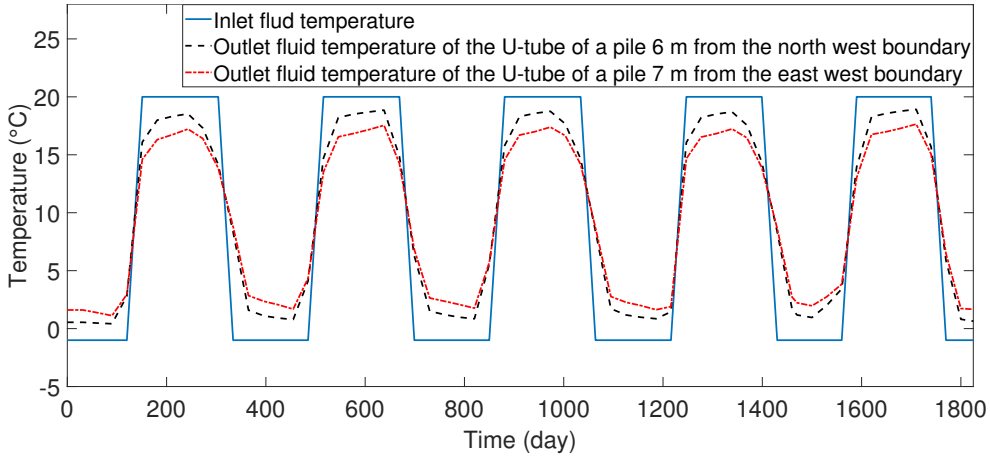

Fig. 4.12: Inlet and outlet heat exchanger fluid temperatures of the U-tubes embedded in 5 m piles over 5 years

Results of Section 4.3.1 showed that in case of supporting 100% of the heating and cooling demand of the building by geothermal piles, thermal imbalance occurs in the soil. Also, the

temperature of the piles and their surrounding soils declines below zero. Therefore, in order to keep the underground thermal balance and preventing the freezing at the soil-pile interface, less amount of energy needs to be extracted/rejected from/into the ground by heat exchanger fluid or auxiliary heating units such as SWHT can be used to facilitates meeting the thermal balance of the soil.

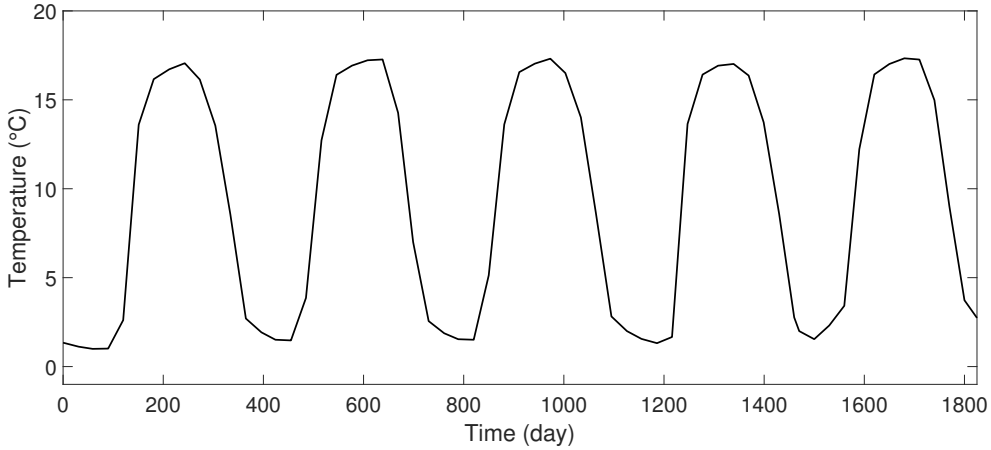

Fig. 4.13: Average temperature variation at the 5 m long pile-soil interface during five years operation of the system

According to the results, during winter and summer 4–15% and 7–41% of the energy demand of the building, respectively, can be supplied by 5 m long thermal piles equipped with U-shape heat carrier fluid pipe without occurrence of the underground thermal imbalance and freezing of the soil-pile interface. However, these values can be alleviated if the length of the piles can be increased which further leads to an increase in the length of the heat exchanger pipe. As such, another simulation is used considering the length of the piles to be 12 m and other variables including inlet temperature the same as for the 5 m long piles. It is observed that 12 m piles used for harvesting energy from the ground can support 20–41% and 39–89 % of the Stanley Pauley building energy demand during winter and summer, respectively. Fig.4.14 compares the

heat supplied to the building using 5 m and 12 m geothermal piles with the energy demand of the building.

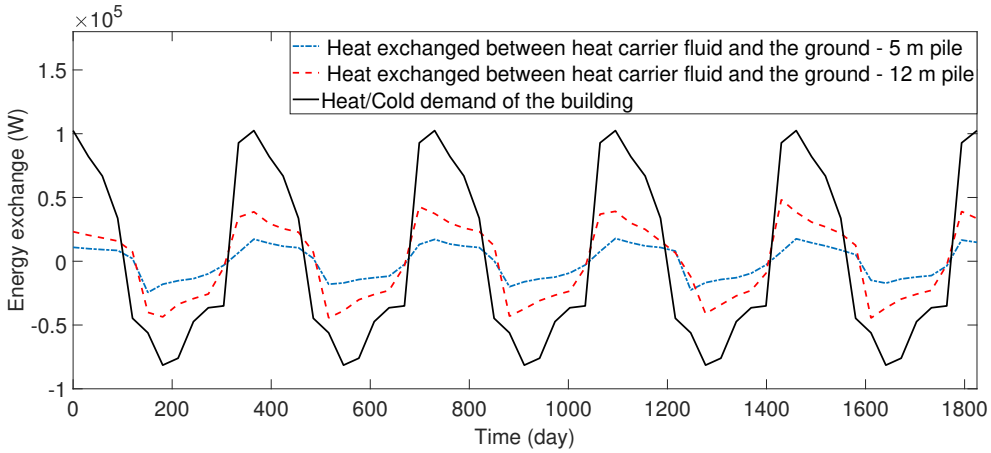

Fig. 4.14: Heat exchanged between the piles and the ground versus monthly heat demand of the building

Fig.4.15 demonstrates the outlet temperature of the heat exchanger U-tube embedded in two 12 m long piles, one of them is affected the most by the surrounding buildings heat loss (i.e, the pile located at a 7 m distance to the east boundary of the model) and the other one is exposed the least to the heat leakage of the surrounding buildings basement (i.e, the pile located at a 6 m distance to the south-west boundary of the model). This can be observed that the outlet temperature of the heat exchanger fluid is relatively the same for two different 12 m long piles close to the boundaries differently affected by the surrounding buildings heat leakage through their basements (Fig.4.12). This verifies the fact that shallower depths of soil are more influenced by surrounding buildings heat loss. Therefore, as the heat carrier fluid circulates in the U-tube embedded in 12 m piles, heat is exchanged between the fluid and the surrounding soil having relatively steady temperature at the higher depths which leads to relatively the same outlet fluid temperature exiting the U-tubes embedded in different piles.

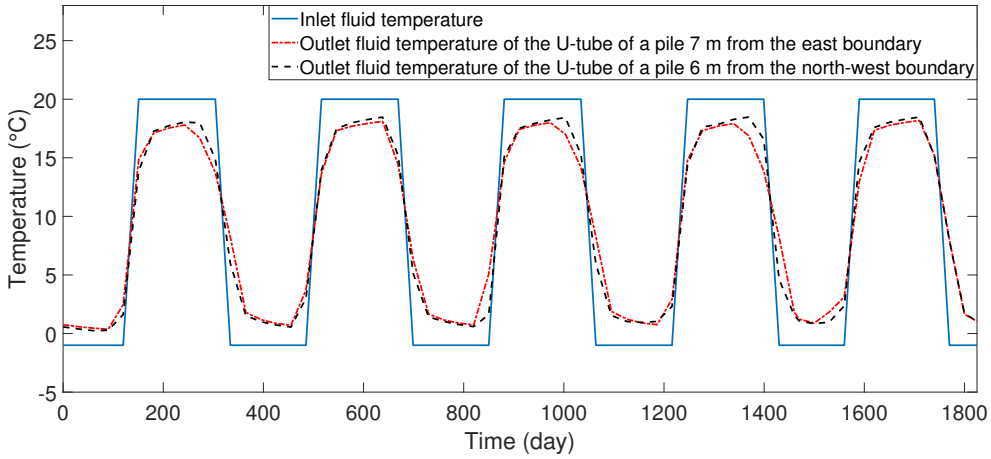

Fig. 4.15: Inlet and outlet heat exchanger fluid temperatures of the U-tubes embedded in 12 m piles over 5 years.

4.4 Conclusion

In the current study, the feasibility of using geothermal pile foundations for the heating and cooling energy demand for the Stanley Pauley engineering building located on the Fort-Garry campus of the University of Manitoba, Winnipeg, Canada is assessed. This is performed by investigating the functionality of the system over 5 years and providing solutions to the potential problems caused by using geothermal piles. The effect of heat loss through the basement of the surrounding buildings on the soil temperature field is also studied. Based on the results, the following conclusions can be drawn:

1. Although the majority of each building heat loss occurs through its walls, the heat loss through the basement floor also influence underground soil temperature significantly. According to the results, the heat leakage through the basement floor of the previously constructed surrounding buildings highly affected the underground temperature field of the Stanley Pauley building at the beginning of the construction process.

2. Geothermal piles are commonly used only for the heating purposes during winters in cold regions. This energy harvesting strategy is not highly suggested due to the occurrence of extreme underground thermal imbalance (Fig.4.5) which leads to a failure of the system.

3. In case of using geothermal piles for extracting and rejecting heat from/into the soil during the winter and summer, respectively, with the purpose of supporting total energy demand of the building through geothermal piles, the underground thermal imbalance occurs and the pile-soil interface freezes. However, at shallower depths of the ground where the soil temperature increases due to the building heat loss, the thermal balance of the soil is met due to the reinjection of heat loss to the ground (Fig.4.6).

4. Changing the operation strategy of geothermal piles can effectively alleviate the thermal imbalance of the soil especially for the depths less affected by the basement heat leakage. The operation strategy presented in this paper is based on the simultaneous extraction and rejection of heat from/into the ground. As such, in winter 50 groups of geothermal piles reject heat from the ground and 69 groups of geothermal piles extract heat into the ground and during the summer the dominant group of piles is used for heat rejection into the ground and the group of 50 piles extract heat from the ground. This heat harvesting strategy significantly alleviated the soil thermal imbalance and kept the soil temperature steady at higher depths of the ground.

5. One of the other proposed solutions for the soil thermal imbalance is the SWHT unit. The presented system obtains heat from the ambient air during June–September, rejects the heated water into the soil and increases the underground temperature. Results showed that this auxiliary heating unit can effectively alleviate underground thermal imbalance.

6. In order to estimate the level of energy supply by thermal piles, each pile is equipped with a U-shape heat exchanger pipe. Results signify that by using 5 m long geothermal piles 4–15% and 7–41% of energy demand of the Stanley Pauley building can be supported during the winter and summer seasons, respectively. These values are obtained while meeting the thermal balance of the soil and preventing the pile-soil interface from freezing (Fig.4.13).

7. Increasing the piles length is an effective approach for increasing the length of the heat exchanger pipe and further increasing energy supply by geothermal piles. Results signify that by increasing the length of the piles to 12 m, 20–41% of the heat demand of the building can be supplied in the winter which is almost 15% more than the heat supply by the 5 m long pile. However, the feasibility of pile length increase needs to be justified from a structural and geotechnical point of view.

5

Thermo-mechanical Performance of a Proposed Geothermal Energy Pile System

1

Abstract

Geothermal energy piles are bi-functional structural elements that are used to support the structural loads of a building and to operate as a geo-heat exchanger for shallow geothermal energy systems. In urban areas, geothermal energy piles can eventually be used to harvest the heat loss through the basement enclosure and re-inject the energy to the building for the heating and cooling purposes. In spite of a higher thermal profile beneath the buildings, an underground thermal imbalance may occur due to the application of geothermal energy piles in cold regions. This paper aims to study the structural performance of a geothermal energy pile in cold regions by meeting the thermal balance in the foundation soil through a numerical Thermo-Mechanical (TM) analysis. Results showed a safe margin between pile settlement and the allowable settlement. However, the axial stress applied to the pile increased by 9% due to thermal loads. In addition, a maximum decrease of 9% in mobilized shaft friction along the pile-soil interface was recorded due to the thermal loads. To consider the thermo-active piles

[1] **Saaly M.,** Maghoul P., Holläder H., 2019. Thermo-mechanical performance of a proposed geothermal energy pile system , *Acta Geotechnica*, Under Review.

as an alternative for buildings energy supply, further considerations should be made to keep the mechanical response of the energy piles in the admissible range.

5.1 Introduction

The energy consumption has increased all over the world due to the population growth and industrial needs. One of the alternatives to address this increasing energy demand is the application of new technologies to harness the energy stored in the ground due to the moderate temperature of the ground all over the year [15, 74]. One of the most promising technologies for the application of geothermal energy is the Ground Source Heat Pump (GSHP). Such a system consist of a heat pump, ground heat exchangers, and a heat distribution system. The ground heat exchangers (GHEs) can be an open-loop or a closed-loop system and its selection depends on various parameters that impact the feasibility of the project such as the availability of natural groundwater, ponds or lakes. Despite the simple design and better thermodynamic performance of an open-loop system, environmental regulations restrict the application of this type of GHE. In fact, changes in groundwater temperature during the operation of GSHP may result in an increase in the bacterial content and suspended particles in groundwater [116].

On the other hand, closed-loop systems can be installed horizontally (straightly horizontal or spirally horizontal loops placed in trenches) or vertically (U-shaped, W-shaped or spiral loops placed in boreholes) depending on the availability of land and energy demand. One of the disadvantages of the application of horizontal loops in cold regions like Canada is that the ground temperature is subjected to seasonal variation at shallow depths [160]. However, the installation costs of vertical closed-loop systems can be fairly high depending on depth and the required number of boreholes [87]. To overcome this issue, a rapidly growing construction tech-

nology, which integrates the geothermal energy technique into the structural pile foundation system has been developed [23, 25, 53, 82]. The geothermal pile operation principle is based on the circulation of a heat carrier fluid in polyethylene pipes embedded in the piles through which heat exchange occurs between the geothermal energy pile and the surrounding medium [154, 51, 46, 18]. This energy further feeds the GSHP system so that the geothermal energy pile acts as heat exchangers in addition to their main function as structural support elements.

Geothermal piles are broadly applied in European countries [20, 82, 21, 10, 6, 22], but in Canada, the application of such foundation systems is not well established and limited knowledge regarding the thermal and mechanical operation of them exists. For example, Laloui et al. [81] have carried out experimental tests on a full-scale pile within the foundation of a four story building in Lausanne, Switzerland. The tested pile was equipped with one U-shape probe for transferring heat. To record the temperature, load, vertical and radial strains, the specific instrumentation such as vibrating strain gauges, fibre optic extensometers and a load cell at the pile toe were used. Based on the results, the effective axial load on the pile is impacted by the thermal cycles especially at the pile toe where the axial load can be twice as effective as only the mechanical loading stage. Further in another analytical study, Laloui et al. [82] showed that thermal loading induced an increase in compressive stress of the pile. Despite the mentioned effects of the thermal loads on the pile, the integrity of the pile was not threatened and the maximum compressive stresses lied within the admissible range. In a large-scale project, Pahud and Hubbuch [118] designed and studied the thermo-mechanical function of 300 geothermal energy piles, which were built for supporting the structural load of the Terminal E of Zürich airport as well as contributing to heating and cooling supply of the building. The designed system included geothermal piles each contained 5 U-pipe heat exchangers which were aimed to provide 3,050 MWh/yr and 1,210 MWh/yr of the building heating and cooling

demand, respectively. Reports signified that performance of the designed geothermal piles was satisfactory, especially for heating purposes, and the GSHP system worked with coefficient of performance (COP) of 4.9 while meeting the piles geotechnical design criteria (i,e., pile settlement and the maximum compressive loads). In another experimental work, Bourne-Webb et al. [20] conducted some in-situ tests on a single thermo-active pile installed in London Clay. The main scope of the in-situ tests was to evaluate the mechanical performance of the pile subjected to thermal cycles. The temperature and strain profiles of the tested pile were recorded using an optical sensor system, vibrating-wire strain gauges, thermistors, and external load control elements. Based on the obtained results, variations in the temperature of the pile, depending on whether the pile is heated or cooled, changed the mobilized shaft friction along the pile- soil interface. It was speculated that if the margin between the pile ultimate shaft resistance and shaft friction along the soil-pile interface is large enough, the pile capacity will not change significantly.

Efforts for the application of energy foundations have recently been expanded in North America. For example, Akrouch et al. [4] carried out an experimental study on the time dependent thermo-mechanical (TM) behavior of a single geothermal energy pile which was installed and instrumented at the campus of the Texas A&M university. One of the important remarks of this study was that the soil properties at the construction site, which included very stiff high plasticity clay in which the creep rate might be an important parameter to consider. The obtained results confirmed that the increase in soil temperature due to the operation of the pile during the cooling mode (heat injection to the ground during summers) increased the creep rate of clay which correspondingly caused the increase in long-term displacement of the pile. Therefore, the application of the thermo-active pile that was installed in highly plastic clay was not suggested for cooling dominated climates (i.e., warm regions).

The above-mentioned experimental studies were mainly aimed at investigating the behavior of single geothermal energy piles. However, in many large-scale projects, piles are designed in a group. Mimouni and Laloui [107] undertook full-scale in-situ experiments on a group of four geothermal energy piles to quantify the group effects caused by thermal load over a span of 25 days. It was observed that heating the entire foundation contributed to an increase in displacement of individual piles although the differential displacements were reduced compared to a thermally-activating an individual pile. While Mimouni and Laloui [107] experimentally investigated the short-term behavior of a group of energy piles, Murphy et al. [111] studied the TM behavior of eight full-scale energy piles, which were constructed for a building at the US air force academy, over 658 days. It was concluded that a 18°C temperature increase in the piles induced the maximum compressive axial stress of 5.1 MPa, which is too small to surpass the allowable axial stress of the pile. In addition, the upward displacement of the piles head ranged between 1.3–1.7 mm, which concluded to be too small to cause angular distortions contributing to structural and aesthetic damage of the building.

Although full-scale in-situ experiments are more reliable to evaluate the TM response of energy piles, they usually require a fair amount of budget and time. An alternative approach to estimate the behavior of the geothermal energy piles is analytical or numerical studies. For example, Pasten and Santamarina [120] evaluated the mechanical behavior of energy piles using the one-dimensional load transfer method. This study emphasized on the importance of the first few cycles of thermal loading in assessing the pile head displacement and corresponding shaft friction variations.

Jeong et al. [69] carried out a three-dimensional (3D) finite element analysis to quantify the axial load and settlement of geothermal energy piles in a group which are subjected to TM

loading. This study highlighted the importance of soil type on the mechanical response of the thermo-active piles. It was concluded that the head displacement of the energy piles embedded in clay was up to 1.5 mm larger than the head displacement of piles installed in sand although both cases were in acceptable limits.

One of the significant advantages of numerical analysis over in-situ tests is the potential for studying the behavior of thermo-active piles over long-term periods. Olgun et al. [115] studied the long-term displacement of different arrangements of geothermal energy piles over a 30-year span of time under different climatic conditions. Impact of climate condition manifested itself as a variation in the ground temperature as well as a variation of energy demand of the building for which the thermo-active foundation was designed. This factor has been studied by Saaly et al. [128] Liu et al. [95], and Andolfi et al. [10].

Although broadly expanded in Europe and US, in Canada, the application of geothermal piles is not well established and limited knowledge regarding the thermal and mechanical operation of such systems exists. In Canada, the operation of GSHP systems may not be satisfactory and may degrade over a few years of the operation of geothermal energy piles [66]. The reason for such malfunction is underground thermal imbalance, which is the term used for the gradual decrease in the ground temperature over years because of an excessive heat extraction for heating the space during the long winter season. As soil temperature decreases, the outlet temperature of the GHE lowers gradually. This contributes to the deterioration of the heating performance of the GSHP. In addition, the underground thermal imbalance and excessive heat extraction can decrease the soil temperature below the freezing point. This causes freezing at the pile-soil interface which temporarily increases the bearing capacity of the geothermal energy pile. However, during spring, thawing occurs at the soil-pile interface, which decreases

the bearing capacity of the piles significantly. The occurrence of such freezing and thawing cycles at the soil-pile interface adversely affects the structural integrity as well as the energy efficiency of such systems [94]. Therefore, it is of paramount importance to consider the potential occurrence of ground thermal imbalance, i.e. the energy performance, in the design of geothermal pile foundation systems in cold regions.

In urban areas, the ground temperature below the buildings base area is fairly higher in comparison to open fields due to the heat dissipation of buildings through their sub-grade enclosures [56]. Such heat can further be re-harvested by a geothermal foundation system which favorably affects the efficiency of the GSHPs. Moreover, this additional dissipated heat from the building basement can ameliorate the potential thermal imbalance in the ground. In this regard, Saaly et al. [128] conducted a study to determine the thermal capacity of a proposed hypothetical geothermal foundation system considering the heat loss through the basement of an institutional building in cold regions. The geothermal energy piles are subjected to both thermal loads due to temperature variations of the fluid heat exchanger whose magnitude is a function of the building heating and cooling demand as well as structural loads [9]. Therefore, aside from the energy performance of the system, the impacts of thermal loading on the structural performance of geothermal piles should be assessed. For example, thermal loads cause volumetric expansion and contraction when piles are heated and cooled, respectively. In addition, the thermo-mechanical properties of soils surrounding the pile foundation are temperature-dependent, which can affect the interaction between the soil and foundation at their interface [26].

This chapter is aimed to investigate the thermo-mechanical behavior of a single pile in a geothermal energy foundation system, which is designed for energy supply of an institutional

building in Winnipeg, Canada. This foundation system is subjected to heat dissipation through the below-grade enclosure of the building. The present work is intended to provide a tool for prediction of the thermo-mechanical response of energy piles by incorporating the knowledge of buildings energy loss.

5.2 Thermo-Mechanical Model

5.2.1 Governing Equations

A coupled thermo-mechanical model has been applied to assess the mechanical and thermal behaviors of one of the piles of the SPEB foundation equipped with a heat exchanger pipe. The governing equations applied to study the thermo-mechanical behavior of the geothermal pile in contact with the surrounding soils are based on the following assumptions:

- Soil is considered to be fully-saturated having two-phases (solid skeleton and water). The soil is modeled as an isotropic, elastoplastic material. The Mohr-Coulomb constitutive model is used to determine the size of the yield surface in the soil.
- Pile material is taken to be solid, isotropic and linear elastic.
- Perfect contact has been assumed at the interface between the soil and pile.
- The solid grains and fluid phase of the soil are modeled as incompressible materials.

Considering the above-mentioned assumptions, the set of governing equations proposed by Laloui et al. [82] and Amatya et al. [6] are applied in the present analysis.

To consider the equilibrium of forces in the domain, the conservation of linear momentum in absence of inertial terms is applied:

$$\nabla.\boldsymbol{\sigma} + \mathbf{b} = 0 \tag{5.1}$$

where $\nabla.$ is the divergence operator, σ is the total (Cauchy) stress tensor and **b** is the body force vector which can be determined as shown below:

$$\mathbf{b} = \rho\, \mathbf{g} \tag{5.2}$$

where, **g** is the gravitational acceleration vector and ρ is the average bulk density of the soil which can be determined by the following equation:

$$\rho = (1 - n)\ \rho_s + n\, \rho_w \tag{5.3}$$

in which ρ_s and ρ_w are the density of solid skeleton and water, respectively. n is the porosity of the soil.

The constitutive law of the solid skeleton describing the stress-strain relations is defined in terms of the effective stress as described in Eq. 5.4.

$$\boldsymbol{\sigma}' = \boldsymbol{D}^{\boldsymbol{e}} \left(\boldsymbol{\varepsilon} - \boldsymbol{\varepsilon}^{\boldsymbol{T}} - \boldsymbol{\varepsilon}_{\boldsymbol{pl}}\right) \tag{5.4}$$

where $\boldsymbol{D^e}$ is the elastic stiffness tensor, $\boldsymbol{\varepsilon}$ is the strain tensor, $\boldsymbol{\varepsilon^T}$ is the thermal strain tensor, and $\boldsymbol{\varepsilon_{pl}}$ is the plastic strain tensor. Plastic strains are computed by the Mohr-Coulomb yield criterion. Also, the thermal strains are computed using the following equation:

$$\boldsymbol{\varepsilon^T} = \frac{1}{3}\ (\alpha_s \nabla T)\ \boldsymbol{I} \tag{5.5}$$

in which $\boldsymbol{\varepsilon^T}$ is the thermal strain tensor, $\boldsymbol{I}$ is the second order unit tensor, α_s is the volumetric thermal expansion coefficient, ∇ is the gradient operator, and T stands for the temperature.

To determine the heat transfer in porous media, the energy conservation equation is described below:

$$\rho C\ \frac{\partial T}{\partial t} + \nabla .\ q_c = 0 \tag{5.6}$$

where ρC is the volumetric heat capacity of the soil which is a function of volumetric heat capacity of solid skeleton ($\rho_s C_s$) and pore water ($\rho_w C_w$) as described below:

$$\rho C = (1-n)\ \rho_s C_s + n\ \rho_w C_w \tag{5.7}$$

In Eq.5.7, q_c [W/m^2] is the conductive heat flux through the volume which is defined by Fourier's law as follows:

$$q_c = -\lambda\ \nabla T \tag{5.8}$$

where λ denotes the effective thermal conductivity of the material whose value for the soil can be determined as described in Eq. 5.9.

$$\lambda = (1 - n)\ \lambda_s + n\ \lambda_w \tag{5.9}$$

in which λ is the effective thermal conductivity of the soil, λ_s is thermal conductivity of solid grains and λ_w is thermal conductivity of water.

5.2.2 Numerical Model

The time-dependent numerical model has been implemented in the finite-element commercial software COMSOL Multiphysics. The dimension of the 2D axisymmetric model applied in this study is 10 m × 10 m. On top of the soil domain, a 0.23 m thick layer of thermal insulation and a 0.2 m thick layer of concrete slab are placed (Fig. 5.1). The modeled pile is a friction pile which has a diameter of 0.4 m and a length of 5 m. The thermo-mechanical properties of the materials used in the model (soil (in wet condition), concrete and insulation) are summarized in Table 5.1.

Based on the structural and design documents, 5 m micro-piles have been used in the foundation of the SPEB considering the structural load and geotechnical parameters.

The boundary conditions of the thermo-mechanical (TM) model are as follows:

- The thermal boundary conditions: constant temperature on the heat exchanger, adiabatic condition at the bottom and surrounding boundaries are considered. Also, to estimate

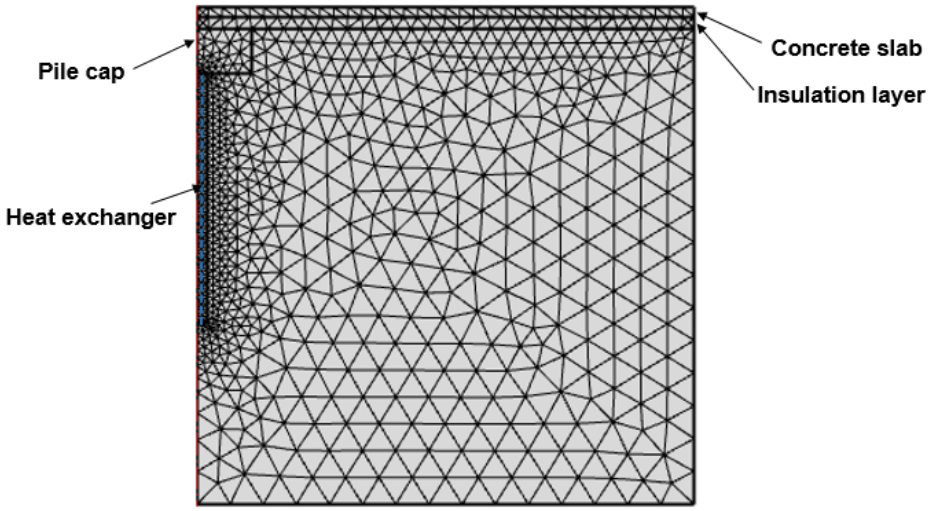

Fig. 5.1: Axisymmetric finite elements model.

the impacts of heat dissipation through the building basement slab, a convective heat flux q_0 $[W/m^2]$ is assigned to the top boundary of the model as follows:

$$q_0 = h\,(T_{indoor} - T_s) \tag{5.10}$$

where h is the convective heat transfer coefficient whose value is assumed to be equal to 6 W/m^2°C [94], T_{indoor} is the basement indoor air temperature that is assumed constant and equal to 20°C, T_s [°C] is the temperature at the ground surface.

- The mechanical boundary conditions: the roller condition on the right boundary of the model, and fixed constraint at the bottom of the domain are considered. An axisymmetric condition is assumed from the left boundary.

The initial temperature of the model is assumed to be equal to 8°C [128]. Also, the initial stress conditions are obtained from the results of another steady-state simulation considering only the gravity effects. In other words, the finite element analysis has been done in two stages.

Soil	
Young's modulus [Pa]	70×10^6
Poisson ratio [-]	0.236
Density [kg/m^3]	1767
Thermal conductivity [W/m°C]	1.483
Specific heat capacity [J/kg°C]	960
Thermal expansion coefficient [1/K]	1.7×10^{-5}
Porosity [-]	0.535
Cohesion [kPa]	5
Friction angle [°]	18

Concrete	
Young's modulus [Pa]	40×10^9
Poisson ratio [-]	0.2
Density [kg/m^3]	2300
Thermal conductivity [W/m°C]	1.5
Specific heat capacity [J/kg°C]	880
Thermal expansion coefficient [1/K]	8.5×10^{-6}

Insulation	
Density [kg/m^3]	34
Thermal conductivity [W/m°C]	0.041
Specific heat capacity [J/kg°C]	1450

Tab. 5.1: Properties of SPEB's numerical model.

Through the first stage, a steady state analysis has been carried out while considering the gravity effects to generate the initial stresses as the input for the transient simulation. In the transient stage, the energy pile response to the applied axial load and thermal cycles has been studied over a five-year span of time.

5.2.3 Model Validation

To validate the implemented TM model in this work, the model has been used to investigate the behavior of the geothermal energy pile that was experimentally studied by Bourne-Webb et al.

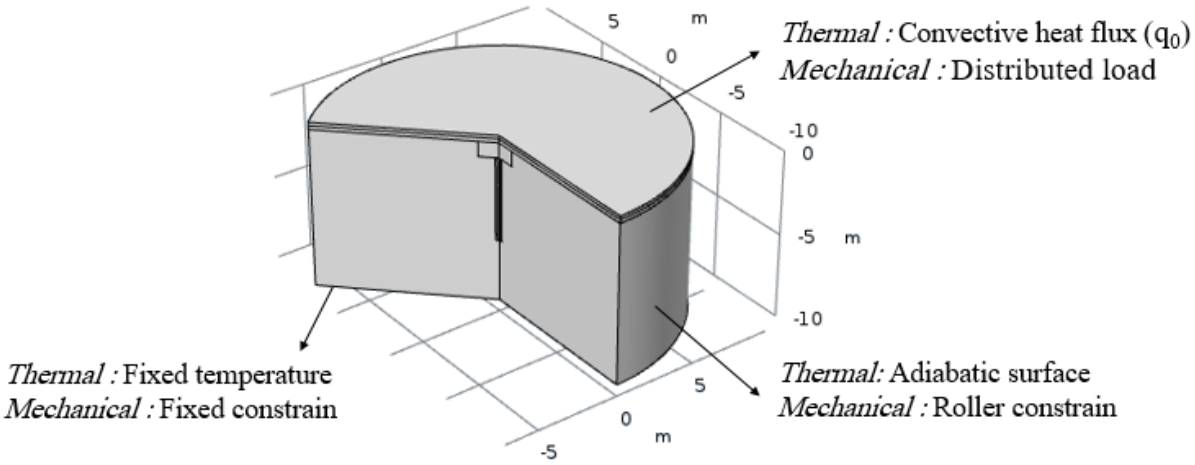

Fig. 5.2: The Thermo-Hydro-Mechanical boundary conditions applied to the model.

[20]. The experimental data has been obtained from the full-scale study that was undertaken on a test pile that was equipped with the heat exchanger pipes. The mentioned pile was designed as part of a 143 piles foundation system of a five-storey building that was located in the Clapham Centre of Lambeth College London and functioned as a geothermal heat exhchanger of a GSHP system. The pile is installed in the London clay whose properties are reported in Table 5.2. The tested pile had a diameter of 0.6 m and a length of 23 m.

Property	Concrete	London Clay
Young's modulus [Pa]	40×10^9	70×10^6
Poisson ratio [-]	0.2	0.236
Unit weight [kN/m^3]	20	20
Thermal conductivity [W/m°C]	2.33	1.79
Specific heat capacity [J/kg°C]	960	910
Thermal expansion coefficient [1/K]	8.5×10^{-6}	4×10^{-5}
Hydraulic conductivity [m/s]	-	1×10^{-11}
Porosity [-]	-	0.4

Tab. 5.2: Characteristics of the validation model's material

The conducted tests included both heating and cooling cycles in conjunction with a mechanical load. The test pile response to the applied thermo-mechanical loads was obtained using Vibrating Wire Strain Gages (VWSG) and Optical Fibre Sensors (OFS). As shown in Fig. 5.3, the first stage of the experiment included applying a 1200 kN mechanical load. During the cooling stage, a thermal load of ΔT = -19°C in addition to the 1200 kN mechanical load was applied to the pile. Finally, the heating phase which consisted of the mechanical load and a thermal gradient of ΔT = +10°C was carried out.

The initial temperature of the pile and soil in the London case had been assumed constant over the entire domain and equal to 19.5°C and the thermo-mechanical loading time applied in this study lasted for almost 1250 days.

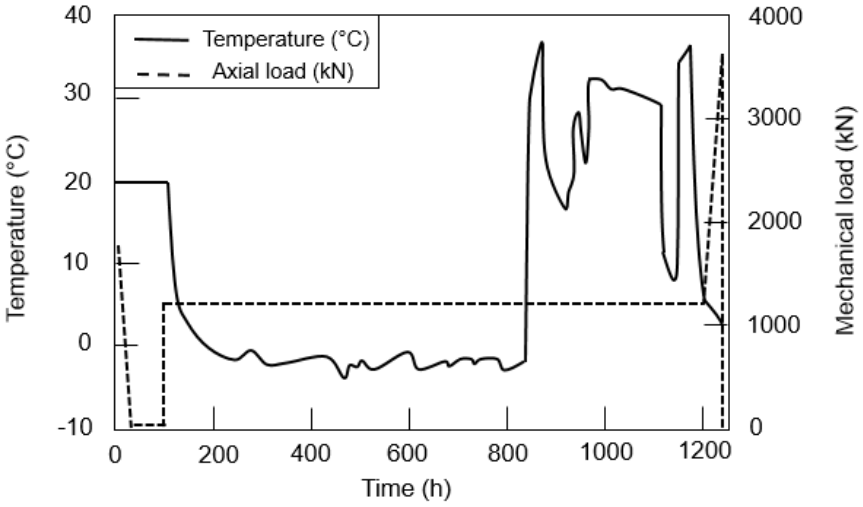

Fig. 5.3: Thermo-mechanical loading history of experimental case (Bourne-Webb et al. 2009).

Comparing the pile head displacements obtained from the experimental tests and the numerical model, good agreement was found during the cooling phase (100 – 860 h) (Fig. 5.4). Although the magnitude of vertical displacement of the pile head during the heating loading is slightly lower in the numerical model, the similarities are acceptable from an engineering

point of view to consider the model an appropriate tool for predicting the thermo-mechanical behavior of the geothermal energy pile.

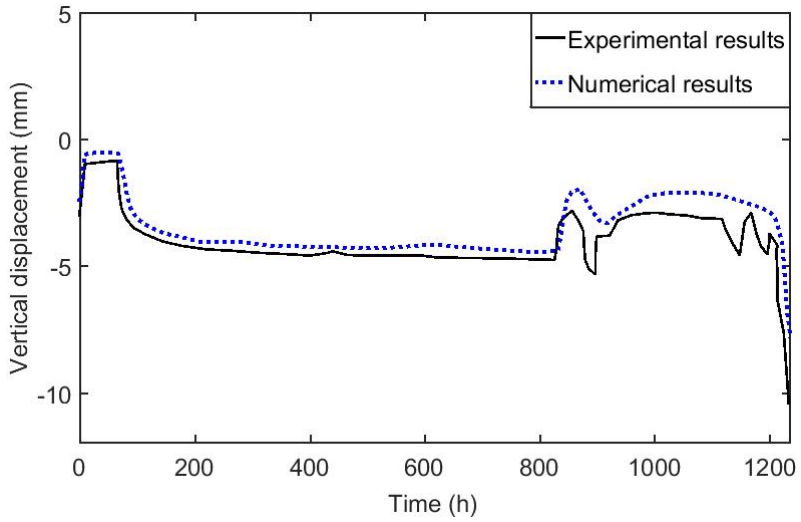

Fig. 5.4: Comparison between the numerical and field data regarding the vertical displacement of the pile head.

5.2.4 Thermo-Mechanical Loading History of the Geothermal Energy Pile in SPEB

The validated numerical model in COMSOL Multiphysics is applied to investigate the behavior of one of the geothermal piles of the SPEB's foundation. The total loading time was 1825 days (five years) which included the seasonally cyclic thermal loads (i.e., 6 months heating and 6 month cooling per year) in addition to a constant mechanical load. The mechanical load was equal to the ultimate capacity of the friction pile (i.e. 1000 kN) that is applied with a factor of safety of 3. It should be noted that the bearing capacity of the pile is computed by the ultimate end-bearing, and ultimate skin friction capacities.

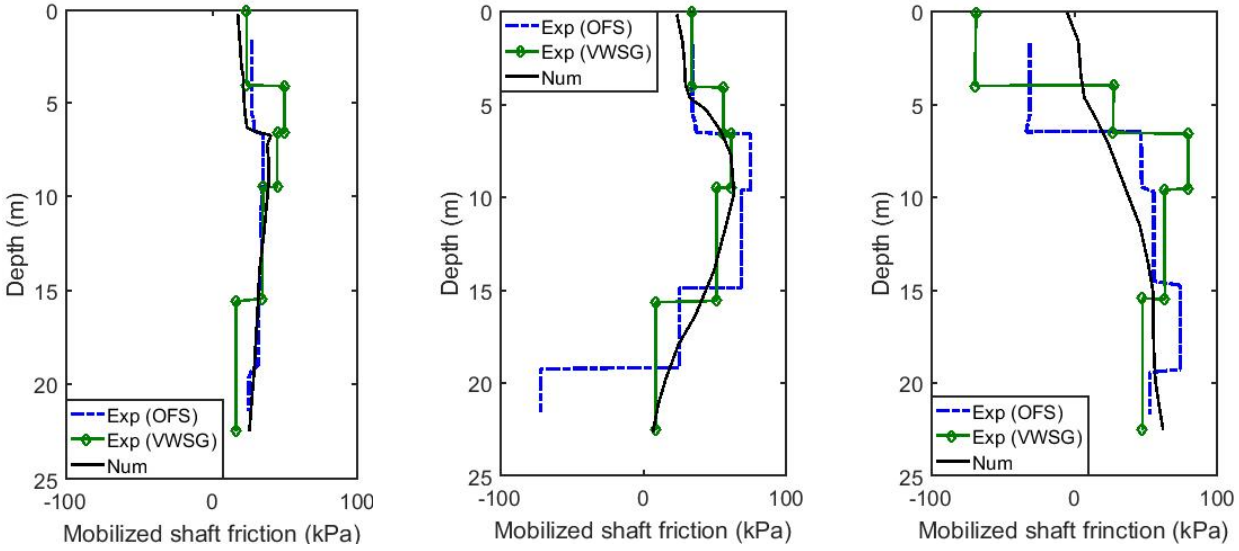

(a) Mechanical (b) Mechanical+Cooling (c) Mechanical+Heating

Fig. 5.5: Comparison between numerical (Num) and experimental (Exp) results of mobilized shaft friction along the pile

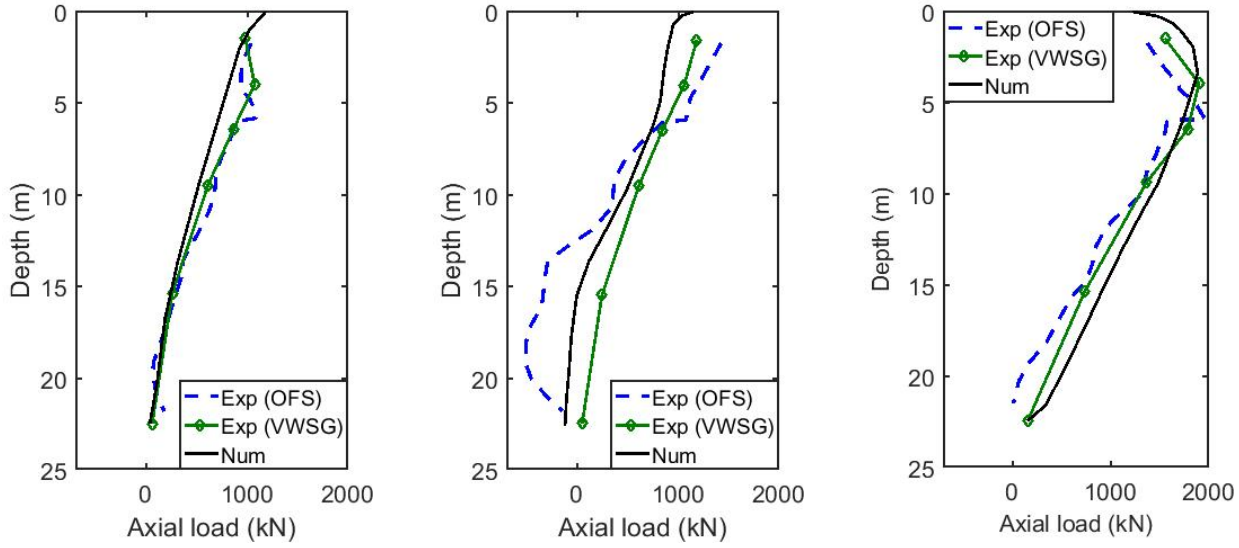

(a) Mechanical (b) Mechanical+Cooling (c) Mechanical+Heating

Fig. 5.6: Comparison between numerical (Num) and experimental (Exp) results of axial load along the pile

As mentioned earlier, the thermal load is applied to the pile while the heat transfer fluid circulates in the heat exchanger pipes. In this work, such a thermal load is represented by a constant temperature, which is equal to the inlet temperature of the heat exchanger fluid, along the length of the heat exchanger pipe. Based on the numerical study carried out by Saaly et al. [128], the inlet temperatures of the pipe have been suggested to be equal to 20°C during May–Oct, and -1°C during the 6 cold months (Nov-Apr) of the year. As mentioned before, the inlet temperatures were chosen to meet the thermal balance of the ground during heat extraction and rejection over the year as well as to avoid freezing at the soil-pile interface. Fig. 5.7 provides the seasonal variation of the inlet temperature of the heat exchanger probes as well as the mechanical load applied to the head of the pile.

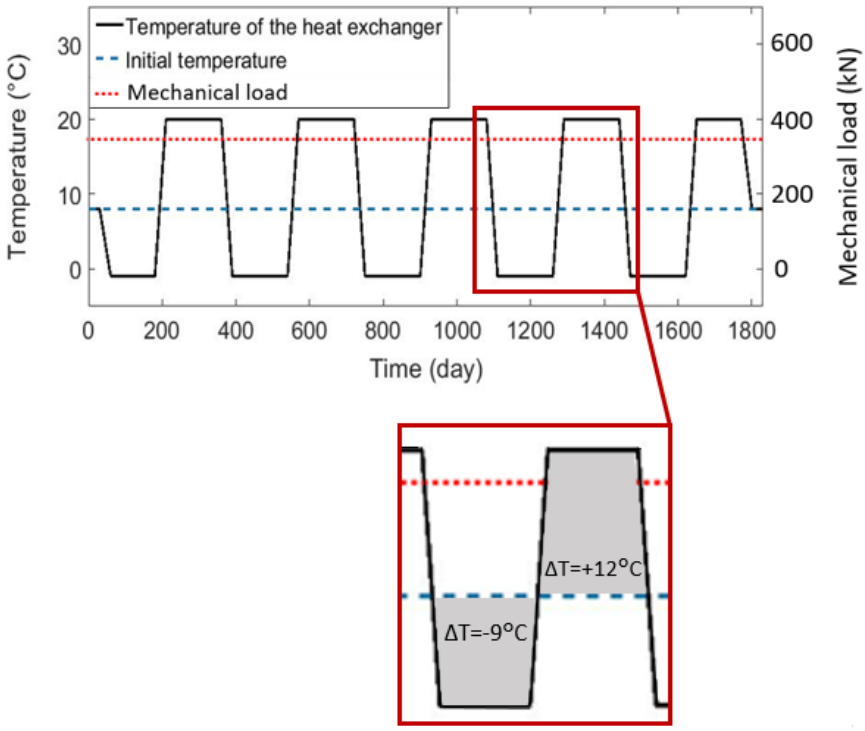

Fig. 5.7: Time histories of applied thermal and mechanical loads.

To demonstrate the initial pile settlement due to only the mechanical load, during the first 30 days of the simulation the temperature in the probes are equal to the initial temperature ($T_{initial}$ = 8°C). In addition, during the last 30 days of the loading time history, the temperature of the probes are equal to 8°C to evaluate the reversibility of pile head displacement induced by the thermal loads.

5.3 Results and Discussion

To study the performance of a thermo-active pile subjected to thermo-mechanical loadings, the vertical displacement of the pile, the maximum axial load induced by the thermo-mechanical loads and the mobilized shaft friction along the pile-soil interface are investigated in this section. The reason is that such factors are considered in the Limit State-based geotechnical design.

The thermo-active pile and its surrounding soils were subjected to an additional thermal load due to the heat loss through the slab of the basement floor. Such heat dissipation from the basement into the ground occurred in spite of insulating the basement envelope [43, 71, 79, 38]. The reason was that the basement slab was in direct contact with the foundation soil whose temperature was different from the regulated temperature of the basement indoor air. Consequently, the thermal gradient between the foundation soil and basement indoor air contributed to heat loss via the thermal conduction through the floor slab [30, 128]. The impacts of such heat leakage is often ignored while assessing the geothermal energy piles behavior. Therefore, this heat loss was incorporated in the model using a convective heat flux which was assigned to the basement slab surface. The geothermal energy pile response to the thermo-mechanical loading is provided for two cases: without considering heat loss through the basement slab (Case 1) and with considering the basement energy loss (Case 2).

5.3.1 Pile Head Displacements

The initial pile head displacement that was induced by the mechanical load at the end of the first 30 days of the simulation time history was equal to -0.79 mm (Fig. 5.8). Once heat extraction from the ground by applying a $\Delta T = -9°C$ began, further pile head displacement occurred whose maximum reached to -1.19 mm at t = 182 days (i.e., the end of the heating season of the first year of the system operation). Such observation was induced due to the contraction of the pile due to the temperature decrease in the probes with respect to the initial temperature of the pile (Fig. 5.7). For the case with no heat loss through the basement (Case 2), the minimum pile head displacement reached -1.18 mm at t = 182 days. This means that during the first few months of the analysis, the heat loss through the slab was not effective enough to influence the pile head displacement. This could be because of the significant thermal mass of the ground in the short time.

In contrast, during the heating loading (May–Oct), the geothermal pile expanded upon a +12°C temperature increase. The maximum expansion, whose value was +0.43 mm relative to the initial settlement, happened at t = 1795 days (i.e., the end of the cooling season of the fifth year of analysis). However, without considering the energy loss from the slab, the maximum expansion reached to +0.31 mm which showed occurrence of 15% less expansion compared to the maximum expansion of the pile head in Case 2. This discrepancy was due to heat leakage through the basement which increased the soil temperature near the basement floor and correspondingly caused more expansion at the pile head. It should be noted that the computed pile displacements (Fig. 5.8) were considerably less than the acceptable settlement (i.e., 25 mm) recommended by the National Building Code of Canada [113].

During the last 30 days of the operation of the system (i.e. at the end of the fifth year; 1795–1825 days), the inlet temperature of the pipes was set equal to the initial temperature of the pile ($T_{initial}$ = 8°C) to evaluate the reversibility of displacement induced by the thermal loads. It was observed that 40% and 25% of the initial pile head displacement left in the pile for the cases with and without considering heat loss, respectively. In other words, the vertical displacements of the pile head were not fully reversible which is believed to be due to the elastoplastic behavior of the soil. In addition, for the case in which the basement energy loss was taken into account, the soil temperature increased up to 1.5°C near the basement floor. Therefore, a larger residual displacement was observed for this case.

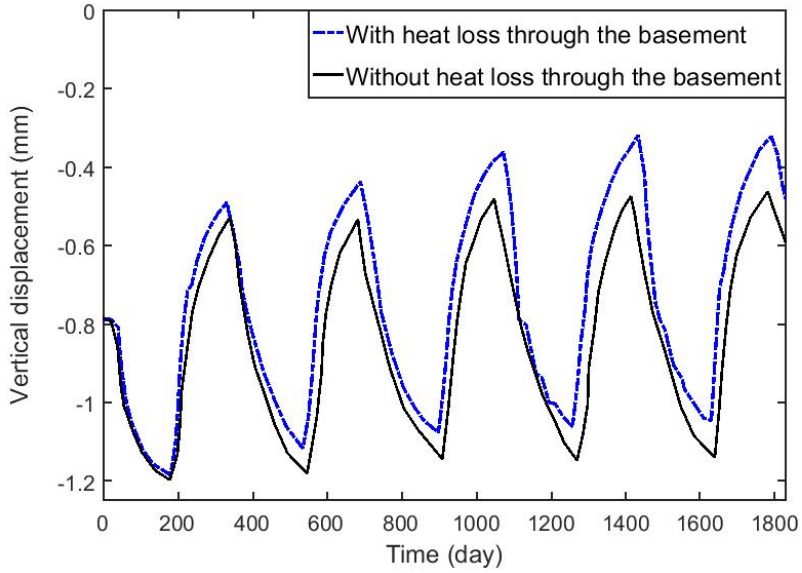

Fig. 5.8: Vertical displacement of the pile head with and without consideration of the heat leakage from the SPEB basement.

5.3.2 Axial Load and Mobilized Shaft Friction Variations

In Case 1, in the stage in which the pile was subjected to only mechanical load, the pile was fully compressed. However, when a cooling load was applied in addition to the mechanical load to

extract heat from the ground ($\Delta T < 0^{\circ}C$), the concrete pile contracted. Pile contraction induced tensile forces in the pile. Therefore, the axial load along the pile length decreased compared to the only mechanical loading stage. The maximum reduction in axial load that was applied on the pile due to the cooling load is 28 kPa (i.e., 9% reduction in the axial load during cooling stage loading compared to mechanical loading stage) that occurred at 0.9 m below the pile head (Fig.5.9a).

Contrary, at the end of the heating loading stage, compressive forces were generated in the pile due to the pile expansion. Consequently, up to 3% increase in compressive load compared to the initial mechanical load applied on the pile (i.e., 333 kN) was observed along the length of the pile.

According to the results regarding the axial load along the pile axis for Case 2, at the end of heating loading stage, the pile was up to 9% more compressed compared to the initial mechanical load applied on the pile (i.e., 333 kN) (Fig. 5.9b). It was observed that the maximum compressive load in Case 2, which was equal to 363 kN, was induced at the pile depth of 0.6 m during the heating loading stage. While the maximum axial load that was induced during heating loading at the same pile depth in Case 1 was 342 kN which was 6% lower than the maximum axial load in Case 2. The reason was the additional pile expansion in Case 2 due to the heat loss through the basement. Such results signify that considering the buildings heat leakage through the underground enclosure in urban areas may be an important factor in assessing the geothermal energy pile response to thermo-mechanical loading.

The axial load distribution illustrated in Fig. 5.9 signified that the thermal cycles change the magnitude of the induced axial load along the pile. In other words, the heating load (i.e., $\Delta T = +12^{\circ}$C) increased the induced axial load along the pile up to 9%. Such an increase in

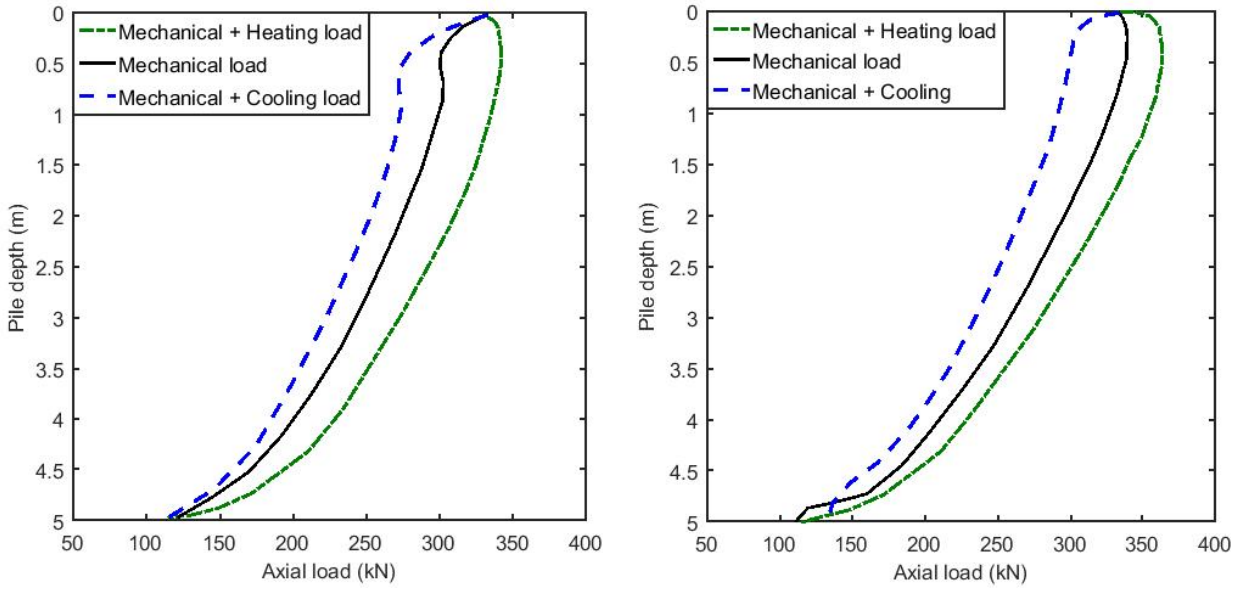

(a) Without considering the heat loss through the basement.

(b) Considering the heat loss through the basement of the SPEB.

Fig. 5.9: Axial load distribution along the pile axis.

the axial load along the pile should be addressed in the geotechnical design by considering a higher factor of safety. For example, in Case 2 that the obtained maximum compressive axial load along the pile axis was 363 kN, 9% increase in the factor of safety (initially considered to be equal to 3.0) is required to ensure safe application of the thermo-active pile since the pile was initially designed for allowable load of 333 kN. In practice, a factor of safety of 3.5 fulfils the required safety margin for the pile that is studied in this work.

The distribution of the mobilized shaft frictions along the pile-soil interface under three different conditions; (i) mechanical loading, (ii) heating and mechanical loadings, and (iii) cooling and mechanical loadings are provided in Fig. 5.10. During only the mechanical loading, the direction of the skin friction was upward and decreased by depth. However, during the cooling loading stage (i.e., winter) the mobilized shaft friction along the length of the pile, upper than

the neutral point, increased (maximum 3% increase in mobilized shaft friction at the pile depth of 0.3 m compared to the mechanical loading stage) while along the length of pile, lower than the neutral point, decreased up to 9% due to the contraction of the concrete pile. Conversely, during the heating loading stage that expansion occurred in the pile, the mobilized shaft friction increased up to 5% along the length of the pile lower than the neutral point while along the upper part of the pile it decreased (maximum 3% decrease in mobilized shaft friction at the pile depth of 0.2 m compared to the mechanical loading stage).

Comparing the mobilized shaft frictions resulted from Case 1 and Case 2, it is observed that in Case 2 in which heat loss through the basement added more heating load to the ground, shaft frictions decreased up to 4% compared to Case 1. This happened since the additional heating load especially close to the basement floor induced more expansion compared to Case 1. This expansion led to a downward pile-soil friction which contributed to a lower shaft friction along the pile-soil interface in Case 2 compared to Case 1.

5.3.3 Thermal Field

The temperature profiles produced by the variation of the inlet temperature of the heat exchanger pipe in Case 1 are illustrated in Fig.5.11. The temperature fields of the model are provided for three stages of loading. In the first stage, the mechanical loading was only applied to the pile (Fig.5.11a). Since no thermal load was implemented in this stage, the temperature of the all domain was equal to the initial temperature ($T_{initial}$ = 8°C).

At the end of the cooling loading stage 5.11c, when the inlet temperature of the heat exchanger fluid was equal to -1°C, the temperature of the pile and the surrounding soil decreased. Despite the noticeable decrease, the average temperature of the soil at the pile-soil interface was equal

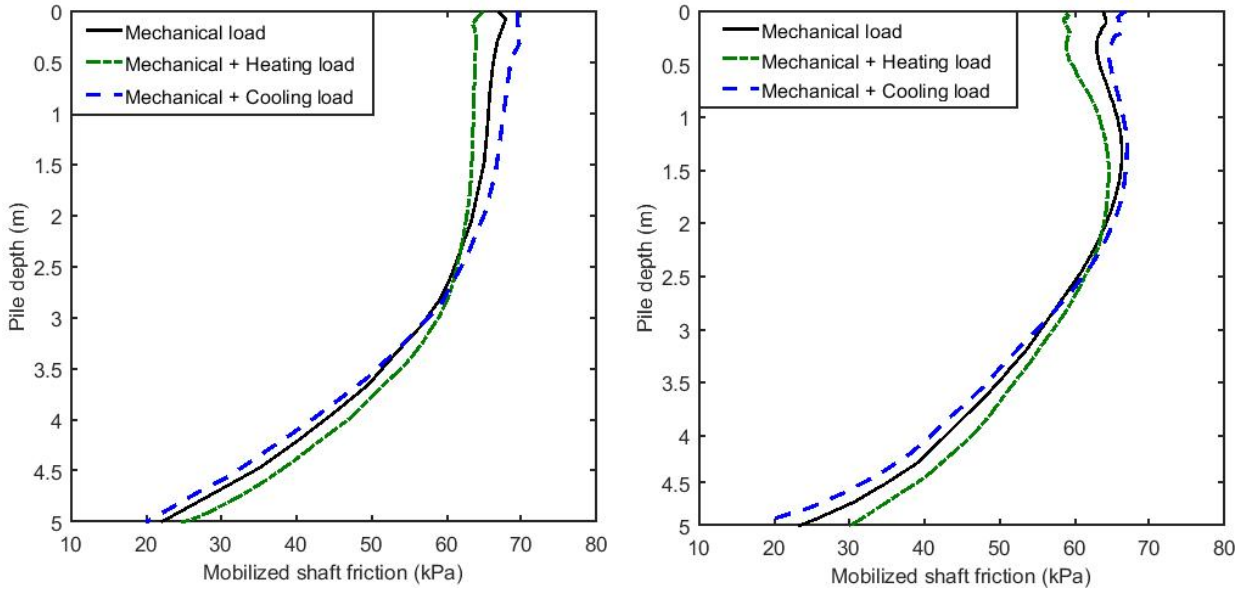

(a) Without considering the heat loss through the basement.

(b) Considering heat loss through the basement of the SPEB.

Fig. 5.10: Mobilized shaft friction distribution along the soil-pile interface.

to 3°C, which is above the freezing point. In other words, the "non freezing pile-soil interface" criterion was met using the inlet temperature of -1°C during the cooling loading stage. The temperature field at the end of the heating loading stage was shown in Fig. 5.11c. According to this figure, the temperature of the soil domain ranged from 8°C to 15°C.

The temperature fields of the model for Case 2 are shown in Fig. 5.12. The top boundary of the axisymmetric model in Case 2 was in direct contact with indoor air of the basement whose temperature assumed to be constant and equal to 20°C. Also, for the side and bottom boundaries of the model, adiabatic condition was considered. At the end of the mechanical loading stage (t = 30 days), the soil did not have enough time to absorb heat from the basement floor. Therefore, the temperature profile of the soil was equal to the initial temperature (Fig. 5.12a). The temperature profile at the end of cooling loading (Nov–Apr), when the inlet temperature of

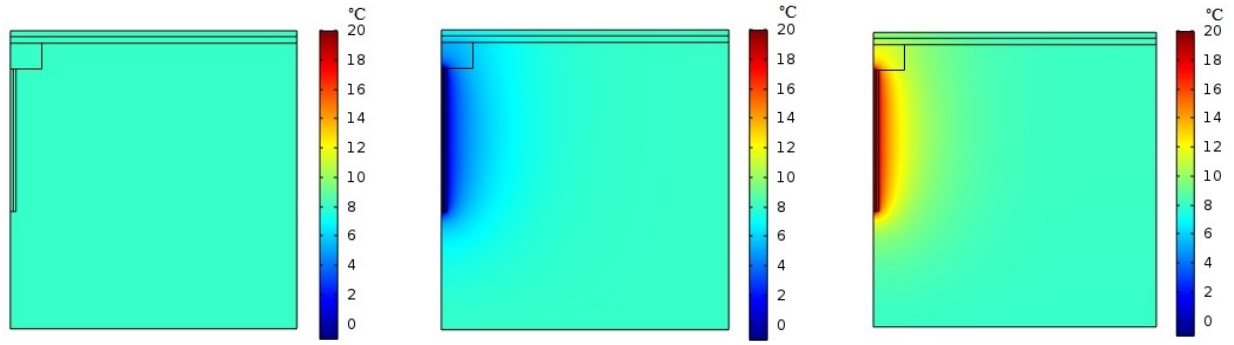

(a) Mechanical (b) Cooling+mechanical (c) Heating+mechanical

Fig. 5.11: Temperature profiles at the end of mechanical loading; cooling and mechanical loading; and heating and mechanical loading stages for Case 1.

the heat exchanger fluid was equal to -1°C, is provided in Fig. 5.12b. According to this figure, the temperature of the soil surrounding the pile decreased up to 5°C although above the freezing point. In addition, the soil temperature near the basement slab increased up to 1.5°C due to the heat loss through the basement.

At the end of the heating loading stage (May–Oct), when the temperature of the heat exchanger fluid was constant and equal to 20°C, the temperature of the pile and its surrounding soil increased compared to the initial temperature (Fig. 5.12c). The temperature of the ground far from the effective diameter of the pile, increased up to 1.5°C especially at shallower depth of soil. This was expected to happen due to the heat dissipation through the basement of the building.

5.4 Conclusion

Geothermal energy pile is the structural element that also serve as a geo-heat exchanger. In cold regions where the heating load of the building is commonly higher than the annual cooling load, the thermal imbalance may occur in the soil due to an excessive heat extraction from the

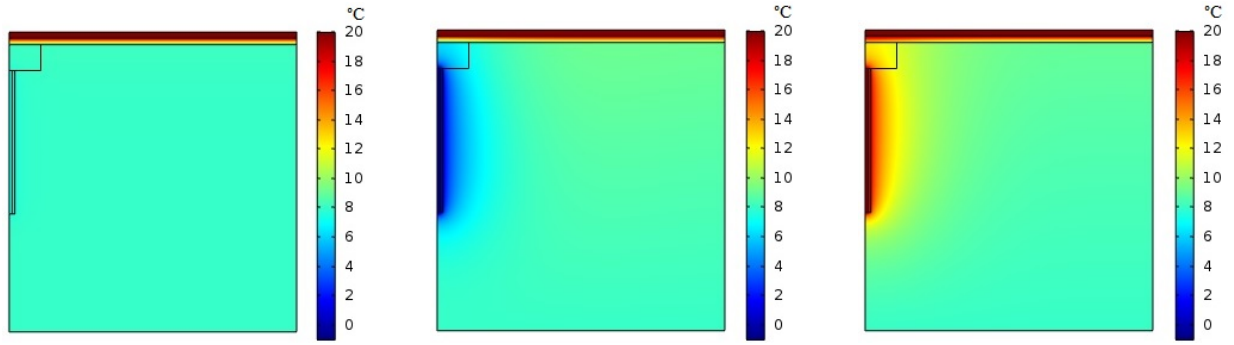

(a) Mechanical **(b)** Cooling+mechanical **(c)** Heating+mechanical

Fig. 5.12: Temperature profiles at the end of mechanical loading; cooling and mechanical loading; and heating and mechanical loading stages for Case 2.

ground. In design of such systems in cold regions, the energy performance of the geothermal energy pile system is of paramount importance. The heat extraction and injection from/to the ground must be designed in such a way to avoid freezing at the pile-soil interface as well as occurring ground thermal imbalance. In addition to the energy performance of the geothermal energy pile systems, their TM behavior should be investigated as well.

Due to the lack of information regarding the effect of heat dissipation through the basement slab on the geothermal energy pile's response, a numerical study was carried out. A single geothermal friction pile of a thermo-active foundation system that was designed for supplying the energy demand of the Stanley Pauley Engineering Building located in the Campus of the University of Manitoba, Winnipeg, Canada was considered. To this end, a 2D TM model was implemented in COMSOL Multiphysics and was validated against the field data obtained from the in-situ tests in the Lambeth College in London [20]. Based on the numerical analysis, the following conclusions can be made:

- During the cooling stage , the pile head downward displacement increased due to pile contraction. Although noticeable, the pile displacements were below the allowable pile settlement according to the National Building Code of Canada [113].

- The results verified that when the energy pile was subjected to heating and cooling loads, the thermal deformations generated additional compressive and tensile stresses during heating stage (May–Oct) and cooling stage (Nov–Apr), respectively. This necessitates further considerations in the geothechnical design and application of geothermal energy pile systems in cold regions. These considerations can be implemented in the form of increasing the factor of safety effective on the allowable load.

- The obtained results showed the importance of considering heat dissipation through the basement in evaluating the thermo-mechanical behavior of geothermal energy piles. The reason was that the heat loss through the basement worked as an additional thermal load which intensified the heating load and weakened the effects of applied cooling load on the pile.

- As the thermal loads were applied to the pile, the mobilized shaft friction along the pile-soil interface varied depending on the type of the loading stage (i.e., heating or cooling). For example, heating load caused up to a 7% decrease in shaft friction along the pile upper than the neutral point compared to shaft frictions induced during the mechanical loading stage. The same thermal load decreased the shaft friction along the pile lower than the neutral point up to 12%.

This work provided an insight into the mechanical behavior of a single pile of a geothermal energy foundation system. Result of this study in conjunction with thermal performance

analysis can facilitate further application of such systems in cold regions and more specifically Canada.

6 Conclusions and Future Works

6.1 Conclusions

In this thesis, a comprehensive numerical study including heat transfer modeling, and coupled thermo-mechanical modeling has been carried out. The set of governing equations were implemented in the commercial software COMSOL Multiphysics. Using numerical modeling, the problems encountered in cold regions were targeted as described bellow:

6.1.1 Energy Performance of the Below-Grade Structures

The energy efficiency of the below-grade envelope of an institutional building in the campus of the University of Manitoba, the Stanley Pauley Engineering Building (SPEB), was investigated using a thermal modeling. To this end, a heat transfer analysis was carried out with and without considering phase change of the soil pore-water. To overcome the energy loss through the sub-grade enclosure of the building, potential solutions were introduced and their corresponding impacts on energy efficiency of the basement envelope of the building were assessed. The important conclusions are drawn as below:

- Despite insulation of below-grade building fabric of the SPEB, energy was dissipated into the ground through the basement walls and floor which impacted the temperature of the ground.

- Modeling of the freezing soil and considering occurrence of phase change is important for an accurate assessment of sub-grade energy efficiency of the building.

- The 3-D thermal model determined the energy performance of the basement more accurately compared to the 2-D analysis. The reason was believed to be less accurate modeling of the basement corners where most of the heat loss through slab and walls occurs due to the thermal bridge. Moreover, the plain strain condition of the 2-D model led to overestimation of the annual energy loss through the basement envelope.

6.1.2 Geothermal Energy Pile Foundation Design

A hypothetical geothermal energy foundation system was proposed for the Stanley Pauley Engineering Building. Potential occurrence of the underground thermal imbalance due to operation of the thermo-active foundation was studied. Furthermore, the mechanical performance of a single pile of the proposed geothermal energy foundation system was analyzed using a coupled thermo-mechanical modeling which was developed in COMSOL Multiphysic. The developed model was validated against the data that was obtained from a full-scale study in the Clapham Centre of Lambeth College London. Then, the validated model was used to assess whether the settlements and stresses induced in the pile due to the thermal and mechanical loadings were in admissible limit.

The important conclusions are drawn as listed below:

- The proposed geothermal energy foundation system is applicable for the SPEB. However, the energy integrity of the system necessitated application of the proposed mitigation strategies for underground thermal imbalance improvement.

- Seasonal temperature changes is an important factor in performance of the proposed geothermal energy foundation system. As such, more analysis should be conducted for such energy foundation system in other regions with different climatic conditions.

- The TM model proposed in this thesis was able to accurately determine the displacement and axial loads along the pile. The numerical results showed a good agreement with the experimental test data.

- The energy loss through the building basement influenced the mechanical behavior of the energy pile since it worked as additional thermal load on the pile.

- Pile head displacements due to thermal loads were not high enough to surpass the admissible limits. The compressive loads effective on the pile increased during cooling season which necessitated further considerations in geothermal pile design.

6.2 Recommendations for Further Works

The recommendations for future work can be summarized as follows:

- The energy integrity of the below-grade structures is highly dependent on thermal properties of the ground. Also, the ground thermal properties are dependent on moisture content. In the present work, due to the actual site conditions, soil was assumed to be saturated. However, such analysis should be carried out on unsaturated soil to evaluate the effects of saturation degree on soil thermal properties and correspondingly the energy integrity of sub-grade envelope of buildings.

- The energy efficiency of the same building can be different in different climatic conditions. Therefore, more analysis should be undertaken to assess the thermal performance of buildings in different cities.

- The thermo-mechanical performance of one single pile of the proposed geothermal energy foundation system was assessed in this thesis. However, there is a need for more analysis into thermo-mechanical performance of groups of thermoactive piles to investigate the group effects on thermo-mechanical response of the piles.

- In present work, the effect of frost heave on structural integrity of thermoactive piles is ignored. Therefore as potential future work, a thermo-mechanical analysis considering the frost heave in the soil is recommended to be carried out.

- This work was based on numerical analyses. However, to better assess the energy performance as well as thermo-mechanical behavior of geothermal energy piles, lab-scale and field experiments are recommended to be conducted as a potential future-work.

Bibliography

[1] M. H. Adjali, M. Davis, C. Ni Riain, and J.G. Littler. „In situ measurements and numerical simulation of heat transfer beneath a heated ground floor slab“. In: *Energy and Buildings* 33 (2000), pp. 75–83 (cit. on pp. 16, 17).

[2] M.H. Adjali, M. Davis, and J. Litter. „Earth-contact heat flows: Review and application of design guidance predictions“. In: *Building Services Engineering Research and Technology* 19.3 (1998), pp. 111–121 (cit. on p. 15).

[3] J. Agemar T.and Weber and R Schulz. „Deep Geothermal Energy Production in Germany“. In: *Energies* 7.7 (2014), pp. 4397–4416 (cit. on p. 49).

[4] G. A. Akrouch, M. Sanchez, and J Briaud. „Thermo-mechanical behavior of energy piles in high plasticity clays“. In: *Acta Geotechnica* 9.3 (2014), pp. 399–412 (cit. on pp. 4, 57–59, 91, 125).

[5] K. Allaerts, M. Coomans, and R. Salenbien. „Hybrid ground-source heat pump system with active air source regeneration“. In: *Energy Conversion and Management* 90 (2015), pp. 230–237 (cit. on p. 82).

[6] B. Amatya, K. Soga, P. Bourne-Webb, T. Amis, and L. Laloui. „Thermo-mechanical behaviour of energy piles“. In: *Géotechnique* 62.6 (2012), pp. 503–519 (cit. on pp. 57, 124, 129).

[7] T. Amis, P. Bourne-webb, C. Davidson, Amatya. B, and K Soga. „The effects of heating and cooling energy piles under working load at Lambeth college: UK“. In: *Conference: 33rd Annual and 11th Intl. Conf. of the Deep Foundations Institute At: New York* (2008) (cit. on pp. 55, 56).

[8] O. B. Andersland and B. Ladanyi. „Frozen Ground Engineering“. In: *Wiley and Sons* (2003) (cit. on p. 17).

[9] M. Andolfi, R. M. S. Maiorano, A. Mauro, and N. Massarotti. „Experimental set-up and thermo hydro mechanical model for an energy pile“. In: *Proceedings of a conference on computational methods for thermal problems* Atlanta, USA, Georgia Tech (2016) (cit. on p. 128).

[10] M. Andolfi, R. M. S. Maiorano, A. Mauro, and N. Massarotti. „On the influence of thermal cycles on the yearly performance of an energy pile“. In: *Geomech Energy Environ* 16 (2018), pp. 32–44 (cit. on pp. 124, 127).

[11] L. Bai and W. Che. „Effects of the soil source heat pump borehole spacing and arrangement on the soil temperature of well group“. In: *Procedia Engineering* 146 (2016), pp. 441–444 (cit. on pp. 66, 67).

[12] K. Bakirci, O. Ozyurt, and O. Comakli. „Energy analysis of a solar-ground source heat pump system with vertical closed-loop for heating applications“. In: *Energy* 36.5 (2011), pp. 3224–3233 (cit. on p. 76).

[13] I. Beausoleil-Morrison and B. Kemery. „Analysis of basement insulation alternatives“. In: *Carleton University: Ottawa, ON* (2009) (cit. on p. 16).

[14] J. Bennet, J. Claesson, and G. Hellström. „Multipole method to compute the conductive heat flows to and between pipes in a composite cylinder“. In: *Notes on Heat Transfer* 3 (1987) (cit. on p. 71).

[15] P. Blum, G. Campillo, W. Munch, and T. Kolbel. „CO2 savings of ground source heat pump systems—a regional analysis“. In: *Energy and Buildings* 35.1 (2010), pp. 122–127 (cit. on pp. 89, 123).

[16] K. Bobko. *Energy Efficiency of Below-Grade Envelope of the Stanley-Pauley Engineering Building in Winnipeg*. Master's thesis, University of Manitoba, Manitoba, Canada, 2018 (cit. on pp. 19, 20, 22, 30, 31).

[17] K. Bobko, P. Maghoul, M. Kavgic, and M. Saaly. „Energy Performance of Below-Grade Envelope of Stanley-Pauley Building in Winnipeg“. In: *71th Canadian Geotechnical Conference–GeoEdmonton* (2018) (cit. on p. 100).

[18] O. Boënnec. „Piling on the Energy“. In: *Geodrilling Int* 150 (2009), pp. 25–28 (cit. on p. 124).

[19] M. T. Bomberg. „Some performance aspects of glass fiber insulation on the outside of basement walls, Symposium on Thermal Insulation Performance“. In: *ASTM Special Technical Publication* 718 (1980), pp. 77–91 (cit. on p. 15).

[20] P. J. Bourne-Webb, B. Amatya, K. Soga, et al. „Energy pile test at Lambeth College, London: geotechncial and thermodynamic aspects of pile response to heat cycles“. In: *Géotechnique* 3 (2009), pp. 237–248 (cit. on pp. 55, 57, 124, 125, 134, 148).

[21] P.J. Bourne-Webb, B. Amatya, and K. Soga. „A framework for understanding energy pile behaviour“. In: *Proceedings of the Institution of Civil Engineers - Geotechnical Engineering* 166.2 (2013), pp. 170–177 (cit. on p. 124).

[22] H Brandl. „Energy foundations and other thermo-active ground structures“. In: *Géotechnique* 56.2 (2006), pp. 81–122 (cit. on pp. 56, 90, 124).

[23] H. Brandl. „Energy piles and diaphragm walls for heat transfer from and into the ground“. In: *Proc. 3rd Int. Symp. on Deep Foundations on Bored and Auger Piles, BAP III, Ghent* (1998), pp. 37–60 (cit. on p. 124).

[24] T. Brettmann and T Amis. „Thermal Conductivity Evaluation of a Pile Group Using Geothermal Energy Piles“. In: *Geo-Frontiers* (2011) (cit. on p. 54).

[25] J.L. Briaud. „The National Geotechnical Experimentation sites at Texas A&M University: Clay and Sand, A Summary“. In: *Geotech Spec Publ J* 93 (2000), pp. 26–51 (cit. on p. 124).

[26] C. Cekerevac and L. Laloui. „Experimental study of thermal effects on the mechanical behavior of a clay“. In: *Int J Numer Anal Methods Geomech* 28.3 (2004), pp. 209–228 (cit. on p. 128).

[27] Y. Chai, T. Sun, H. Han, F. Cao, and Y. Liu. „Modularly Design for Waste Heat Recovery System in Subway Based on Air Source Heat Pump“. In: *Procedia Engineering* 205 (2017), pp. 273–280 (cit. on p. 85).

[28] K. S. Chang and M.J. Kim. „Analysis and thermal response test for vertical ground heat exchanger with two U-loop configuration“. In: *International Journal of Energy Research* 40.2 (2016), pp. 189–197 (cit. on p. 62).

[29] D. Chen. „Dynamic three-dimensional heat transfer calculation for uninsulated slab-on-ground constructions“. In: *Energy and Building* 60 (2013), pp. 420–428 (cit. on p. 15).

[30] D. Chen. „Heat Loss via Concrete Slab Floors in Australian Houses“. In: *Procedia Eng* 205 (2017), pp. 108–115 (cit. on pp. 15, 140).

[31] X. Chen, L. Lu, and HX Yang. „Long term operation of a solar assisted ground coupled heat pump system for space heating and domestic hot water“. In: *Energy Build* 43.8 (2011), pp. 1835–1844 (cit. on pp. 60, 73).

[32] X. Chen and H. Yang. „Performance analysis of a proposed solar assisted ground coupled heat pump system“. In: *Applied Energy* 97 (2012), pp. 888–896 (cit. on pp. 76–78).

[33] A.D. Chiasson, S.J. Rees, and J.D. Spitler. „A preliminary assessment of the effects of groundwater flow on closed-loop ground source heat pump systems“. In: *JStillwater, (OK, US): Oklahoma State Univ* (2000) (cit. on p. 70).

[34] J. Claesson and G. Hellström. „Multipole method to calculate borehole thermal resistances in a borehole heat exchanger“. In: *Science and Technology for the Built Environment* 17.6 (2011), pp. 895–911 (cit. on p. 71).

[35] Canada Green Building Council. *LEED v4 Green Associate Study Guide*. 2015 (cit. on p. 14).

[36] C. Dai and Y. Chen. „Classification of shallow and deep geothermal energy“. In: *Geothermal Resource Council Transactions* 32 (2008), pp. 317–320 (cit. on pp. 48, 49).

[37] L. Dai, S. Li, L. DuanMu, et al. „Experimental performance analysis of a solar assisted ground source heat pump system under different heating operation modes“. In: *Applied Thermal Engineering* 75 (2015), pp. 325–333 (cit. on pp. 80, 91).

[38] M. G. Davies. „Heat loss from a solid gound floor“. In: *Build Environ* 28.3 (1993), pp. 347–359 (cit. on pp. 15, 140).

[39] M. De Moel, P. M. Bach, A. Bouazza, Singh R. M., and J O. Sun. „Technological Advances and Application of Geothermal Energy Pile Foundations and their Feasibility in Australia“. In: *Renewable and Sustainable Energy Reviews* 14.9 (2010), pp. 2683–2696 (cit. on p. 54).

[40] Decagon Devices, Pullman, WA. *KD2 Pro thermal properties analyzer operator's manual version 4*. 2013 (cit. on p. 21).

[41] B. Dehghan, A. Sisman, and M. Aydin. „Optimizing the distance between boreholes with helical shaped ground heat exchanger“. In: *In : Proceedings World Geothermal Congress* (2015) (cit. on p. 66).

[42] F. Delaleux, X. Py, R. Olives, and A. Dominguez. „Enhancement of geothermal borehole heat exchangers performances by improvement of bentonite grouts conductivity“. In: *Applied Thermal Engineering* 33–34 (12 2012), pp. 92–99 (cit. on pp. 71, 72).

[43] A. E. Delsante, A. N. Stokes, and P. J. Walsh. „Application of Fourier Transforms to Periodic Heat Flow Into the Ground Under a Building“. In: *Int J Heat Mass Tran* 26 (1982), pp. 121–132 (cit. on pp. 16, 140).

[44] M. P. Deru and A. T. Kirkpatrick. „Ground-Coupled Heat and Moisture Transfer from Buildings: Part1–Application.“ In: *Journal of Solar Energy Engineering* 124.1 (2002), pp. 10–16 (cit. on pp. 17, 33).

[45] M. Deru and P. Burns. „Model for Ground-Coupled Heat and Moisture Transfer from Buildings“. In: *National Renewable Energy Laboratory (NREL)* (2003) (cit. on pp. 15, 17).

[46] N. Diao and Z. Li Q. Fang. „Heat transfer in ground heat exchangers with groundwater advection“. In: *Int J Therm Sci* 43 (2004), pp. 1203–1211 (cit. on p. 124).

[47] A. Dikici and A. Akbulut. „Exergetic performance evaluation of heat pump systems having various heat sources“. In: *International Journal of Energy Research* 32.14 (2008), pp. 1279–1296 (cit. on p. 75).

[48] *Energy Efficiency Trends in Canada 1990 to 2009*. 2011 (cit. on pp. 2, 14, 15).

[49] U.S. Department of Energy's (DOE) Building Technologies Office (BTO). „EnergyPlus, version 8.9“. In: (2018) (cit. on p. 23).

[50] *Environment and Climate Change Canada, Winnipeg Historical Temperature*. Dec. 2018 (cit. on p. 113).

[51] H. Esen, M. Inalli, and Y. Esen. „Temperature distributions in boreholes of a vertical ground-coupled heat pump system“. In: *Renewable Energy* 34.12 (2009), pp. 2672–2679 (cit. on pp. 54, 124).

[52] D. Essex, K. Joe, H. Arvinder, et al. *Project Manual. Volume I of II Stanley Pauley Engineering Building 97 Dafoe Road (Vol. I). University of Manitoba*. 2017 (cit. on p. 19).

[53] J. Fadejev, J. Kurnitski, and Y. Chen. „Geothermal energy piles and boreholes design with heat pump in a whole building simulation software“. In: *Energy and Buildings* 106 (2015), pp. 23–24 (cit. on pp. 89, 124).

[54] H. Fang, J. Xia, A. Lu, and Y. Jiang. „An operation strategy for using a ground heat exchanger system for industrial waste heat storage and extraction“. In: *Building Simulation* 7.2 (2014), pp. 197–204 (cit. on p. 85).

[55] O. T. Farouki. „The thermal properties of soils in cold regions“. In: *Cold Regions Science and Technology* 5.1 (1981), pp. 67–7 (cit. on p. 17).

[56] A. Fergusen and A. D. Woodbury. „Subsurface heat flow in an urban environment“. In: *J Geophys Res* 109 (2004), pp. 1–9 (cit. on pp. 18, 33, 93, 100, 128).

[57] G. Florides and S Kalogirou. „First in situ determination of the thermal performance of a U-pipe borehole heat exchanger in Cyprus“. In: *Applies Thermal Energy* 28.2-3 (2008), pp. 157–163 (cit. on p. 54).

[58] J. Gao, X. Zhang, J. Liu, K. Li, and J. Yang. „Numerical and experimental assessment of thermal performance of vertical energy piles: an application“. In: *Applied Energy* 85.10 (2008), pp. 901–910 (cit. on p. 54).

[59] J. Gao, Xu. Zhang, J. Liu, K.S. Li, and J. Yang. „Thermal performance and ground temperature of vertical pile-foundation heat exchangers: a case study“. In: *Applied Thermal Engineering* 28.17-18 (2008), pp. 2295–2304 (cit. on p. 54).

[60] S. Gehlin, J. Spitler, and G. Hellström. „Deep Boreholes for Ground Source Heat Pump Systems-Scandinavian Experience and Future Prospects“. In: *Meeting, Orlando, Florida, January 23-27* (2016) (cit. on p. 67).

[61] N. Ghabra, L. Rodriguez, and P. Oldfield. „Energy-Saving Potential of Building Envelope Designs in Residential Houses in Taiwan“. In: *International Journal of Low-Carbon Technologies* 12.4 (2017), pp. 411–419 (cit. on p. 15).

[62] N. GhaffarianHoseini A. Dalilah Dahlan, U. Berardi, A. GhaffarianHoseini, N. Makaremi, and M. GhaffarianHoseini. „Sustainable energy performances of green buildings: A review of current theories, implementations and challenges“. In: *Renewable and sustainable energy reviews* 25 (2013), pp. 1–14 (cit. on p. 89).

[63] S. Hackel and A. Pertzborn. „Effective design and operation of hybrid ground-source heat pumps: Three case studies“. In: *Energy and Buildings* 43 (2011), pp. 3497–3504 (cit. on p. 84).

[64] C. E. Hagentoft. „Heat loss to the ground form a building. Slab on the ground and cellar. Thèse de doctorat,Lund, Suède,“ in: *Lund Institute of Technology* (1988) (cit. on p. 16).

[65] Z. Han, M. Zheng, F. Kong, et al. „Numerical simulation of solar assisted ground-source heat pump heating system with latent heat energy storage in severely cold area“. In: *Applied Thermal Engineering* 28.11-12 (2008), pp. 1427–1436 (cit. on p. 74).

[66] A. Hepbasli, O. Akdemir, and E. Hancioglu. „Experimental study of a closed loop vertical ground source heat pump system“. In: *Energy Conversion and Management* 44.4 (2003), pp. 527–548 (cit. on pp. 60, 127).

[67] F.P. Incropera, D. P. Dewitt, T. L. Bergman, and A. S. Lavine. *Fundamentals of Heat and Mass Transfer*. Wiley, 2007 (cit. on pp. 32, 99).

[68] A. Al-Janabi, M. Kavgic, A. Mohammadzadeh, and A. Azzouz. „Comparison of EnergyPlus and IES to model a complex university building using three scenarios: Free-floating, ideal air load system, and detailed“. In: *J Build Eng* 22 (2019), pp. 262–280 (cit. on pp. 23–25, 45).

[69] J. Jeong, T. Hong, J. Kim, M. Chae, and C. Ji. „Multi-Criteria analysis of a self-consumption strategy for building sectors focused on ground source heat pump systems“. In: *Journal of cleaner Production* 186 (2018), pp. 68–80 (cit. on pp. 65, 108, 126).

[70] O. Johansen. „Thermal conductivity of soils“. In: *Cold Regions Research and Engineering Lab Hanover NH* (1997) (cit. on p. 17).

[71] M. Karti, D. E. Claridge, and J.F. Kreider. „ITPE technique applications to time-varying three-dimensional groundcoupling problems“. In: *ournal of Heat Transfer (ASME)* 112 (1990), pp. 849–852 (cit. on pp. 16, 44, 140).

[72] M. Karti, D. E. Claridge, and J.F. Kreider. „ITPE technique applications to time-varying two-dimensional groundcoupling problems“. In: *International Journal of Heat and Mass Transfer* 31.9 (1988), pp. 1899–1911 (cit. on pp. 16, 44).

[73] M. Karti, D. E. Claridge, and J.F. Kreider. „The ITPE technique applied to steady-state ground-coupling problems“. In: *International Journal of Heat and Mass Transfer* 31.9 (1988), pp. 1855–1898 (cit. on pp. 16, 44).

[74] M. Kharseh, L. Altorkmany, M. Al-Khawaja, and F. Hassani. „Analysis of the effect of global climate change on ground source heat pump systems in different climate categories“. In: *Renew. Energy* 78 (2015), pp. 219–225 (cit. on pp. 62, 92, 123).

[75] E. Kjellsson, G. Hellströmb, and B. Perers. „Optimization of systems with the combination of ground-source heat pump and solar collectors in dwellings“. In: *Energy* 35.6 (2010), pp. 2667–2673 (cit. on p. 75).

[76] R. Kothari, V. V. Tyagi, and A. Pathak. „Waste-to-energy: A way from renewable energy sources to sustainable development“. In: *Renewable and Sustainable Energy Reviews* 14.9 (2010), pp. 3164–3170 (cit. on p. 89).

[77] C.A. Kramer, O. Ghasemi Far, and P Basu. „Laboratory Thermal Performance Tests on a Model Heat Exchanger Pile in Sand“. In: *Geotechnical and Geological Engineering* 32.2 (2015), pp. 253–271 (cit. on p. 55).

[78] T. Kurevija, D. Vulin, and V. Krapec. „Effect of borehole array geometry and thermal interferences on geothermal heat pump system“. In: *Energy Conversion and Management* 60 (2012), pp. 134–142 (cit. on pp. 67–69).

[79] A. H. Lachenbruch. „Three-Dimensional Heat Conduction in Permafrost Beneath Heated Buildings“. In: *Geological Survey Bulletin 1052-B, U.S. Government Printing Office, Washington, DC.* (1967) (cit. on pp. 16, 44, 140).

[80] C. M. Lai and Y. Wang. „Energy-Saving Potential of Building Envelope Designs in Residential Houses in Taiwan“. In: *Energies* 4.11 (2011), pp. 2061–2076 (cit. on p. 15).

[81] L. Laloui, M. Moreni, and L Vulliet. „Comportement d'un pieu bi-fonction, fondation et échangeur de chaleur“. In: *Canadian Geotechnical Journal* 40.2 (2003), pp. 388–402 (cit. on pp. 56, 124).

[82] L. Laloui, N. Nuth, and L Vulliet. „Experimental and Numerical Investigations of the behavior of a Heat exchanger pile“. In: *International Journal for numerical and analytical methods in geomechanics* (2006) (cit. on pp. 56, 89, 124, 129).

[83] K.A. Landman and A.E. Delsante. „Steady-state heat losses from a building floor slab with vertical edge insulation - I“. In: *Building and Environment* 21 (1986), pp. 177–182 (cit. on p. 15).

[84] C. Lee, K. Lee, H. Choi, and H.P. Choi. „Characteristics of thermally-enhanced bentonite grouts for geothermal heat exchanger in South Korea“. In: *Science in China Series E: Technological Sciences* 53.1 (2010), pp. 123–128 (cit. on p. 71).

[85] C. Lee, M. Park, T.B. Nguyen, et al. „Performance evaluation of closed-loop vertical ground heat exchangers by conducting in-situ thermal response tests“. In: *Renewable Energy* 42 (2012), pp. 77–83 (cit. on p. 72).

[86] J. H. Lee, C. H. Lee S.H. Choi, and S. U. S. Jang S. P. Choi. „A review of thermal conductivity data, mechanism and models for nanofluids“. In: *International Journal of Micro-Nano Scale Transport* 4 (2010), pp. 269–322 (cit. on p. 72).

[87] J. U. Lee, T. Kim, and S. B. Leight. „Thermal performance analysis of a ground-coupled heat pump integrated with building foundation in summer“. In: *Energy Build* 59 (2013), pp. 37–43 (cit. on pp. 90, 123).

[88] WH. Leong, VR. Tarnawski, and A. Aittomäki. „Effect of soil type and moisture content on ground heat pump performance: Effet du type et de l'humidité du sol sur la performance des pompes à chaleur à capteurs enterrés“. In: *International Journal of Refrigeration* 21.8 (1998), pp. 595–606 (cit. on p. 70).

[89] H. Q. Li, S. S. Kang, Z. Yu, B. Cai, and G. Q. Zhang. „A feasible system integrating combined heating and power system with ground-source heat pump“. In: *Energy* (2014), pp. 240–247 (cit. on p. 85).

[90] K Li. „Comparison of geothermal with solar and wind power generation systems“. In: *38th Workshop on Geothermal Reservoir Engineering Stanford University* (2013) (cit. on p. 48).

[91] S. Li, W. Yang, and X. Zhang. „Soil temperature distribution around a U-tube heat exchanger in a multi-function ground source heat pump system“. In: *Applied Thermal Engineering* 29.17-18 (2009), pp. 3679–3686 (cit. on p. 61).

[92] X. Li, Z. Chen, and J. Zhao. „Simulation and experiment on the thermal performance of U-vertical ground coupled heat exchanger“. In: *Applied Thermal Engineering* 26.14-15 (2006), pp. 1564–1571 (cit. on pp. 61, 92).

[93] H. Liu, P. Maghoul, A. Bahari, and M. Kavgic. „Feasibility study of snow melting system for bridge decks using geothermal energy piles integrated with heat pump in Canada“. In: *Renewable Energy* (2019) (cit. on p. 54).

[94] H. Liu, P. Maghoul, A. Bahari, and M. Kavgic. „Feasibility Study of Snow Melting System Using Geothermal Energy Heat Pumps in Canada“. In: *International Journal of Renewable Energy (Elsevier)* Submitted (2018) (cit. on pp. 33, 99, 128, 133).

[95] H. Liu, P. Maghoul, and H. Holländer. „Sensitivity analysis and optimum design of a hydronic snow melting system during snowfall“. In: *Phys Chem Earth, Parts A/B/C* (2019) (cit. on p. 127).

[96] J. Liu, X. Zhang, J. Gao, and J. Yang. „Evaluation of heat exchange rate of GHE in geothermal heat pump systems“. In: *Renewable Energy* 34.12 (2009), pp. 2898–2904 (cit. on p. 71).

[97] Y. Liu, B. X. Li, and X. H. Xu. „Study on the heating system combined subway exhaust heat with geothermal source heat pump“. In: *Acta Energiae Solaris Sinica* 31.6 (2010), pp. 754–758 (cit. on p. 85).

[98] Z. Liu, W. Xu, C. Qian, and G. Jin. „Investigation on the feasibility and performance of ground source heat pump (GSHP) in three cities in cold climate zone, China“. In: *Renewable Energy* 84 (2015), pp. 89–96 (cit. on pp. 62, 92).

[99] J. Lu and M. Chen. „The analysis and simulation on operating characteristics of GSHP in summer“. In: *Journal of Superconductivity and Novel Magnetism* 23.6 (2010), pp. 1091–1093 (cit. on p. 63).

[100] J. Lund, B. Sanner, L. Rybach, R. Curtis, and G. Hellström. „Geothermal (groundsource) heat pumps: a world overview“. In: *GHC Bulletin* (2004), pp. 1–10 (cit. on p. 60).

[101] *Manitoba Energy Code for Buildings (MECB)*. 2011 (cit. on p. 23).

[102] *Manitoba Hydro historical electricity and natural gas rates*. 2019 (cit. on p. 44).

[103] A. B. Mcguire. „Ground-source heat pumps: Keys to design, installation“. In: (2009) (cit. on p. 65).

[104] P.D. Metz. „The use of ground-coupled tanks in solar-assisted heat-pump systems“. In: *Journal of Solar Energy Engineering* 104.4 (1982), pp. 366–372 (cit. on p. 72).

[105] R.L. Michalowski. „A Constitutive Model of Saturated Soils for Frost Heave Simulations“. In: *Cold Regions Science and Technol* 22 (1993), pp. 47–63 (cit. on pp. 29, 97).

[106] A. Michopoulos, D. Bozis, P. Kikidis, K. Papakostas, and N.A. Kyriakis. „Three-years operation experience of a ground source heat pump system in Northern Greece“. In: *Energy and Buildings* 39.3 (2007), pp. 328–334 (cit. on p. 84).

[107] T. Mimouni and L. Laloui. „Behaviour of a group of energy piles“. In: *Can Geotech J* 52.12 (2015), pp. 1913–1929 (cit. on p. 126).

[108] G. P. Mitalas. „Calculation of basement heat loss“. In: *ASHRAE Transactions* 89.1 (1983), pp. 420–437 (cit. on p. 16).

[109] G. P. Mitalas. „Calculation of below-grade residential heat loss: low-rise residential building“. In: *ASHRAE Transactions* 93.1 (1987), pp. 743–784 (cit. on p. 16).

[110] M. Mokhtar, M. Stables, x. Liu, and J. Howe. „Intelligent multi-agent system for building heat distribution control with combined gas boilers and ground source heat pump“. In: *Energy and Buildings* 62 (2013), pp. 615–626 (cit. on p. 92).

[111] K. D. Murphy, J. S. McCartney, and K. S Henry. „Evaluation of thermo-mechanical and thermal behavior of full-scale energy foundations“. In: *Acta Geotechnica* 10.2 (2015), pp. 179–195 (cit. on pp. 57–59, 91, 126).

[112] Y. Nam, R. Ooka, and Y. Shiba. „Development of dual-source hybrid heat pump system using groundwater and air“. In: *Energy and Buildings* 42.6 (2010), pp. 909–916 (cit. on p. 81).

[113] National Research Council Canada. „The National Building Code of Canada (NBC)“. In: (2015) (cit. on pp. 141, 149).

[114] L. Ni, W. Song, F. Zeng, and Y. Yao. „Energy Saving and Economic Analyses of Design Heating Load Ratio of Ground Source Heat Pump with Gas Boiler As Auxiliary Heat Source“. In: *2011 International Conference on Electric Technology and Civil Engineering (ICETCE)* (2011), pp. 1197–1200 (cit. on p. 84).

[115] C. G. Olgun, T. Y. Ozudogru, S. L. Abdelaziz, and A. Senol. „Long-term performance of heat exchanger piles“. In: *Acta Geotechnica* 10 (2015), pp. 553–569 (cit. on pp. 55, 127).

[116] A. M Omer. „Ground-source heat pumps systems and applications“. In: *Renewable and Sustainable Energy Reviews* 12.2 (2008), pp. 344–371 (cit. on pp. 3, 50, 51, 89, 123).

[117] O. Ozgener and A. Hepbasli. „Experimental performance analysis of a solar assisted ground-source heat pump greenhouse heating system“. In: *Energy and Buildings* 37.1 (2005), pp. 101–110 (cit. on pp. 73, 92).

[118] D. Pahud and M. Hubbuch. „Measured thermal performances of the energy pile system of the dock midfield at Zürich airport“. In: *In: Proceedings European geothermal congress 2007. May 31-June 01 Unterhatching, Germany* (2007) (cit. on pp. 90, 124).

[119] N. Pardo, Á. Montero, J. Martos, and J.F. Urchueguía. „Optimization of hybrid–ground coupled and air source–heat pump systems in combination with thermal storage“. In: *Applied Thermal Engineering* 30.8-9 (2010), pp. 1073–1077 (cit. on pp. 81, 92).

[120] C. Pasten and J.C. Santamarina. „Thermally Induced Long-Term Displacement of Thermoactive Piles“. In: *J Geotech Geoenviron Eng* 140.5 (2014) (cit. on p. 126).

[121] H. Qian and Y. Wang. „Modeling the interactions between the performance of ground source heat pumps and soil temperature variations“. In: *Energy for Sustainable Development* 23 (2014), pp. 115–121 (cit. on pp. 61, 65, 108).

[122] J. Rantala and V. Leivo. „Heat loss into ground from a slab-on-ground structure in a floor heating system“. In: *Internaltional Journal of Energy Research* 30 (2006), pp. 929–938 (cit. on p. 15).

[123] R.H.D. Rawlings and J. R Sykulski. „Ground-source heat pump systems: A technology review“. In: *Building Services Engineering Research and Technology* 20.3 (1999), pp. 119–129 (cit. on pp. 50, 52, 53).

[124] S. W. Rees, Z. Zhou, and H. R. Thomas. „The influence of soil moisture content variations on heat losses from earth-contact structures: an initial assessment“. In: *Building and Environment* 36 (2001), pp. 157–165 (cit. on p. 15).

[125] B.A. Rock. „Sensitivity study of slab-on-grade transient heat transfer model parameters“. In: *ASHRAE Transactions* 110.1 (2004), pp. 177–184 (cit. on p. 15).

[126] P. Roth, A. Georgiev, and A. Busso. „First in situ determination of ground and borehole thermal properties in Latin America“. In: *Renewable Energy* 29 (12 2004), pp. 1947–1963 (cit. on p. 71).

[127] R. Ruparathna, Kasun. Hewage, and R. Sadiq. „Improving the energy efficiency of the existing building stock: A critical review of commercial and institutional buildings“. In: *Renewable and Sustainable Energy Reviews* 53 (2016), pp. 1032–1045 (cit. on p. 25).

[128] M. Saaly, P. Maghoul, M. Kavgic, and D. Polyzois. „Performance analysis of a proposed geothermal pile system for heating and cooling energy demand for a building in cold regions“. In: *Sustainable Cities and Society* 45 (2019), pp. 669–682 (cit. on pp. 54, 127, 128, 133, 139, 140).

[129] Y. Shang, M. Dong, and S. Li. „Intermittent experimental study of a vertical ground source heat pump system“. In: *Appl Energy* 136 (2014), pp. 628–635 (cit. on pp. 63, 65, 70).

[130] M.H. Sharqawy, E.M. Mokheimer, and H.M. Badr. „Effective pipe-to-borehole thermal resistance for vertical ground heat exchangers“. In: *Geothermics* 38 (2009), pp. 271–277 (cit. on p. 71).

[131] Q. Si, M. Okumiya, and X. Zhang. „Performance evaluation and optimization of a novel solar-groundsource heat pump system“. In: *Energy and Buildings* 70 (2014), pp. 237–247 (cit. on pp. 77, 79).

[132] H. Sozer. „Improving energy efficiency through the design of the building envelope“. In: *Building and Environment* 45 (2010), pp. 2581–2593 (cit. on p. 15).

[133] M. C. Swinton and R. E. Platts. „Engineering method for estimating basement heat loss and insulation performance“. In: *ASHRAE Tran* 87.2 (1981) (cit. on p. 16).

[134] The Energy Saver. Compiled by NIFES Consulting Group, Gee Ltd. *The complete guide to energy effciency* (cit. on pp. 14, 15).

[135] E. W. Tiedje and P. Guo. „Modeling the influence of particulate geometry on the thermal conductivity of composites“. In: *Journal of Materials Science* 49.16 (2014), pp. 5586–559 (cit. on p. 71).

[136] V. Trillat-Berdal, B. Souyri, and G. Fraisse. „Experimental study of a ground-coupled heat pump combined with thermal solar collectors“. In: *Energy and Buildings* 38.12 (2006), pp. 1477–1484 (cit. on p. 74).

[137] A. Tulsyan, S. Dhaka, J. Mathur, and J. V. Yadav. „Potential of energy savings through implementation of Energy Conservation Building Code in Jaipur city, India“. In: *Energy and Buildings* 58 (2013), pp. 123–130 (cit. on p. 15).

[138] J.F. Urchueguía, M. Zacarés, J.M. Corberán, et al. „Comparison between the energy performance of a ground coupled water to water heat pump system and an air to water heat pump system for heating and cooling in typical conditions of the European Mediterranean coast“. In: *Energy Conversion and Management* 49.10 (2008), pp. 2917–2923 (cit. on p. 81).

[139] K.K.W. Wan, D.H.W. Li, W. Pan, and J.C. Lam. „Impact of climate change on building energy use in different climate zones and mitigation and adaptation implications“. In: *Applied Energy* 97 (2012), pp. 274–282 (cit. on p. 62).

[140] B. Wang, A. Bouazza, and C Haberfield. „Preliminary Observations from Laboratory Scale Model Geothermal Pile subjected to Thermo-Mechanical Loading“. In: *Geo-Frontiers 2011 Proceeding* (2011) (cit. on p. 89).

[141] E. Wang, A. S. Fung, C. Qi, and W. H. Leong. „Performance prediction of a hybrid solar ground source heat pump system“. In: *Energy and Buildings* 47 (2012), pp. 600–611 (cit. on p. 92).

[142] H.J. Wang and C. Qi. „Performance study of underground thermal storage in a solar-ground coupled heat pump system for residential buildings“. In: *Energy and Buildings* 40.7 (2008), pp. 1278–1286 (cit. on p. 74).

[143] X. Wang, M. Zheng, W. Zhang, S. Zhang, and T. Yang. „Experimental study of a solar-assisted ground-coupled heat pump system with solar seasonal thermal storage in severe cold areas“. In: *Energy and Buildings* 42.11 (2010), pp. 2104–2110 (cit. on p. 75).

[144] W. Wei, B. Wang, T. You, W. Shi, and X Li. „A Potential solution for thermal imbalance of ground source heat pump system in cold regions: Ground source absorption heat pump“. In: *Renewable Energy* 59 (2013), pp. 39–48 (cit. on p. 60).

[145] W. Wu, T. Li, B. Wang, and W Shi. „Hybrid ground source absorption heat pump in cold regions: thermal balance keeping and borehole number reduction“. In: *Applied Thermal Engineering* 90 (2015), pp. 322–334 (cit. on p. 92).

[146] C. Xi, L. Lin, and Y. Hongxing. „Long term operation of a solar assisted ground coupled heat pump system for space heating and domestic hot water“. In: *Energy and Buildings* 43.8 (2011), pp. 1835–1844 (cit. on p. 92).

[147] L. Yang, B. Qiao, W. Xu, and Q. Zhou. „Analysis of the influence of borehole depth on energy efficiency and cost of ground source heat pump system“. In: *in: proceeding of 12th IEA Heat Pump Conference, Rotterdam* (2017) (cit. on p. 69).

[148] W. Yang, Y. Chen, M. Shi, and J.D. Spitler. „Numerical investigation on the underground thermal imbalance of ground-coupled heat pump operated in cooling-dominated district“. In: *Applied Thermal Engineering* 58.1-2 (2013), pp. 626–637 (cit. on p. 60).

[149] W. Yang, L. Kong, and Y. Chen. „Numerical evaluation on the effects of soil freezing on underground temperature variations of soil around ground heat exchangers“. In: *Applied Thermal Engineering* 75 (2015), pp. 259–269 (cit. on p. 70).

[150] W. Yang, P. Lu, and Y. Chen. „Laboratory investigations of the thermal performance of an energy pile with spiral coil ground heat exchanger“. In: *Energy and Buildings* 128 (2016), pp. 491–502 (cit. on p. 92).

[151] W. Yang, L. Sun, and Y. Chen. „Experimental investigations of the performance of a solar-ground source heat pump system operated in heating modes“. In: *Energy and Buildings* 89 (2015), pp. 97–111 (cit. on p. 92).

[152] W. Yang, L. Sun, and Y. Chen. „Experimental investigations of the performance of a solar-ground source heat pump system operated in heating modesWeibo“. In: *Energy and Buildings* 89 (2015), pp. 97–111 (cit. on pp. 79, 80).

[153] W. Yang, J. Zhou, W. Xu, and G.Q. Zhang. „Current status of ground-source heat pumps in China“. In: *Energy Policy* 38.1 (2010), pp. 323–333 (cit. on p. 60).

[154] M. Yari and N. Javani. „Performance assessment of a horizontal coil geothermal heat pump“. In: *Int J Energy Res* 31.6 (2006), pp. 288–299 (cit. on p. 124).

[155] N. Yavari, A.M. Tang, J. Pereira, and G Hassen. „Experimental study on the mechanical behaviour of a heat exchanger pile using physical modelling“. In: *Acta Geotechnica* 9.3 (2014), pp. 385–398 (cit. on p. 55).

[156] T. You, W. Shi, B. Wang, W. WU, and X. Li. „A new ground-coupled heat pump system integrated with a multi-mode air-source heat compensator to eliminate thermal imbalance in cold regions“. In: *Energy and Buildings* 107 (2015), pp. 103–112 (cit. on pp. 82, 83).

[157] T. You, B. Wang, W. Wu, W. Shi, and X. Li. „A new solution for underground thermal imbalance of ground-coupled heat pump systems in cold regions: heat compensation

unit with thermosyphon“. In: *Applied Thermal Engineering* 64.1-2 (2014), pp. 283–292 (cit. on pp. 60, 62, 82, 91, 105).

[158] T. You, B. Wang, W. Wu, W. Shi, and X. Li. „A new solution for underground thermal imbalance of ground-coupled heat pump systems in cold regions: heat compensation unit with thermosyphon“. In: *Applied Thermal Engineering* 64 (2014), pp. 283–292 (cit. on p. 92).

[159] T. You, W. Wu, W. Shi, B. Wang, and X. Li. „An overview of the problems and solutions of soil thermal imbalance of ground-coupled heat pumps in cold regions“. In: *Applied Energy* 177.14-15 (2016), pp. 515–536 (cit. on pp. 4, 60, 92).

[160] M. Younis and D.S.K Bolisseti T.and Ting. „Ground source heat pump systems: Current status“. In: *International Journal of Environmental Studies* 67.3 (2010), pp. 405–415 (cit. on pp. 50–53, 123).

[161] T. Yu, Z. Liu, G. Chu, and Y. Ou. „Influence of intermittent operation on soil temperature and energy storage duration of ground-source heat pump system for residential building“. In: *In: Proceedings of the 8th international symposium on heating, ventilation and air conditioning* (2014), pp. 203–213 (cit. on p. 62).

[162] X.Q. Zhai, M. Qu, X. Yu, Y. Yang, and R.Z. Wang. „A review for the applications and integrated approaches of ground-coupled heat pump systems“. In: *Renewable and Sustainable Energy Reviews* 15.6 (2011), pp. 3133–3140 (cit. on p. 60).

[163] Y. Zhou, Y. Zhang, and Y. Xu. „Influence of grout thermal properties on heat-transfer performance of ground source heat exchangers“. In: *Science and Technology for the Built Environment* 24 (2018), pp. 461–469 (cit. on p. 71).

[164] J. Zhu, K. Hu, X. Lu, et al. „A review of geothermal energy resources, development, and applications in China: Current status and prospects“. In: *Energy* 93 (2015), pp. 466–483 (cit. on pp. 28, 29, 48).